5. SITE 556[1]

Shipboard Scientific Party[2]

HOLE 556

Date occupied: 22 September 1981

Date departed: 29 September 1981

Time on hole: 172.9 hr.

Position (latitude; longitude): 38°56.38′N; 34°41.12′W

Water depth (sea level; corrected m, echo-sounding): 3672

Water depth (rig floor; corrected m, echo-sounding): 3682

Bottom felt (m, drill pipe); 3690

Penetration (m): 639.0

Number of cores: 22

Total length of cored section (m): 184

Total core recovered (m): 85.21

Core recovery (%): 46

Oldest sediment cored:
Depth sub-bottom (m): 471.0
Nature: Basalt limestone breccia
Age: latest early Oligocene
Measured velocity (km/s): 5.61

Basement:
Depth sub-bottom (m): 461.5
Nature: Basalt, basalt breccias, gabbro, and gabbro breccias

Principal results: Hole 556 (Site MAR-2) was drilled on Anomaly 12 on the west flank of the Mid-Atlantic Ridge, about 50 miles north of the Pico Fracture Zone, on a flow line passing through the Azores Triple Junction (Fig. 1). The seismic profile collected on the way to the site indicated approximately 500 m of sediment overlying basement.

After washing down through 461 m of sediment, we cored 177 m into the basement until bit destruction. Three different basaltic and basalt breccia units were cored down to 96 m sub-basement. Below, gabbro and gabbro breccias were recovered down to the bottom of the hole (177 m sub-basement) interrupted by a thin basaltic layer. Nannofossils found in the basalt breccias at 10 m sub-basement are dated at 30 to 34 Ma in agreement with the magnetic anomaly age.

The concentrations of the magmaphile trace elements in the 33 basaltic samples analyzed on board with the X-ray fluorescence (XRF) unit are representative of depleted Mid-Oceanic Ridge Basalts. Typical concentrations in these basalts are: Nb = 1.5 ppm, Zr = 85 ppm, Ti = 8400 ppm, Y = 36 ppm, V = 270 ppm. This unexpected result demonstrates that if an Azores Mantle Plume exists, it either has been active for a shorter period of time than previously thought or is an intermittent process.

The average core remanent magnetization inclinations within the upper part of the pillow and massive basaltic units are closely grouped (−25 to −30°), whereas the lower basaltic units have more scattered inclinations (−12 to −46°).

Three temperature measurements were made at different depths when washing down to the basement; they showed a geothermal gradient of 36°C/km. A successful suite of logs were run after bit destruction. A constant temperature of about 2°C was observed down to the sediment-basement interface, suggesting seawater flow into the hole.

OPERATIONS

Approach to the Site

The exact location of Site 556 was required to fulfill three criteria. It should be at the latitude of the Azores Triple Junction, near Magnetic Anomaly 13, contain sediments as thin as possible, and avoid basement peaks or ridges and fracture zones. No previous site survey had been performed; the closest useful data was a reflection profile record along an east-west track some 15 miles north of the tentative site location.

A westward course was set just south of 39°N, and magnetic and seismic profiler records were monitored (Figs. 2 and 3). Magnetic Anomalies 11 and 12 were situated over sediment thicknesses of about 0.5 s overlying a strongly reflecting acoustic basement (2230Z, 21 September). In places, the reflector became weak and was difficult to distinguish. Continuing west to Anomaly 13 (0015Z, 22 September), the basement topography became rough, with a prominent peak at 0030Z. This correlated with a peak on the profiler record to the north, indicating a prominent basement ridge underlying Anomaly 13.

To avoid this ridge, we decide to return to the area of strong basement reflectors previously noted underlying Anomaly 12. An eastward course was set diverging to the north from the westward track, to determine the linearity of features seen on that track. A pass across the site was made to the south to check for basement peaks, and the beacon dropped at 0351 hr., 22 September on a final northward pass. The correlation of magnetic anomalies along these tracks with previous data tracks in the area precludes the possibility of any significant offset fracture zones close to this site.

On-Site Operations

At Site 556 (MAR-2), we decide that, in addition to the basic program of drilling the basement until bit de-

[1] Bougault, H., Cande, S. C., et al., *Init. Repts. DSDP*, 82: Washington (U.S. Govt. Printing Office).

[2] Henri Bougault (Co-Chief Scientist), IFREMER (formerly CNEXO), Centre de Brest, B. P. 337, 29273 Brest Cedex, France; Steven C. Cande (Co-Chief Scientist), Lamont-Doherty Geological Observatory, Columbia University, Palisades, New York; Joyce Brannon, Department of Earth and Planetary Sciences, Washington University, St. Louis, Missouri; David M. Christie, Hawaii Institute of Geophysics, University of Hawaii at Manoa, Honolulu, Hawaii; Murlene Clark, Department of Geology, Florida State University, Tallahassee, Florida; Doris M. Curtis, Curtis and Echols, Geological Consultants, Houston, Texas; Natalie Drake, Department of Geology, University of Massachusetts, Amherst, Massachusetts; Dorothy Echols, Department of Earth and Planetary Sciences, Washington University, St. Louis, Missouri (present address: Curtis and Echols, Geological Consultants, 300 Anderson, Houston, Texas 77401); Ian Ashley Hill, Department of Geology, University of Leicester, Leicester LE1 7RH, United Kingdom; M. Javed Khan, Lamont-Doherty Geological Observatory, Columbia University, Palisades, New York (present address: Department of Geology, Peshawar University, Peshawar, Pakistan); William Mills, Deep Sea Drilling Project, Scripps Institution of Oceanography, La Jolla, California (present address: Ocean Drilling Program, Texas A&M University, College Station, Texas 77843); Rolf Neuser, Institut für Geologie, Ruhr Universität Bochum, 4630 Bochum 1, Federal Republic of Germany; Marion Rideout, Graduate School of Oceanography, University of Rhode Island, Kingston, Rhode Island (present address: Department of Geology, Rice University, P.O. Box 1892, Houston, Texas 77251); and Barry L. Weaver, Department of Geology, University of Leicester, Leicester, LE1 7RH, United Kingdom (present address: School of Geology and Geophysics, University of Oklahoma, Norman, Oklahoma 73019).

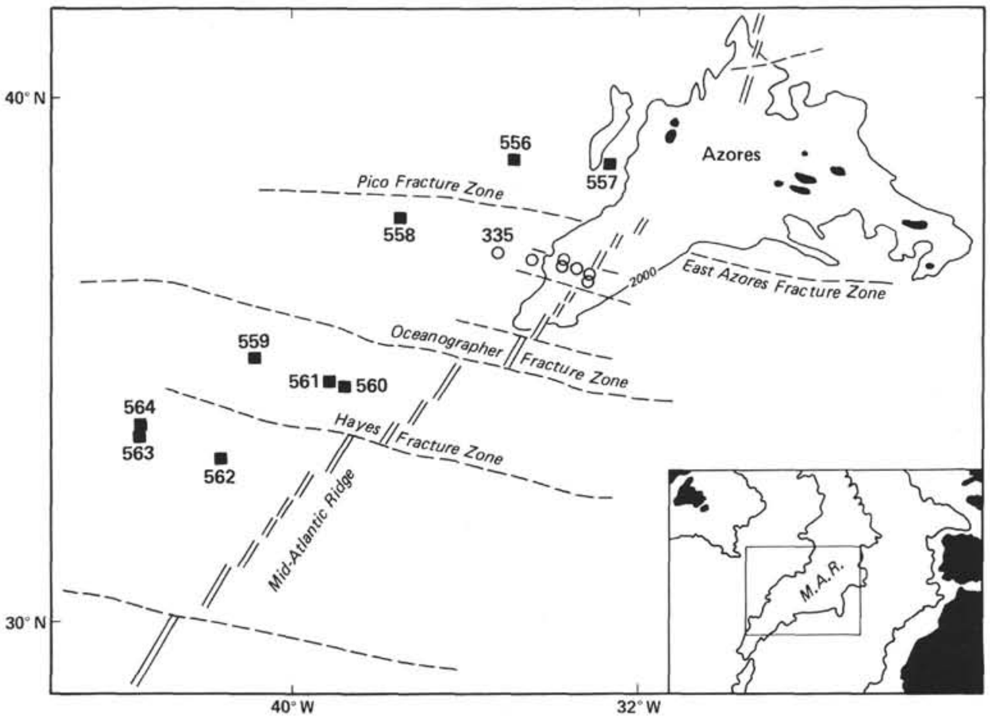

Figure 1. Site location map, Leg 82. M.A.R. = Mid-Atlantic Ridge.

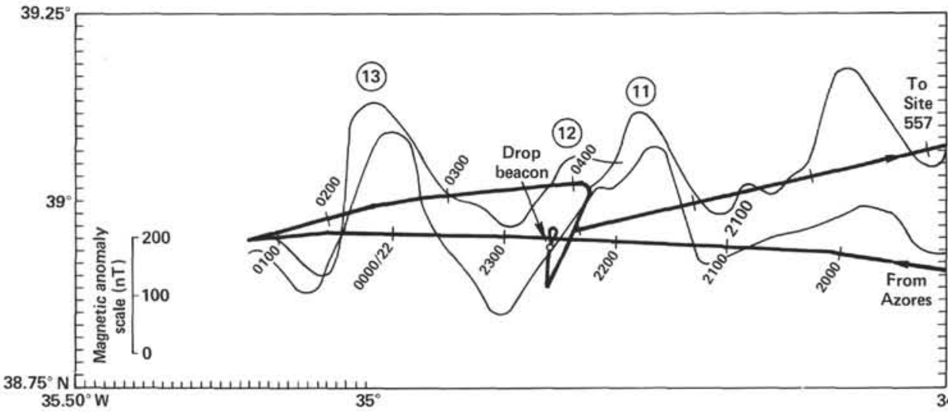

Figure 2. Approach and site survey tracks for Site 556. Heavy line is the ship's track with hour marks in GMT. Faint line is magnetic anomaly line projected perpendicularly from the ship's track. Circled numbers are magnetic anomalies based on work at Lamont-Doherty Geological Observatory. Beacon position is 38°56.38′N, 34°41.12′W.

struction, we would also make heat flow measurements. A logging option was included in the program in the event of basement penetration exceeding 100 m.

The mudline core was recovered at 1805 hr. on 22 September, establishing the correct depth at 3690 m below the drill floor. Sediments were washed down to a depth of 97.5 m below mudline, where the first heat-flow station was taken. Additional temperature measurements were made at 145.0 and 192.5 m below the mudline. Wash cores were recovered at each of these stations. Basement was felt at 461.5 m (below mudline), and a wash core containing the first basaltic pieces was recovered at 1930 hr., 23 September. We then continuously cored basalts, breccias, gabbros, and gabbro breccias down to 639 m below mudline, for a total basement penetration of 177.5 m. The bit failed during the drilling of Core 22. The last core was recovered at 1925 hr. on 27 September. In the upper part of the hole (basalt and basalt breccia), the average recovery was fairly good (65%), but it decreased in the lower part (gabbro, serpentinized gabbro breccia) to approximately 20%. The good basement penetration was probably the result of several factors, including the good condition of the drilling equipment, the good weather, and the consolidation of the basement rocks. Table 1 contains the coring summary for Site 556.

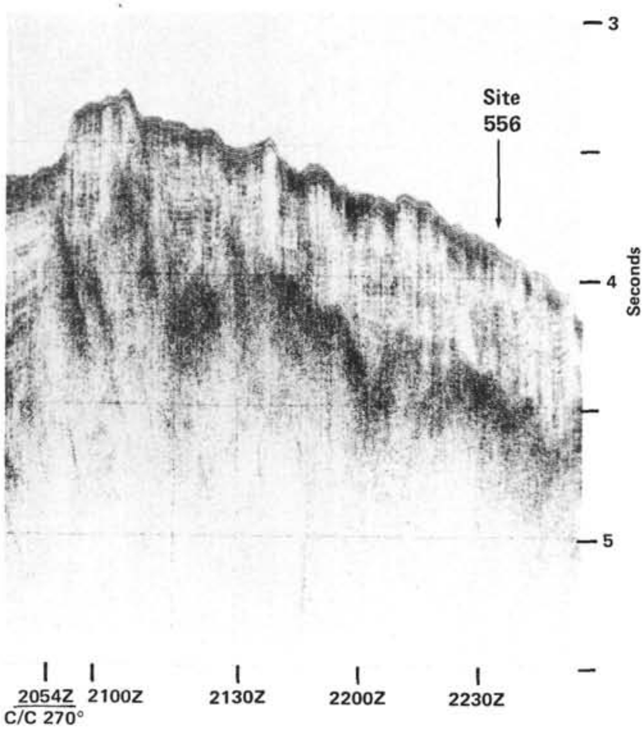

Figure 3. *Glomar Challenger* seismic profile approaching Site 556. See Figure 2 for location of profile. C/C = course change.

A suite of logs was run on 28 September:

Tools	Time at the bottom of the hole (hr.)
The sonic, caliper, and natural gamma ray	0200
Dual laterolog, S.P., and natural gamma ray	0900
Formation density and neutron porosity, caliper and natural gamma ray	1500
Temperature log	2130

The first three logs were run the total depth of the hole; the temperature log could only be lowered to 20 m below the sediment/basement interface because of blockage at that level.

SEDIMENTOLOGY

A single bit hole was drilled at Site 556; 639 m were penetrated, including 461 m of sediment (lower Pleistocene to upper lower Oligocene) above the first major basalt unit. Of these sediments, a mudline punch core, four wash cores, and a single rotary core at the base of the sedimentary section (see coring summary) were taken. These recovered sediments were divided into two major units (see Table 2) based on lithology and depositional style. These are Unit 1, calcareous biogenic ooze and chalk, and Unit 2, limestone basalt breccia. We have also included in this section a description of interpillow sediments and Unit 7, a basalt breccia, and a discussion of its probable tectonic origin.

Table 1. Coring summary, Hole 556.

Core	Date (Sept. 1981)	Time (Z)	Depth from drill floor (m)	Depth below seafloor (m)	Length cored (m)	Length recovered (m)	Percent recovered
1	22	1805	3690.0–3696.5	0.0–6.5	6.5	6.09	94
H1	22	2128	3696.5–3787.5	6.5–97.5	0.0	0.00	0
H2	23	0135	3787.5–3835.0	97.5–145.0	0.0	0.00	0
H3	23	0600	3835.0–3882.5	145.0–192.5	0.0	0.00	0
H4	23	1930	3882.5–4151.5	192.5–461.5	0.0	0.00	0
2	24	0148	4151.5–4161.0	461.5–471.0	9.5	6.24	66
3	24	0810	4161.0–4170.0	471.0–480.0	9.0	2.91	32
4	24	1250	4170.0–4179.0	480.0–489.0	9.0	8.40	93
5	24	2022	4179.0–4188.0	489.0–498.0	9.0	7.06	78
6	25	0203	4188.0–4197.0	498.0–507.0	9.0	7.23	80
7	25	0638	4197.0–4206.0	507.0–516.0	9.0	4.22	47
8	25	1134	4206.0–4215.0	516.0–525.0	9.0	5.17	57
9	25	1632	4215.0–4224.0	525.0–534.0	9.0	5.83	65
10	25	2117	4224.0–4233.0	534.0–543.0	9.0	5.80	64
11	26	0051	4233.0–4242.0	543.0–552.0	9.0	2.65	29
12	26	0507	4242.0–4251.0	552.0–561.0	9.0	4.45	49
13	26	0900	4251.0–4255.5	561.0–565.5	4.5	0.77	17
14	26	1227	4255.5–4264.5	565.5–574.5	9.0	3.01	33
15	26	1731	4264.5–4273.5	574.5–583.5	9.0	4.03	45
16	26	2255	4273.5–4282.5	583.5–592.5	9.0	2.40	27
17	27	0217	4282.5–4291.5	592.5–601.5	9.0	2.06	23
18	27	0514	4291.5–4300.5	601.5–610.5	9.0	1.30	14
19	27	0713	4300.5–4309.5	610.5–619.5	9.0	1.28	14
20	27	1056	4309.5–4318.5	619.5–628.5	9.0	1.74	19
21	27	1450	4318.5–4327.5	628.5–637.5	9.0	1.98	22
22	27	1925	4327.5–4329.0	637.5–639.0	1.5	0.59	39
					184.0	85.21	46

Unit 1

One-half meter (556-H4-4, 90–143 cm) of pinkish white (5Y 8/2) nannofossil chalk (upper Oligocene to lower Miocene) overlies Unit 2. Although the chalk of this unit is similar to the matrix and limestone clasts of Unit 2, it contains no clasts of basalt or of reworked limestone and has no apparent transport structures. The sediment components are nannofossils (93–95%), foraminifers (1–3%) and traces of quartz, feldspar, heavy minerals, volcanic glass, palagonite, and sponge spicules. No distinct bioturbation or bedding is observed.

In the remaining upper portion of Core 556-H4, the lithology is a white (2.5YN8-5Y 8/1), firm nannofossil ooze with interbedded Miocene chalk. The color change with the underlying sediment is sharp. The sediment components are nannofossils (95%) and unspecified carbonate (5%). No distinct bioturbation is observed, but rare, faint black streaks were observed. Bedding is indistinct.

Starting at the bottom of Section 556-1 up to 556-1-4, 105 cm the lithology is a light yellowish brown (10YR 6/4), firm foraminiferal-nannofossil to nannofossil ooze dated early Pleistocene and older(?). The sediment components include nannofossils (85–90%), foraminifers (5–15%), and traces of clay, volcanic glass, and palagonite. No distinct bedding, bioturbation, or black streaks were observed.

In the remaining upper portion of Core 556-1, the lithology is a light gray (2.5RN7), soft to firm nannofossil to foraminiferal-nannofossil ooze (lower Pleistocene). The contact with the underlying sediment is sharp. The sediment components include nannofossils (82–95%), foraminifers (3–14%), and traces of clay minerals, feldspar, volcanic glass, palagonite, pyrite, diatoms, radiolarians, sponge spicules, and silicoflagellates. Interbedded are layers of greenish gray (5GY 6/1) firm siliceous

Table 2. Sediment lithology summary, Hole 556.

Interval	Unit designation	Depth and thickness (m)	Main colors	Main lithology	Main components	Structure	Age
556-1-1, 0 cm washed to 556-H4-2, 143 cm	1	0–461.0 (461.0)	White, light gray, light yellowish brown, and pinkish white	Nannofossil ooze, foraminiferal-nannofossil ooze, nannofossil chalk	Nannofossil, foraminifers, and siliceous fossils	Homogeneous with slight mottling	early Pleistocene to middle Miocene
556-H4-2, 143 cm to 556-3-1, 5 cm	2	461.0–471.1 (10 m)	Pinkish white to gray matrix with pinkish gray to gray clasts	Limestone basalt breccia	Volcaniclasts, limestone clasts, limestone matrix	Crudely graded	late Oligocene

nannofossil ooze. There appears to be a direct relationship between the color changes and the higher percentage of siliceous microfossils in these greenish gray layers. The sediment components of these layers are: nannofossils (80%), foraminifers (3–5%), diatoms (10%), radiolarians (3–5%), sponge spicules (2%), and traces of silicoflagellates, feldspar, volcanic glass, palagonite, and pyrite. No distinct bedding or bioturbation was present, although rare, faint black streaks (pyrite?) and mottling were observed.

Unit 2

This unit consists of approximately 10 m (Core 556-H4-2, 143–150 cm; all of Core 556-2 and 556-3-1, 0–5 cm) of a limestone basalt breccia (uppermost lower Oligocene) (see Fig. 4). The basalt clasts (moderately plagioclase phyric) range in size from boulders to silt-size particles, with sand and finer particles considered as part of the matrix. The basalt clasts are poorly sorted, although three crudely fining-upward sequences can be recognized: (1) from Core 556-H4-2, 143 cm to 556-2-2, 150 cm; (2) 556-2-3, 0 cm to 556-2-5, 30 cm, and (3) 556-2-5, 32 cm to 556-3-1, 5 cm. The basalt clasts are subrounded to angular, gray (7.5YR N5) to pinkish gray (7.5YR N6/2) in color, fresh and altered respectively. Also included with the basalts are angular clasts of grayish green (5G 4/2) to dark brown (7.5YR 3/2) volcanic glass.

The limestone clasts are subrounded, 5 mm to 5+ cm in diameter and are occasionally attached to basalt to form a composite clast. The limestone clasts are similar in color to the calcareous matrix, pinkish white (5YR 8/2) to light gray (10YR 7/1), but are easily distinguished from the matrix in both thin section and hand specimen. In thin section, the limestone clasts are microcrystalline (biomicrite), similar to the chalks of Subunit 1d, but much more indurated.

The matrix is also a microcrystalline (biomicrite) limestone that contains minor amounts of volcanic material similar to the basalt clasts. In hand specimen, the matrix often appears to have flowed around clasts and to infill cracks in the basalt clasts assumed to have formed during deposition. The matrix also appears as light-colored halos around some of the basalt clasts. Thin-section examination showed that this halo effect is the result of the finer crystal size of the microcrystalline matrix adjacent to the basalt clasts. Also in thin section we observed discontinuous recrystallization, as irregular patches of both matrix and limestone clasts, to sparry calcite. Often these veins are rimmed by dendritic manganese oxide (see Fig. 5). In parts of this unit, both matrix and limestone clasts were completely recrystallized to sparry calcite by fluids subsequent to deposition, which left occasional solution vugs lines with yellow-stained, "dog tooth" calcite.

Intrapillow Sediments

In the basalt of Core 556-5, pinkish white (5YR 8/2) micritic limestone occurs between flow margins. In Core 556-4, pale yellow (5Y 7/3) chalk with small rounded (1 to 5 mm) intraclasts have infilled cracks in basalts. These infilling sediments show well-preserved geopetal structures (see Fig. 6).

Unit 7

This unit consists of 28.8 m (556-9-3, 30 cm to 556-12-4, 63 cm) of predominantly basalt breccia. The basalts are mostly very angular to occasionally subrounded and range in size from boulder to clay, with the sand-size and finer fraction considered as matrix. From 556-9-3 cm to 556-12-1, 135 cm, the clasts are all uniformly medium gray (5Y 5/1), aphyric to moderately plagioclase phyric basalt (see Fig. 7). The matrix, except for minor amounts of microcrystalline calcite, is predominantly basalt-derived, clay-size to sand-size particles clearly derived from the adjacent basalt clasts. X-ray diffraction (XRD) analysis shows that no clay minerals are present in the matrix in this section of the breccia, and thin-section examination shows no obvious alteration of clasts or matrix.

Beginning in 556-12-1, 135 cm, the compositions of both clasts and matrix change to include more basaltic glass rims, light brownish gray (10YR 6/1) to reddish brown (2.5YR 4/4) altered basalt and rare, pale red (10R 6/3) chalk clasts (see Fig. 8). The matrix also reflects this change in the clasts composition by mimicking, as a finer-grain equivalent, the neighboring clasts.

The boundary between Units 7 and 8 occurs in the bottom of Section 556-12-4 and is recognized as a transitional change from basaltic clasts to gabbroic clasts.

Discussion

The basalt breccias observed at Site 556 are quite dissimilar in character and origin. The first one, cored im-

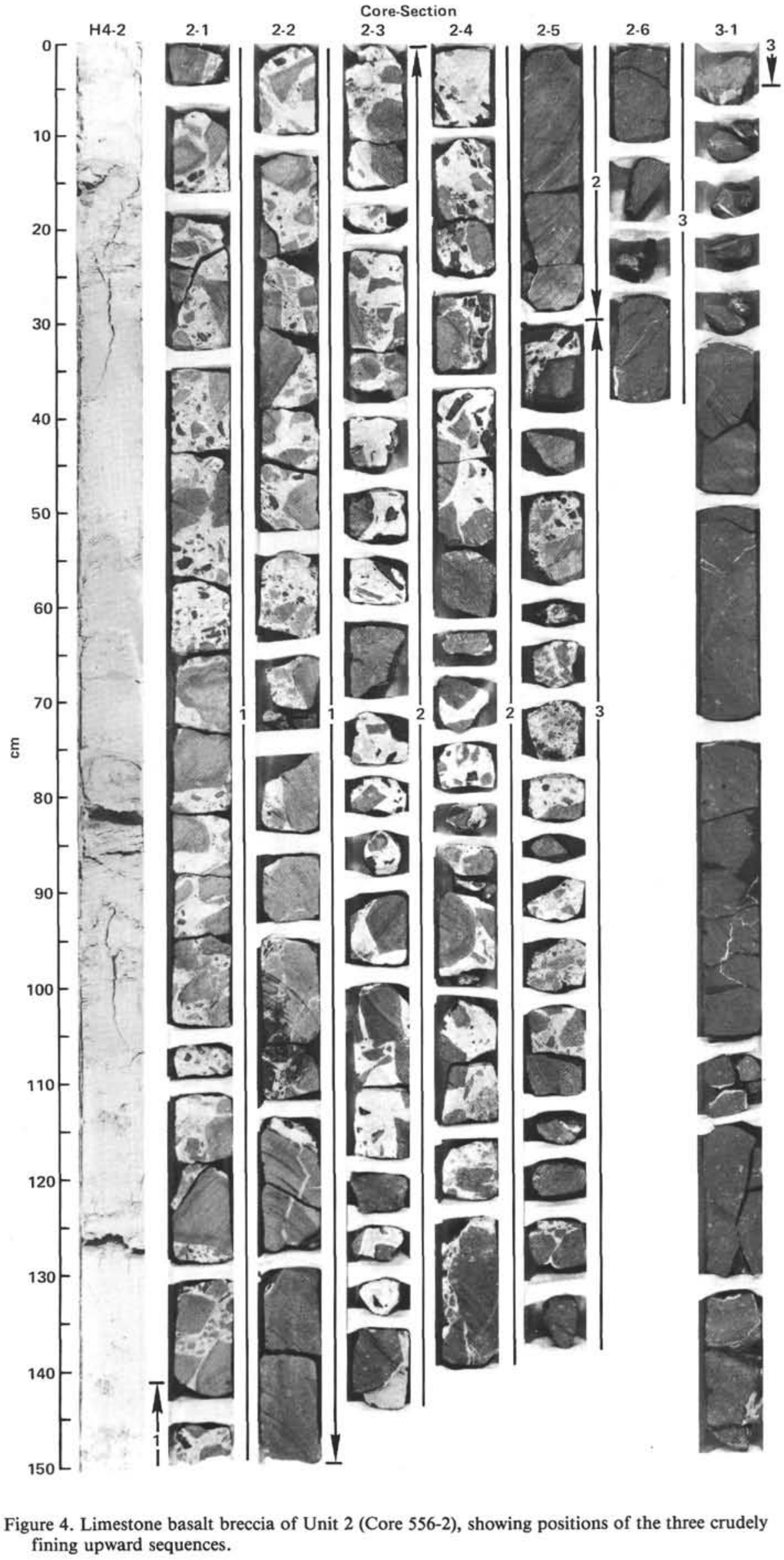

Figure 4. Limestone basalt breccia of Unit 2 (Core 556-2), showing positions of the three crudely fining upward sequences.

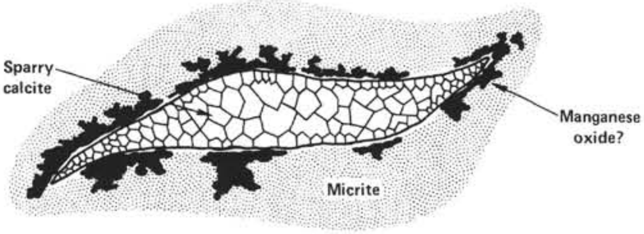

Figure 5. Sketch of sparite patches in limestone, rimmed by dendritic manganese oxide(?).

mediately below the nannofossil oozes and chalks of Unit 1, is a limestone basalt breccia, designated as Unit 2. The second breccia, cored between a basalt flow and a gabbroic or polymict breccia, is a basalt breccia, designated as Unit 7. Table 3 is a summary of the contrasting characteristics of each breccia.

On the basis of the comparison listed in Table 3, we believe that Unit 7 (basalt breccia) did not originate as a slump or debris flow as in the case of Unit 2 (limestone basalt breccia), nor do we believe that Unit 7 is an autoclastic breccia as described from DSDP Sites 407, 408, and 410 (Luyendyk, Cann, et al., 1979) and discussed by Varet and Demange (1978).

With only preliminary data it is impossible to give a specific origin for Unit 7, but we do believe that it is related to local tectonics and to the emplacement of the serpentinized gabbros of Units 8 and 10.

BIOSTRATIGRAPHY

One rotary core and four wash cores were obtained at Site 556. Zonation of wash core catchers was attempted to permit tentative correlation between age and depth at several points. Sediments ranged in age from early Pleistocene ($\pm$1.6 to 1.8 Ma) to late early Oligocene (30 to 34 Ma). In both fossil groups, preservation is moderate to good, and assemblages are characteristic of temperate to warm-temperate regions. Figure 7 in the Explanatory Notes chapter (this volume), shows the zonations for nannofossils and foraminifers as well as the magnetostratigraphy correlation used for all site chapters, the numerical time scale, and the European stages.

Nannofossils

Core 556-1 is early Pleistocene in age based on the presence of *Calcidiscus macintyrei* and *Helicopontosphaera sellii* above the last appearance datum (LAD) of *Discoaster brouweri*. Core 556-1 is placed in the *C. macintyrei* Zone (bottom of NN19) (Gartner, 1977). The presence of *Gephyrocapsa caribbeanica* in the top of Core 556-1 indicates that a younger age for the upper sediment is possible if reworking of *C. macintyrei* has occurred.

The Pliocene/Pleistocene boundary is located between 556-1,CC and 556-H1-1, 70 cm. An abundance of *D. brouweri* and *C. macintyrei* is contained in 556-H1-1, 70 cm; it is late Pliocene in age, NN18 or CN12D (Okada and Bukry, 1980). The core catcher of 556-H1 contains *Reticulofenestra pseudoumbilica, Discoaster tamalis, D. brouweri, D. asymmetricus*, and *C. macintyrei*. Because *R. pseudoumbilica* is rare, 556-H1,CC is placed within either the *D. asymmetricus* Subzone 11b (Okada and Bukry, 1980) (upper NN15) or the *D. tamalis* Subzone 12a (Okada and Bukry, 1980) (lower NN16).

The core catcher of Core 556-H2 is assigned to the *Discoaster neohamatus* Zone CN8–NN10, upper Miocene, because of an abundance of *D. neohamatus* in an assemblage composed of *Triquetrorhabdulus rugosus, Discoaster variabilis, D. pentaradiatus*, and possibly a

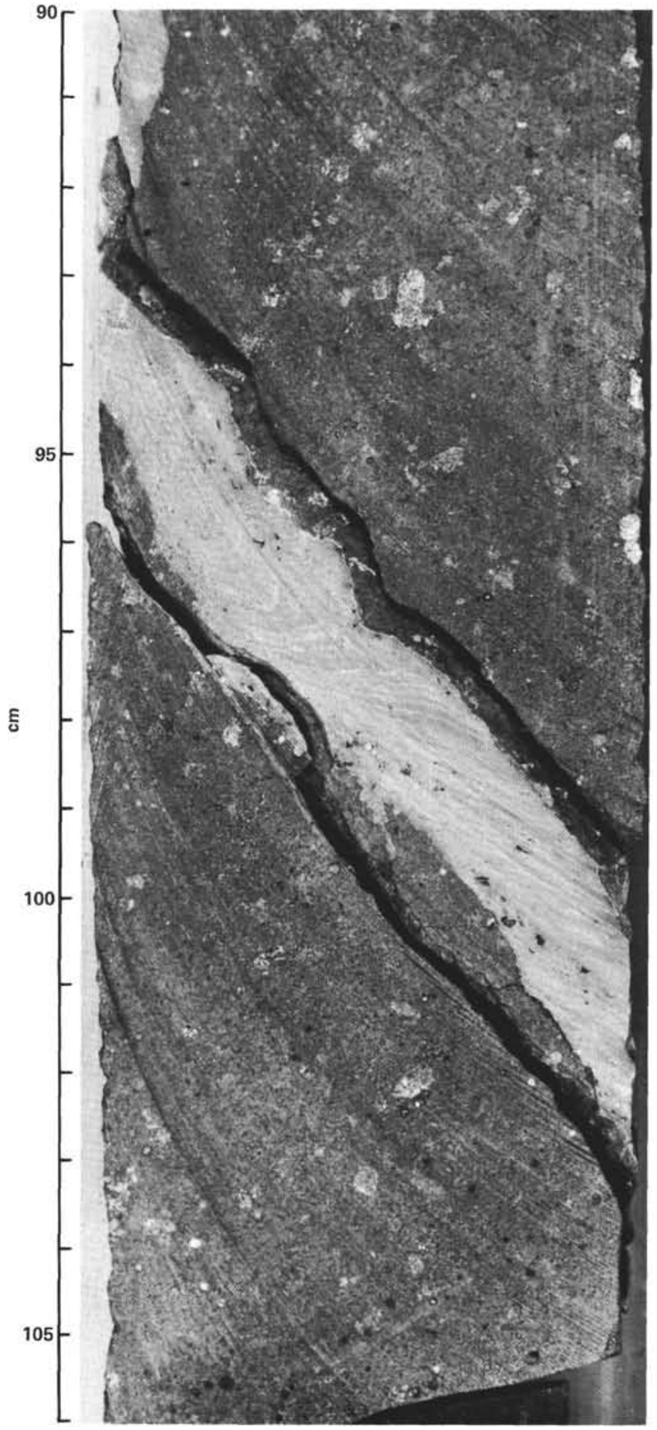

Figure 6. 556-4-1, 90–106 cm; nannofossil chalk infilling cracks in basalt flow. Note the geopetal structures.

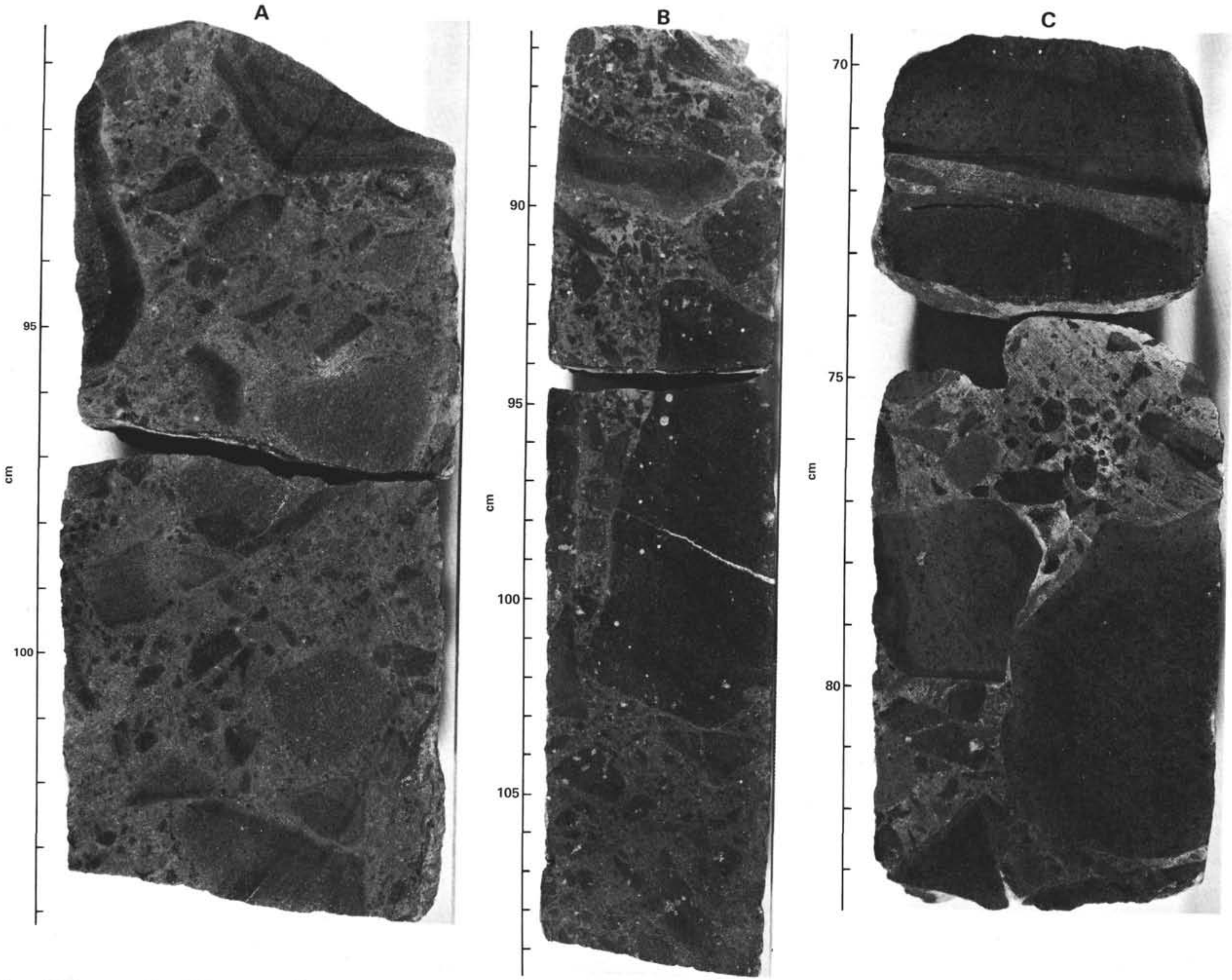

Figure 7. Three examples of the upper position of the basalt breccia (Unit 7). A, 556-9-3, 91–103 cm; B, 556-10-2, 86–110 cm; C, 556-10-4, 70–83 cm. In Figure 7C, note the replacement of original matrix by calcite (lighter-colored area between 74 and 78 cm) and the formation of vugs by fluids subsequent to the breccia's development.

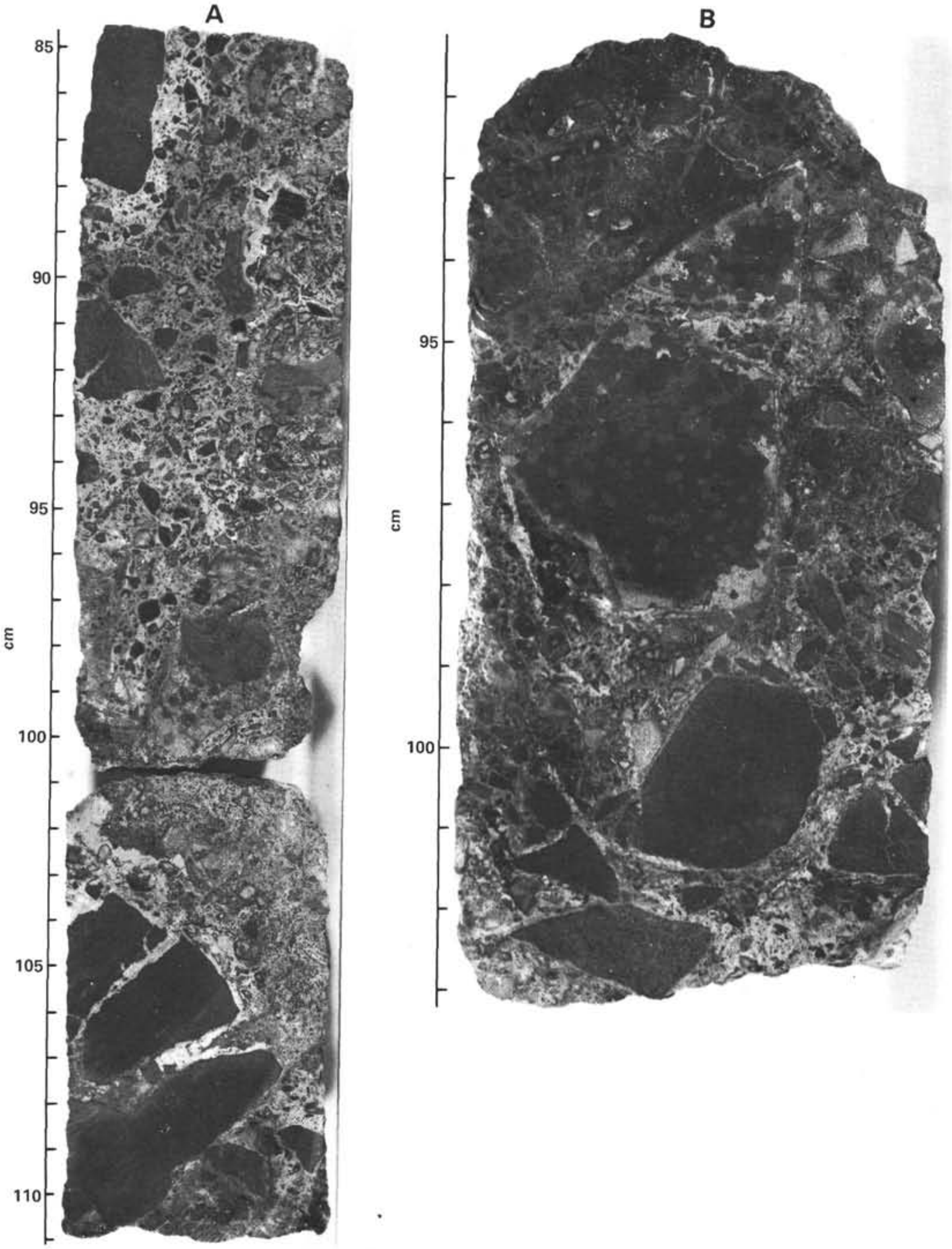

Figure 8. Two examples of the lower position of the basalt breccia (Unit 7). A, 556-12-2, 85–111; B, 556-12-2, 91–103 cm. Compare to Figure 7 and notice the change in both clasts and matrix.

few *D. berggrenii*. The tentative presence of *D. berggrenii* may extend the zonation into CN9a (lower NN11).

The rare occurrence *hamatus* in 556-H3,CC indicates the upper middle Miocene or lower upper Miocene *D. hamatus* Zone CN7–NN9.

Two samples taken within 556-H4, 556-H4-2, 72 cm and 556-H4-2, 92 cm contain *D. exilis*. The deeper sample also contains *Sphenolithus heteromorphus*. The upper sample falls into the *D. exilis* Zone CN5 (NN6–7) and the lower one is within the *S. heteromorphus* Zone CN4 (NN5). Both samples are middle Miocene.

The base of the sediment column, 556-H4,CC, contains *S. ciperoensis, S. distentus*, and *S. predistentus*. The presence of these species indicates an age of 30–24 Ma (late Oligocene) (NP23–24) (CP18/19). Core 556-3, which is composed primarily of basalt, contains a pocket of nannofossil chalk at the top of the section that can be assigned to the *S. predistentus* Zone CP17 (N23), dat-

Table 3. Comparison between basalt breccias of Unit 2 and Unit 7 of Site 556.

Unit 2: limestone basalt breccia	Unit 7: basalt breccia
Clasts	
Predominantly basalt, with minor limestone and volcanic glass; glass appears to be randomly distributed throughout the unit.	Almost entirely basalt, with rare limestone; glass in lower part (556-12, 4 cm).
Clast subrounded to angular.	Clasts mostly angular to subangular; some subrounded.
Altered basalt common, but mixture of altered and fresh basalt occurs throughout the unit; both fresh and altered glass present.	Altered basalt is common in the lower part of the unit, associated with altered glass rinds, pillows, and sedimentary clasts; fresh basalt predominates above 556-12-4.
Clasts range from boulders to silt and clay size. Particles smaller than sand size are considered part of the matrix. The boulders to sand-size clasts occur in crudely graded sequences with boulders at the base of each fining-upward sequence. Part of the nannofossil chalk overlying the breccia (Subunit 1d) could be the youngest fining-upward sequence.	Clasts range from boulders to clay size. Silt-size and clay-size fragments make up the matrix. The boulders to sand-size clasts show no apparent grading; size of clasts and clast: matrix ratio appears to increase downward from Section 556-9-3 through Core 556-11.
Matrix	
Matrix predominantly microcrystalline limestone of biogenic origin; silt-size and clay-size particles of basalt-derived material are a very minor constituent.	Matrix predominantly basalt-derived clay-size lithic and mineral fragments; no biogenic limestone except in rare clasts, as in 556-12-4.
Calcite also occurs in vugs and as veins and fracture fillings; microcrystalline calcite commonly forms light-colored rims around the basalt clasts.	Calcite is a very minor constituent of the matrix, probably secondary; calcite also occurs in veins and veinlets.
Matrix has flow lines.	Matrix does not have flow lines.
XRD analysis shows small amount of clay.	XRD analysis shows no clay.

Note: XRD = X-ray diffraction.

ed 30–34 Ma (latest early Oligocene). This date matches the proposed basement age for Anomaly 12.

Foraminifers

Core 556-1 recovered a Pleistocene nannofossil–foraminiferal ooze. The core catcher sediments examined for foraminifers contain an assemblage of lower Pleistocene planktonic and benthic species, which characterize Zone N22. This correlates, in the present study, with nannofossil Zones CN13–NN19.

The planktonic fauna is made up of abundant *Globorotalia truncatulinoides, G. menardii* s.l. complex, *G. inflata, G. scitula; Globigerina bulloides, G. aequilateralis, G. falconensis, G. calida* and *G. rubescens; Globigerinoides conglobatus, G. ruber*, and *G. sacculifer; Orbulina universa; Pulleniatina obliquiloculata;* and *Sphaeroidinella dehiscens*. The assemblage is dominated by species characteristic of temperate to warm-temperate regions.

The benthics are not common but are represented by a fairly diverse group of deep-water forms. Ostracodes, diatoms, silicoflagellates, and radiolarians are also present.

The core catcher of Core 556-H1 contains a lower Pliocene planktonic foraminiferal fauna and is assigned to the upper part of foraminiferal Zone N19 *(Globoratalia margaritae)* within the PL2, *G. margaritae–G. prehirsuta* in the subdivision of the Pliocene (Fig. 9). This assignment is based on abundant *G. margaritae* and the absence of *Globigerina nepenthes*, which was extinct by 3.7 Ma. Well-preserved ostracodes and a few benthic foraminifers are present.

Preservation in general is good but with some indication of crystalline overgrowth on the globorotalid forms. The fauna is considered characteristic of temperate to warm-temperate regions.

The core catcher of Core 556-H2 is a white chalky nannofossil marl that contains Miocene planktonic and benthic foraminifers. In this sample there is a high benthic-to-planktonic ratio, and the thin-walled planktonic forms show dissolution. *G. nepenthes, S. subdehiscens*, and *S. seminulina* and the accompanying fauna indicate an upper Miocene assignment.

The core catcher of Core 556-H3 is a nannofossil ooze with common to abundant planktonic and few benthic foraminifers. The sediment is lower upper Miocene, foraminiferal Zone N14 *(G. nepenthes–Globorotalia siakensis)*. This agrees well with the nannofossil determination (CN7–NN9).

On the basis of the planktonic foraminifers, the core catcher of Core 556-H4 is upper Oligocene and falls in the upper portion of foraminiferal Zone P21 *(Globorotalia opima opima)*. The planktonic foraminifers are common, and preservation is moderate to good.

IGNEOUS PETROLOGY AND GEOCHEMISTRY

Basalt occurs as clasts in breccias, as pillowed flows, and as massive flows throughout the basement section. Gabbro, in both fresh and serpentinized forms, occurs as clasts in breccia. We have recognized ten lithologic units (Table 4) and five chemical groups. Lithologic units are indicated by Arabic numbers (1, 2, 3...) and petrographic or chemical groups by Roman numerals (I, II, III...) throughout this volume.

Lithologic Units

Unit 2. Basalt-Carbonate Breccia (462–469.5 m)

The breccia of Unit 2 is composed of angular basalt clasts set in a matrix of biogenic limestone (as described in the Sedimentary and Biostratigraphy section). Clasts range downwards in size from a maximum of about 10

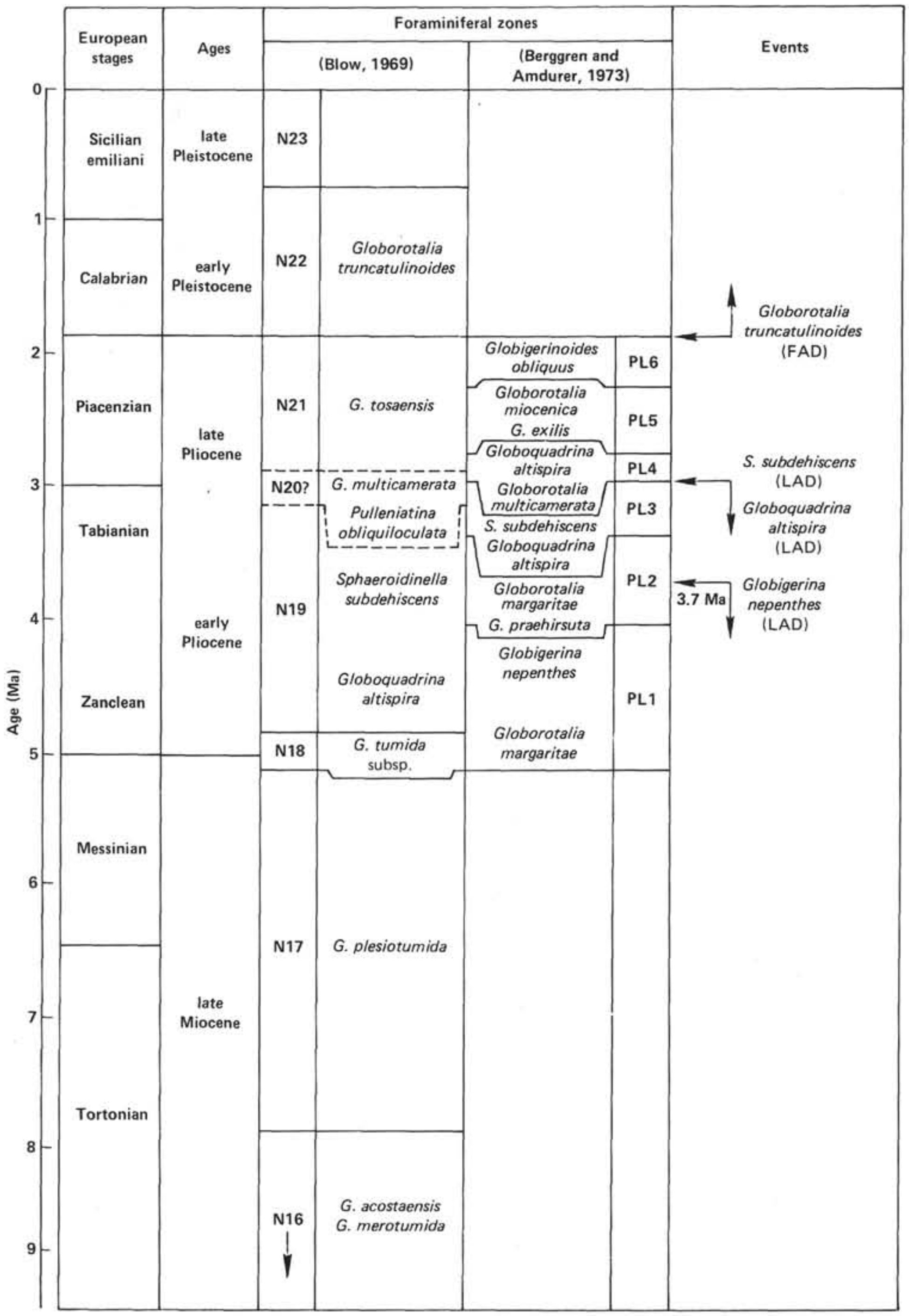

Figure 9. Foraminiferal biostratigraphic zonation, Site 556. FAD = first appearance datum; LAD = last appearance datum.

cm to a few millimeters or less. Glass rims and isolated glass fragments are occasionally present. A majority of clasts have light brown weathered rims, up to 2 cm thick, and relatively fresh cores. Within the breccia, there is a downward transition from aphyric basalt (Petrographic Group I) to moderately plagioclase phyric basalt (Petrographic Group II); the latter is chemically identical with that of the underlying unit.

Unit 3. Upper Pillow Basalts (469.5–505 m)

Basalts of Unit 3 are plagioclase phyric, ranging from 2–5% phenocrysts with occasional patches of higher or lower concentration. Within this section of the core, 30 recognized pillows or flow lobes are separated by narrow bands of glass. This glass, generally only 2 to 3 cm thick, is moderately palagonitized and may be veined

Table 4. Site 556 lithologic units and petrographic and chemical groups.

Sub-bottom depth (m)	Lithologic unit	Lithology	Petrographic and chemical groups
461.0	1	Nannofossil ooze	
465.0	2	Basalt carbonate breccia	I
469.5			
	3	Upper pillow basalts	II
505.0			
	4	Massive aphyric basalts	
512.0			
	5	Small pillow basalts and pillow breccia	III
526.5			
	6	Massive aphyric basalt	
528.5			
543.0	7	Basalt breccia	
546.0			IV
561.0			III
	8	Gabbro breccia (serpentinized)	V
586.0			
	9	Aphyric basalt	IV
587.0			
	10	Talc serpentinized gabbro breccia	V
693.0			

Note: Sub-bottom depth column not to scale.

with calcite, or have glassy rinds separated by calcite veins. Pillow thicknesses range from 30 to 170 cm and average 73.5 cm; a basalt(?) flow 300 cm thick is also present. No interpillow sedimentary material was recovered; calcite cement filling in fractures, however, is common in the upper third of the unit and rare in the lower part of the unit.

The unit is chemically and petrographically homogeneous. The plagioclase phyric clasts of the overlying breccia and Unit 3 compose Petrographic Group II.

Unit 4. Massive Aphyric Basalt (505–512 m)

This unit appears to be composed of two massive flows, separated at 507.2 m by a narrow glass band with associated calcite veining and palagonitization. Calcite-filled fractures are also common near the upper and lower boundaries of the unit. The basalt is fine-grained and light gray in color, with approximately 1% plagioclase phenocrysts in the upper 1.5 m and scattered equant plagioclase phenocrysts in the remainder of the unit. The basalts of Unit 4 belong to the Petrographic Group III.

Unit 5. Pillow Basalts and Pillow Breccia (512–526.5 m)

Unit 5 consists of approximately 4 m of small basalt pillows grading down the core into pillow breccia. Pillow diameters appear to be a few tens of centimeters. Glass margins are strongly palagonitized, although fresh glass is still present in very small quantities. Interpillow spaces are filled by angular glass fragments and calcite cement. Pillow centers are aphyric basalt identical to that of the overlying massive Unit 4. Well-formed pillows give way downwards to pillow breccia, composed of angular basalt and glass fragments in a matrix of smaller glass fragments and calcite cement. The basalts of this unit are classified as Petrographic Group III.

Unit 6. Massive Aphyric Basalt (526.5–528.5 m)

This unit is a single flow of strongly fractured and weathered aphyric fine-grained basalt, similar to that of Unit 4 and also classified as Petrographic Group III.

Unit 7. Basalt Breccia (528.5–561 m)

This breccia is texturally very similar to that of Unit 2, yet significantly different in its matrix composition. Matrix material is gray green in color and appears to be composed of a mixture of carbonate and finely comminuted basaltic material (per description of matrix in the Sedimentology and Biostratigraphy sections). Basalt clasts are predominantly aphyric with scattered plagioclase phenocrysts; occasionally, phenocrysts range up to 5% of the basalt content. The olivene occurs as microphenocrysts (1 mm in diameter) and composes up to 5% of the basalt content. Petrographic and chemical studies demonstrate that clasts of both Petrographic Groups III and IV occur throughout most of this unit.

Unit 8. Serpentinized Gabbro Breccia (561–586 m)

This unit consists of a largely serpentinized gabbro breccia, the matrix of which appears to be composed of finely comminuted serpentinized material. Clast size varies from a few millimeters to about half a meter in diameter. Serpentinization is virtually complete in the upper half of the unit, but some fresh gabbro clasts are present further down the core.

Serpentinized gabbro clasts are composed of up to 15% brown, prismatic, altered orthopyroxene phenocrysts up to 10 mm long. These phenocrysts are set in a dark green black foliated matrix, composed almost entirely of serpentine. The dominant serpentine mineral is antigorite as determined by XRD.

Fresh gabbro clasts are coarse grained (3–10 mm in diameter), equigranular, dark gray to black aggregates of (in order of decreasing abundance) plagioclase, orthopyroxene, clinopyroxene, and minor olivine. The clasts show varied stages of alteration, ranging from completely fresh to completely altered.

Also present as smaller (1–2 cm in diameter) clasts within this unit are pieces of anorthosite (plagioclase-clinopyroxene–composed rock), some of which appear to have formed as small veins within the gabbro. Occasionally, prismatic clinopyroxene crystals up to 1 cm long are also present in the breccia. This unit (along with Unit 10) is classified as Petrographic Group V.

Unit 9. Aphyric Basalt (586–587 m)

This light gray, aphyric basalt occupies slightly less than 1 m of core separating two units of gabbro breccia. It is not clear whether this is an unusually large clast or a flow of a narrow intrusive body. However, the presence of small, petrographically and/or chemically identical clasts (Petrographic Group IV) within Unit 7 may suggest that this is simply a large clast.

Unit 10. Talc-Serpentinized Gabbro Breccia (587–639 m)

This lowermost unit of Hole 556 differs from Unit 8 only by the presence of blue green talc as an alteration mineral in addition to serpentine. No fresh gabbro was recovered in this interval. Petrographic Group V comprises the gabbroic breccia units (8 and 10).

Petrographic Groups

The samples recovered at Site 556 have been classified into five groups, based upon macroscopic and microscopic descriptions and chemical analyses (see Fig. 10 and Table 5).

Group I

This group coincides with the upper part of Lithologic Unit 2, consisting of basalt carbonate breccia. The aphyric basaltic clasts are reasonably fresh, although weathering occurs around the rims and along fractures. Rare equant plagioclase phenocrysts (3-5 mm) are present in a dominantly intergranular groundmass. Group I basalt clasts have a distinctive groundmass: lath-shaped to acicular-shaped plagioclase that comprises 30-35% of the groundmass ranges in size from 0.6 to 0.1 mm in length; clinopyroxene (about 40%) occurs mostly as fine-grained (0.1 mm) aggregates interstitial to plagioclase with scattered larger (0.5 mm) granules; altered granular olivine (5%, 0.1-0.2 mm), granular magnetite (3%), and up to 15% dark brown mesostasis are distributed throughout the groundmass.

The two samples analyzed (556-2-1, 78-82 cm; 556-2-2, 145-150 cm) are very similar in both major and trace element composition. Noteworthy are the relatively high CaO (~13%) and Al_2O_3 (~16%) concentrations.

Group II

The lower part of Lithologic Unit 2 and all of Unit 3 compose Group II. The recovered samples are fresh to moderately altered. These basalts are moderately to sparsely plagioclase phyric, containing 2-5% equant to prismatic plagioclase phenocrysts, some of which form glomerocrysts. The plagioclase is unzoned or normally zoned. Optically determined compositions cluster around AN_{70}, occasionally ranging to An_{60} at the rims. Some prismatic olivine phenocrysts (2-3 mm), altered to a variable extent to green or brown clay, are also present[3].

The groundmass texture varies from hyalophitic to intergranular and slightly subophitic. This variation corresponds to position within the pillow relative to the cooling margin. In all cases skeletal, swallowtail to narrow lath-shaped plagioclase make up 35 to 40% of the groundmass. Fine granular magnetite is relatively abundant (5%). Interstitial clinopyroxene varies from extremely fine intergranular branches of sheaf aggregates in hyalophitic and intersertal textures to coarser (0.2 mm) granules forming aggregates up to 1 mm in coarser-grained textures. Olivine (about 5%) occurs both as diamond-shaped microphenocrysts (up to 1 mm) and scattered small granules altered to clay. Clay contents, mainly after olivine and mesostasis, vary from 5-10% in the freshest samples to 20-30% in moderately weathered samples.

Sixteen samples were analyzed for trace elements and seven for major elements. The chemical composition of this group is fairly homogeneous. This composition is typical of oceanic tholeiite with TiO_2 concentrations (1.46%) falling in the upper range of values for oceanic tholeiites.

Group III

Lithologic Units 4, 5, 6, and the majority of Unit 7 form Group III. The extent of weathering is quite variable.

Although lithologically, petrographically, and chemically heterogeneous as a basalt type, the petrology and major and trace element characteristics of samples from this group are distinctive from the other identified groups. Most of the basalts composing this group are aphyric, but concentrations of up to 5% of plagioclase phenocrysts may occur, and scattered phenocrysts are common. Within the group, intersertal textures are common with 15-20% altered mesostasis in most samples. Some varieties are more granular and richer in glass. Plagioclase laths frequently radiate from a single nucleus with interstitial granular clinopyroxene. Interstitial plagioclase and relatively large prismatic pyroxene grains are also common. The amount of plagioclase present (about 30%) is always subordinate to clinopyroxene (about 40%). Olivine is only present as microphenocrysts (about 5%) and is completely altered to green brown clays.

The chemical heterogeneity of Group II is reflected by the greater variation of TiO_2 (0.82-1.06%), Al_2O_3 (14.9-17.6%), and CaO (12.5-14.5%) abundances. Al_2O_3 and CaO have been plotted versus TiO_2 in Figure 11; it is clear from this figure that it is difficult to find more than two samples that could define separate subgroups. A notable feature for some samples is the high CaO content (~14%), as noted in Group I, but not necessarily related to high Al_2O_3 content. This high CaO content cannot be accounted for by calcite contamination alone. The average values given in Table 6 are uninformative because of the heterogeneity in this group.

Group IV

This group is represented by two samples, one of which occurs in Unit 7 and the other in Unit 9. They are aphyric basalts characterized by a greater abundance of plagioclase in the groundmass than in the other groups, and by an almost complete lack of olivine. Plagioclase laths frequently radiate from a single nucleus and are surrounded by granular clinopyroxene forming rounded patches of subophitic texture. The patches are separated by irregularly shaped areas of mesostasis, largely altered to green brown clay, and contain up to 5% granular magnetite. The SiO_2 content (~52%) is the highest encountered among the four basaltic groups.

Group V

Gabbros of Site 556 are fairly uniform in grain size (3-5 mm) but variable in mineralogy and in degree of alteration. Primary minerals are plagioclase (An_{60}), clinopyroxene, orthopyroxene, and minor amphibole and

[3] Preliminary shore-based microprobe studies suggest phenocryst core compositions of AN_{87} and rim compositions of An_{70}.

magnetite. Relative proportions of orthopyroxene and clinopyroxene vary widely from orthopyroxene less than 5% (clinopyroxene 35%) to orthopyroxene 20% (clinopyroxene 15%). Clinopyroxene occurs in large (3–7 mm) prismatic grains showing extensive twinning, evolution, and alteration. Orthopyroxene is generally less altered and occurs as slightly smaller prismatic or subhedral grains. Occasional unaltered, pleochroic (dark to light brown) amphibole grains may also be primary. Magnetite(?) is present in trace amounts only. Olivine has not been identified.

Both pyroxenes are altered to masses of green or colorless fibrous amphibole and to chlorite. Plagioclase is altered to prehnite. The degree of alteration varies from almost none to as much as 30–40%.

Serpentinized gabbros generally display very little relict structure. Isolated prismatic grains of pyroxene and rare plagioclase are surrounded by weakly foliated serpentine (antigorite by XRD).

Small (1–2 cm diameter) fragments of anorthosite (80% plagioclase, 20% clinopyroxene), are strongly altered to prehnite; talc(?), amphibole, and chlorite also occur within the breccia. They appear to have formed as small veins within the gabbro.

Geochemistry

At Site 556, 33 samples were analyzed for trace and major elements. The data are presented in Table 5 and plotted in Figure 10 (Zr, Ti, Al_2O_3, CaO, Fe_2O_3, MgO); they contribute to the definition of petrographic groups together with lithology and the description of the samples. Groups I and IV are represented by only two samples each. Group I samples are chemically similar to those of Group III, whereas Group IV samples are chemically similar to those of Group II. Inspection of Table 5 and Figure 10 shows that samples of Group II are homogeneous compared to Group III samples, except for K_2O concentrations. The first standard deviation of K_2O for 16 Group II samples is 0.12 wt.% or 54 relative percent of the mean value (0.22 wt.%), which is far larger than the analytical uncertainty (0.02 wt.% or 9 relative percent). This effect is attributable to low-temperature weathering rather than magmatic processes. The distinction between Group II and Group III is obvious when one considers the wide range of variation of certain plotted elements in Group III, which do not overlap with the narrow range of variation in Group II (Zr, Ti).

All of the compositions found are characteristic of mid-ocean ridge basalt (MORB). A peculiar feature is the high CaO content in some of the analyzed samples (up to 14%) in Group III; there is no covariation of CaO and Al_2O_3 concentrations (Fig. 11), excluding the possibility of plagioclase accumulation (an exclusion that is supported by the macro and micro descriptions of the rocks). Part of the CaO content could be accounted for by calcite contamination, but such contamination is no more pervasive in Group III than in the other petrographic groups. This hypothesis of calcite contamination is also discounted by the variations of other elements in Group III.

None of the samples can be considered as primary liquids in view of phenocryst assemblages and chemical composition. In general, it is difficult to relate basalt groups by fractional crystallization; Group II could possibly be related to Groups I or III by such a process, but that would require an extensive degree of fractionation (from Zr and Ti values), which in detail is incompatible with the major and trace element variations. The chemistry of gabbros composing petrographic Group V clearly indicates that they are cumulates (low Zr, Ti concentrations and high Mg′-numbers).

Magmaphile elements (Nb, Zr, Ti, and V) are plotted in Figure 12 normalized to chondritic values, in an extended Coryell-Masuda plot (see Introduction, this volume). Error bars for a single determination are shown for the Nb values. The proportion of Nb-normalized values relative to that of Zr, Ti, and Y defines a depleted character for all samples recovered at Site 556. Compared to similar results obtained at various sites (e.g., 22°N, Leg 45; Melson, Rabinowitz, et al., 1979), the La-normalized values are inferred to be twice the Nb-normalized values; dashed lines have been drawn through these hypothetical points to suggest the probable rare earth element patterns.

The probability of finding depleted basalts at Site 556 (MAR-2 of scientific prospectus) was thought to be low according to extrapolation of zero-age data and assuming the influence of Azores mantle plume at the time of formation of this crust. The only previous evidence of depleted character between 33°N and the Azores Triple Junction area was the slightly depleted signature at Site 335 (on the FAMOUS flow line at 16 Ma; Aumento, Melson, et al., 1977). The results of Site 556 together with the previous Site 335 results suggest that the present enriched character of the Azores Triple Junction has not been constant with time. We drilled at MAR-1 to obtain a better resolution of the temporal evolution of the enriched or depleted character of the inferred mantle source(s).

MAGNETICS

Basalt Paleomagnetism

The major aim at Site 556 was to get the maximum basalt from the basement before the destruction of the drilling bit. One hundred seventy-seven meters of basalt were cored with 44% recovery. Four different units were identified based on petrographic studies done onboard. These units are described in detail in the Igneous Petrology and Geochemistry section. Phyric and aphyric basalts were studied for present paleomagnetic studies. One sample from each core was taken for detailed studies of the general paleomagnetic properties of these rocks. Natural remanent magnetization (NRM) of these samples varies between 10^{-4} and $\sim 10^{-2}$ emu/cm^3 Oe (Table 7). After the NRM was measured, each sample was subjected to alternating field (AF) demagnetization at various steps from 25 to 600 Oe, and in some cases up to 900 Oe. Plots of natural remanent magnetization versus AF demagnetizing field (Fig. 13) suggest the presence of

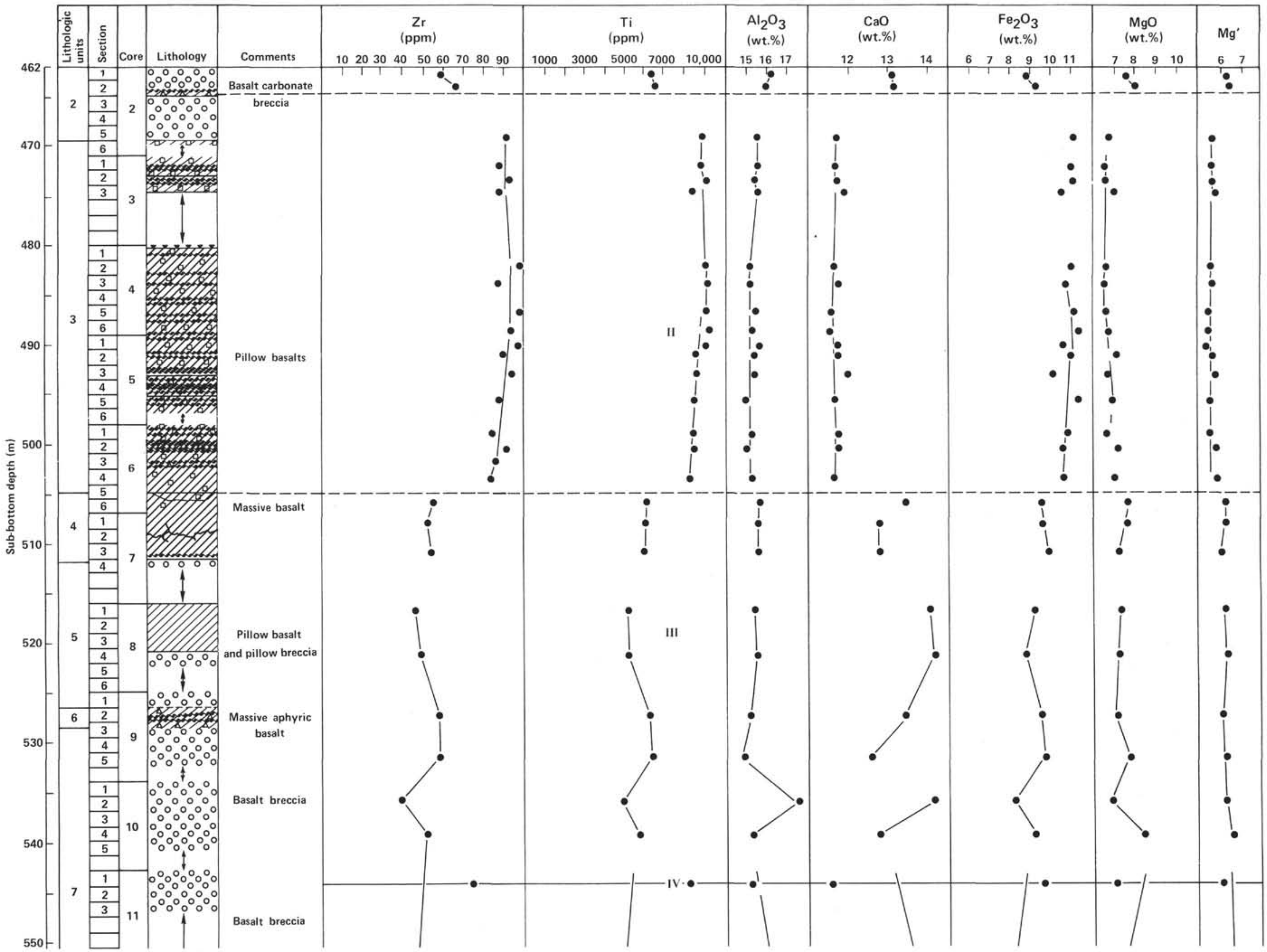

Lithologic units
Section
Core
Lithology
Comments
Zr (ppm)
10 20 30 40 50 60 70 80 90
Ti (ppm)
1000 3000 5000 7000 10,000
Al_2O_3 (wt.%)
15 16 17
CaO (wt.%)
12 13 14
Fe_2O_3 (wt.%)
6 7 8 9 10 11
MgO (wt.%)
7 8 9 10
Mg′
6 7
Sub-bottom depth (m)
462
470
480
490
500
510
520
530
540
550
Basalt carbonate breccia
Pillow basalts
Massive basalt
Pillow basalt and pillow breccia
Massive aphyric basalt
Basalt breccia
Basalt breccia
II
III
IV

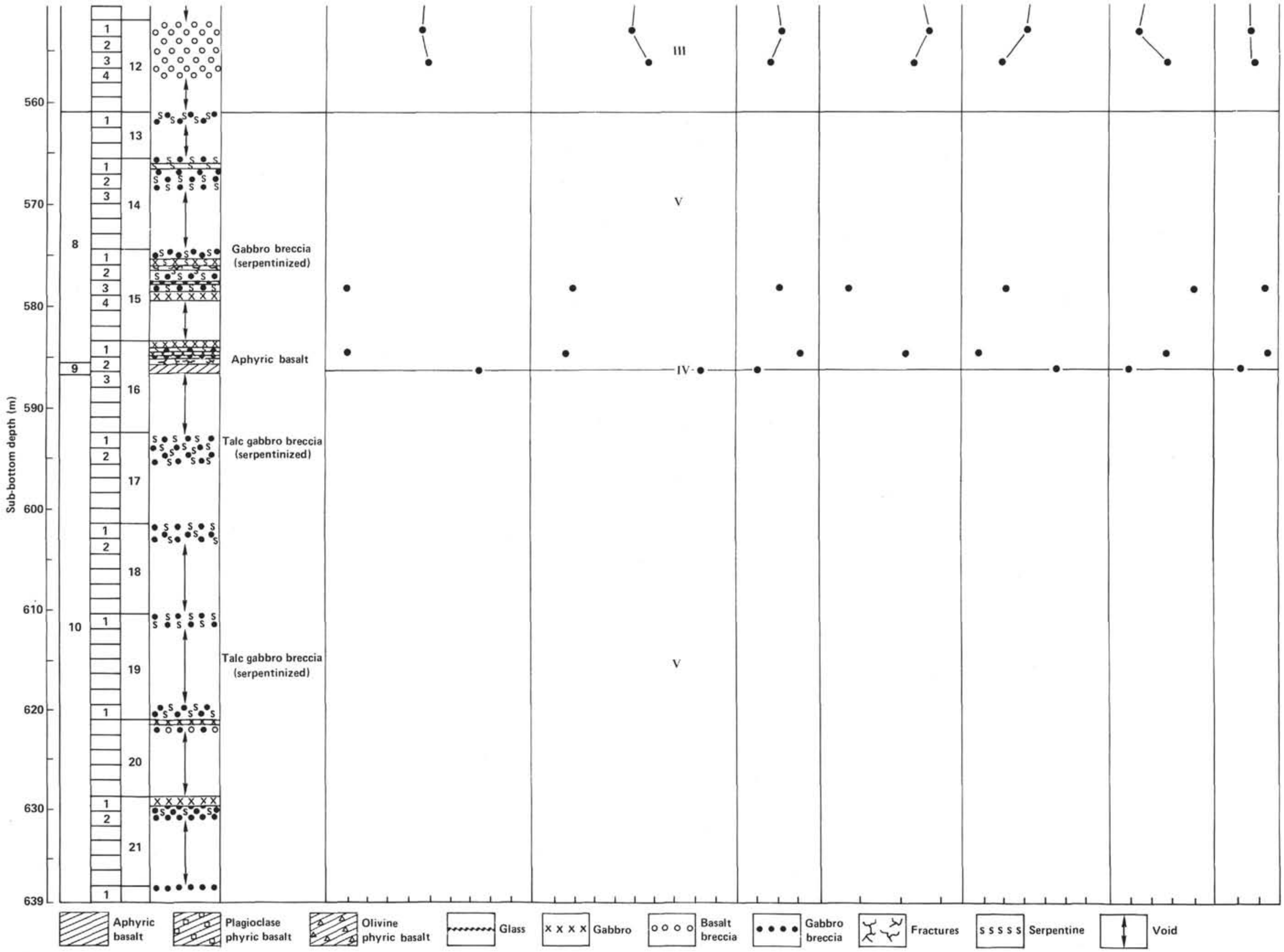

Figure 10. Lithology column and downhole plot of chemical abundances, Hole 556 basalts. Roman numerals are chemical groups. Zr and Ti expressed in ppm; others in wt.%. MG′ = 100 × (Mg/[Mg + Fe^{2+}]), calculated using an assumed Fe_2O_3 ratio of 0.15.

Table 5. Major (in wt. %) and trace (ppm) element analysis of basalts and gabbros from Hole 556.[a]

Core-Section, interval in cm (piece number)	Depth (m)	Chemical group	SiO_2	TiO_2	Al_2O_3	Fe_2O_3[b]	MnO	MgO	CaO	K_2O	P_2O_5	Total	Mg′[c]	Ti	V	Sr	Y	Zr	Nb
2-1, 78–82 (4E)	462.8	I	50.92	1.05	16.17	8.71	0.16	7.55	13.09	0.16	0.11	97.92	66	6300	277	106	28.0	59	0.8
2-2, 145–150 (9B)	464.5	I	50.54	1.07	15.97	9.27	0.16	7.92	13.10	0.17	0.12	98.32	66	6420	279	98	27.7	66	0.9
2-5, 12–16 (1A)	468.2	II	50.58	1.46	15.59	11.06	0.18	6.71	11.71	0.33	0.15	97.77	58	8760	280	98	38.3	91	0.9
3-1, 60–70 (7)	471.5	II	50.42	1.46	15.60	11.06	0.17	6.50	11.71	0.27	0.15	96.34	57	8760	292	97	39.3	88	2.2
3-2, 52–56 (4B)	473.0	II	49.83	1.50	15.46	11.14	0.18	6.52	11.74	0.30	0.16	96.83	57	9000	299	96	40.3	93	1.5
3-3, 70–74 (7)	474.6	II	50.44	1.41	15.58	10.62	0.17	6.92	11.94	0.14	0.15	97.37	59	8460	270	97	37.0	88	2.9
4-2, 77–84 (2C)	482.3	II	49.68	1.51	15.24	11.08	0.19	6.66	11.69	0.20	0.15	96.40	57	9052	293	93	40.2	98	3.2
4-3, 132–136 (1L)	483.9	II	50.37	1.53	15.09	10.89	0.20	6.56	11.78	0.09	0.16	96.67	58	9172	307	91	39.4	88	2.8
4-5, 31–33 (2B)	486.4	II	50.14	1.51	15.47	11.20	0.18	6.65	11.60	0.18	0.15	97.08	57	9060	286	92	38.7	99	1.8
4-6, 61–63 (2A)	488.1	II	50.25	1.53	15.36	11.46	0.17	6.62	11.58	0.40	0.18	97.55	57	9180	300	95	41.2	94	2.4
5-1, 73–75 (3E)	489.7	II	50.72	1.51	15.78	10.86	0.17	6.10	11.78	0.36	0.16	97.44	56	9060	297	96	40.5	98	1.5
5-2, 65–73 (1D)	491.0	II	50.07	1.42	15.44	11.15	0.18	7.18	11.79	0.29	0.14	97.66	59	8520	283	96	38.6	90	1.7
5-3, 75–80 (4)	492.8	II	50.62	1.42	15.45	10.22	0.16	6.72	12.05	0.32	0.14	97.10	60	8520	279	103	38.9	95	1.9
5-5, 145–150 (7)	497.3	II	50.46	1.40	14.98	11.43	0.17	6.99	11.71	0.07	0.14	97.35	58	8393	268	94	36.0	88	2.8
6-1, 66–70 (3A)	498.7	II	50.11	1.41	15.43	10.93	0.15	6.74	11.85	0.26	0.13	97.01	58	8460	269	110	36.0	85	1.9
6-2, 30–34 (2A)	499.9	II	50.87	1.41	15.11	10.73	0.17	7.28	11.77	0.19	0.16	97.69	60	8460	273	93	36.0	92	1.9
6-3, 82–86 (1D)	501.9	II	50.67	1.42	15.10	11.06	0.16	7.33	11.53	0.05	0.14	97.46	60	8540	274	92	35.1	86	0.7
6-4, 121–126 (5B)	503.7	II	50.08	1.36	15.35	10.78	0.16	7.18	11.70	0.02	0.14	96.77	60	8160	257	94	35.3	84	1.7
6-6, 44–48 (2A)	505.9	III	49.89	1.02	15.75	9.68	0.16	7.82	13.50	0.16	0.09	98.07	64	6120	249	94	26.1	56	2.0
7-1, 123–126 (5A)	508.1	III	50.56	1.01	15.67	9.68	0.17	7.78	12.81	0.14	0.10	97.92	64	6055	241	98	25.7	53	0.1
7-3, 12–15 (1B)	510.3	III	50.57	1.01	15.74	10.03	0.16	7.34	12.71	0.15	0.11	97.82	62	6055	245	98	26.9	55	0.9
8-1, 107–111 (7)	517.1	III	50.01	0.87	15.50	9.32	0.15	7.41	14.04	0.37	0.11	97.78	64	5220	257	96	24.7	47	1.1
8-4, 60-63 (3B)	521.1	III	50.03	0.87	15.60	8.86	0.16	7.24	14.46	0.35	0.12	97.69	65	5216	248	97	24.3	50	0.6
9-2, 82–84 (4B)	527.4	III	50.53	1.05	15.33	9.52	0.17	7.12	13.42	0.24	0.12	97.50	63	6295	275	97	26.1	59	2.1
9-5,64–68 (8A)	531.8	III	51.22	1.06	14.94	9.71	0.17	7.75	12.54	0.22	0.09	97.70	64	6360	282	101	28.7	59	1.3
10-2, 137–141 (3B)	536.8	III	49.87	0.82	17.58	8.17	0.14	6.86	14.13	0.26	0.10	97.93	65	4920	250	94	23.0	41	2.4
10-4, 50–54 (4)	538.9	III	50.37	0.95	15.38	9.22	0.16	8.49	12.73	0.21	0.09	97.60	67	5700	247	85	24.8	53	1.2
11-1, 105–115 (13)	544.1	IV	51.84	1.38	15.23	9.73	0.19	7.06	11.63	0.12	0.15	97.33	62	8273	333	107	37.7	77	2.5
12-1, 55–59 (4B)	552.6	III	49.81	0.83	17.24	8.16	0.13	7.41	13.69	0.24	0.09	97.60	67	4976	247	94	21.8	48	1.5
12-3, 118–122 (5B)	556.1	III	50.85	0.96	15.64	8.74	0.15	8.83	12.49	0.17	0.09	97.92	69	5755	243	87	24.6	51	0.7
15-3, 33–35 (2B)	577.9	V	52.51	0.32	15.98	7.17	0.14	10.16	11.85	0.00	0.03	98.16	76	1918	163	84	8.7	10	<0.1
16-1, 21–27 (3B)	583.8	V	52.61	0.28	17.21	5.92	0.12	8.82	13.21	0.00	0.03	98.20	77	1680	164	90	9.9	10	<0.1
16-2, 137–140 (15)	586.3	IV	52.46	1.38	15.06	9.66	0.14	6.86	11.06	0.29	0.15	97.06	63	8273	326	108	36.2	77	1.8

[a] On-board measurements were made on ignited samples. Onshore analyses of loss on ignition are less than 1% in most cases. Compiled data tables in Appendix at the end of the volume include volatile components.
[b] Total Fe as Fe_2O_3.
[c] Mg′ is the atomic ratio of 100 × Mg/(Mg + Fe^{2+}); calculated using an assumed Fe_2O_3/FeO ratio of 0.15.

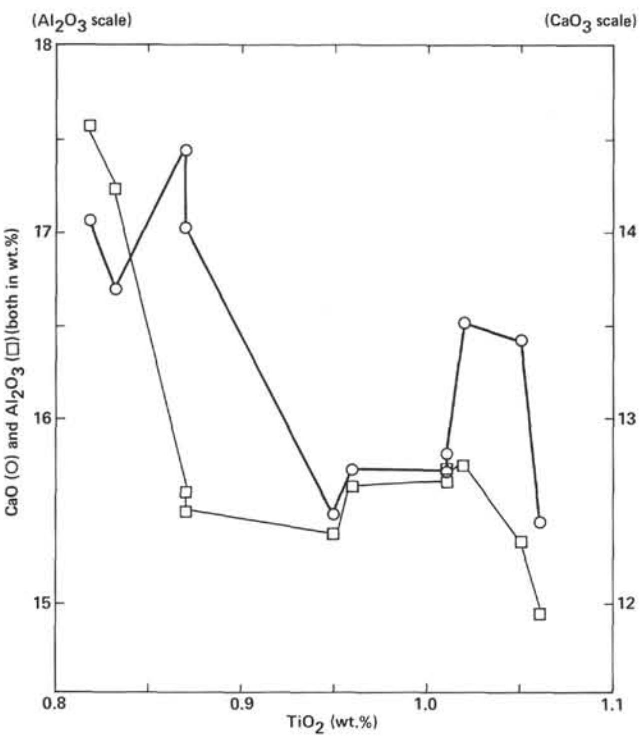

Figure 11. Variation of TiO_2 with CaO and Al_2O_3 for heterogeneous Chemical Group III, Hole 556.

Table 6. Average analyses for the five chemical groups from Hole 556.

Chemical group	I	II	III[a]	IV	V
N[b]	2	16	11	2	2
SiO_2 (wt.%)	50.73	50.31	50.34	52.15	52.55
TiO_2	1.06	1.46	0.95	1.38	0.30
Al_2O_3	16.07	15.40	15.85	15.15	16.60
Fe_2O_3[c]	8.99	10.97	9.19	9.70	6.54
MnO	0.16	0.17	0.16	0.17	0.13
MgO	7.74	6.76	7.64	6.96	9.49
CaO	13.10	11.76	13.32	11.35	12.53
K_2O	0.17	0.23	0.23	0.21	
P_2O_5	0.12	0.15	0.10	0.15	0.03
Ti (ppm)	6360	8722	5697	8273	1800
V	278	283	253	330	164
Sr	102	96	95	108	87
Y	27.9	38.0	25.2	37.0	9.3
Zr	63	91	52	77	10
Nb	0.9	2.0	1.3	2.2	<0.1
Mg′[d]	66	58	65	63	77
Al_2O_3/TiO_2	15.2	10.5	16.9	11.0	56
Ti/Zr	102	96	110	107	(180)

[a] A heterogeneous chemical group.
[b] Number of samples on which the mean is based.
[c] Total Fe as Fe_2O_3.
[d] Mg′ is the atomic ratio of 100 × Mg/(Mg + Fe^{2+}); calculated using an assumed Fe_2O_3/FeO ratio of 0.15.

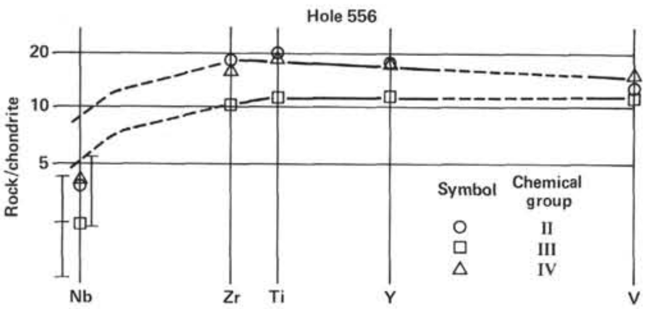

Figure 12. Extended Coryell-Masuda diagram for averages of Chemical Groups II, III, and IV. Error bars for Nb are shown at the left.

Table 7. Paleomagnetic properties, Hole 556.

Core-Section (interval in cm)	J_{NRM} ($\times 10^{-3}$ emu/cm^3)	NRM inc.	Stable inc.	($\times 10^{-6}$ g/cm^{-3} Oe)	Q ($= J_{NRM}/0.45\ \chi$)
3-1, 42-44	2.07	−36.4	−32.0	52	89
3-1, 102-105	3.22	−31.5	−30.8	40	179
3-2, 116-119	2.77	−42.5	−39.6	43	143
4-1, 118-120	6.97	−38.7	−33.9	100	155
4-2, 62-65	5.32	−35.5	−35.8	45	263
4-3, 63-66	1.64	−31.8	−31.9	198	184
4-4, 95-98	5.84	−33.7	−29.9	65	200
4-5, 71-74	7.75	−22.4	−34.4	355	49
4-6, 23-26	1.92	−36.3	−36.9	57	75
5-1, 38-41	1.72	−25.7	−26.5	45	85
5-3, 139-142	1.71	−40.4	−38.9	65	59
5-4, 102-105	3.38	−30.0	−26.7	58	130
5-5, 126-129	1.13	−27.7	−31.3	56	45
6-1, 112-115	0.64	−25.4	−24.5	64	22
6-2, 125-128	2.94	−20.8	−25.6	91	67
6-3, 103-106	5.15	−13.4	−28.9	383	30
6-4, 75-78	9.5	−25.0	−23.3	94	225
6-5, 73-76	4.32	−25.3	−31.1	70	137
7-1, 12-15	1.46	−10.1	−17.1	80	41
7-2, 95-98	0.33	− 2.1	−20.5	76	10
7-3, 97-100	0.73	−23.2	−27.0	85	19
8-2, 105-108	2.67	−49.4	−49.9	104	57
8-3, 96-99	3.35	−42.5	−43.6	85	88

Note: J_{NRM} = natural remanent magnetization; inc. = inclination; χ = susceptibility; Q = Königsberger ratio.

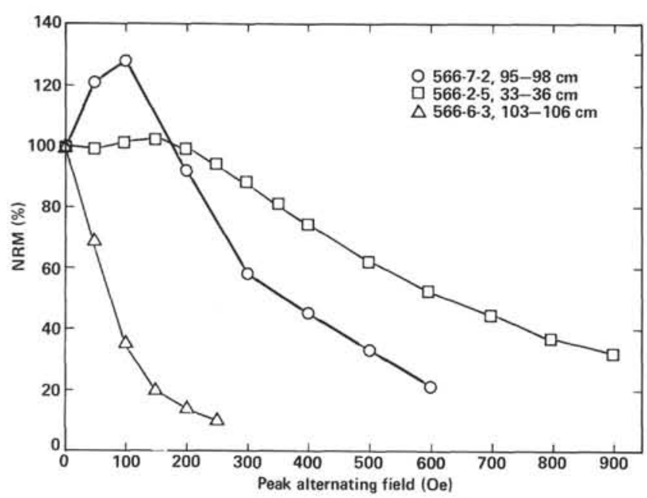

Figure 13. Plots of natural remanent magnetization (NRM) versus alternating field demagnetization, Hole 556.

a weak secondary component of magnetization that is removed after demagnetization at 150 Oe. To observe this secondary component, vertical component of magnetization z was plotted against horizontal component of magnetization x (Fig. 14). This orthogonal plot clearly indicates the secondary component of magnetization,

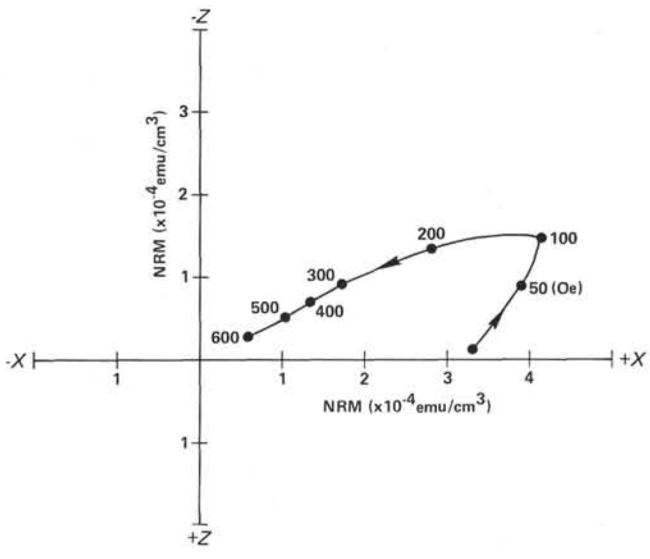

Figure 14. Vertical versus horizontal component of magnetization, Hole 556 (556-7-2, 95–98 cm).

which in some cases has antiparallel orientation with respect to the main component of magnetization.

Inclination values of individual samples are given in Table 8. Inclination values observed are shallower than expected and may be the result of tectonic rotation of the oceanic crust since the acquisition of remanent magnetization.

Susceptibility of the samples was measured using Bison's Magnetic Susceptibility System, Model 3101. The susceptibility values are given in Table 7.

PHYSICAL PROPERTIES

The drill string was washed down through the sediments, but some sediment was recovered in the mudline core and in wash cores taken at points of temperature

Table 8. Magnetic inclinations, Hole 556.

Core-Section (interval in cm)	Inclination after AF demag. (°)[a]	Core mean inclination (°)[b]
3-1, 42-44	−33.6	
3-1, 102-105	−30.8	−34.6
3-2, 116-119	−39.6	
4-1, 118-120	−34.8	
4-2, 62-65	−35.8	
4-3, 63-66	−31.9	−34.0
4-4, 95-98	−30.2	
4-5, 71-74	−34.4	
4-6, 23-26	−36.9	
5-1, 38-41	−26.5	
5-3, 139-142	−38.9	−30.8
5-4, 102-105	−26.7	
5-5, 126-125	−31.3	
6-1, 12-15	−24.5	
6-2, 125-128	−25.6	
6-3, 103-106	−28.9	−26.6
6-4, 75-78	−23.3	
6-5, 73-76	−31.1	
7-1, 12-15	−17.1	−21.5
7-2, 95-98	−20.5	
7-3, 97-100	−27.0	
8-2, 105-108	−49.9	−46.7
8-3, 96-99	−43.6	

[a] AF demag. = alternating - field demagnetization.
[b] Core mean inclination was calculated by assuming same declination for all samples.

measurements for heat flow calculations. Because all of these sediment samples were highly disturbed and their depth of origin unknown, no physical properties measurements were made. The basement was continuously cored to bit destruction through pillow basalts, breccia, and gabbros with high core recovery. Measurements were made of seismic velocity, density, and thermal conductivity. Details of basement physical properties measurements are described in the following paragraphs, and the downhole temperature data are included in the discussion of wireline logging.

Basement Section

The drilled sequence of pillow basalts, basalt, and gabbro was sampled to determine typical values for fresh rocks. Altered specimens were difficult to sample but did indicate the range of values with alteration. All measured values are shown in Table 9, and plotted in Figure 15.

Seismic velocities were measured in the Hamilton frame velocimeter on seawater-saturated samples to an estimated accuracy of 0.02 km/s. Densities were determined by 2-minute GRAPE and gravimetric methods to an accuracy of about 0.02 g/cm^3. Thermal conductivities were measured on saturated specimens in a water bath to an accuracy of about 5%. Values in Table 9 are in units of $\text{mcal}\cdot\text{cm}^{-1}\cdot\text{deg}^{-1}\cdot\text{s}^{-1}$ under laboratory conditions. The correction to *in situ* conditions is small compared to the measurement error.

The values in Table 9 should be compared with bulk *in situ* values determined by the downhole measurements (see Downhole Measurements section) to estimate the degree of alteration of the rock units for which there was no core recovery.

Densities determined by GRAPE and gravimetric methods agree quite well; discrepancies are mainly due to the fact that each measurement was made on separate but adjacent samples, and in altered rocks there is variability over this small distance. Seismic velocities vary systematically with density as would be expected. The thermal conductivity values give mean values for basalt and gabbro, which are very similar to those determined on Leg 37 (FAMOUS area; Aumento, Melson, et al., 1977) for similar lithologies.

Comparison with the downhole geophysical log records shows excellent agreement; the bulk downhole values for density and velocity are lower than the laboratory values by an amount that reflects the degree of jointing and fracturing of the rock.

DOWNHOLE MEASUREMENTS

Heat Flow Measurements

Measurements were made at depths of 97.5, 145.0 and 192.5 m sub-bottom using the downhole thermal probe. This is inserted above the drill bit in place of the core barrel, with the thermistor probe protruding about 1 m through the center of the drill bit. The bit is then lowered to the base of the hole so that the probe is inserted into "undisturbed" sediment. The first measurement was not taken until 97.5 m sub-bottom because the sediment above this depth would not support the weight of the bit.

For each measurement, the probe was lowered to seabed depth and left to equilibrate for 20 minutes, then lowered to the drill bit, inserted in the sediments, and again left to equilibrate for 20 minutes. Resulting temperatures are accurate to better then $\pm 0.1°C$.

The three measurements (Fig. 16) yield four points on a temperature-depth plot (Fig. 17). This gives a linear gradient of 36°C/km over the interval from 97.5 to 192.5 m. The sea-bottom temperature lies below this

Table 9. Physical property measurements for Hole 556.

Core-Section (interval in cm)	Sub-bottom depth (m)	Sonic velocity (km/s) V.	Sonic velocity (km/s) H.	T(°C)	Thermal conductivity (mcal · cm^{-1} · deg^{-1} · s^{-1})	GRAPE density (g/cm^3) V.	GRAPE density (g/cm^3) H.	Gravimetric data: Wet-bulk density (g/cm^3)	Gravimetric data: Water content (%)	Gravimetric data: Porosity (%)	Acoustic impedance (× 10^5 g · cm^{-1} · s^{-1})	Lithology and remarks
2-5, 33-36	467.8	5.61		21.5	4.06	2.80		2.82	2	4	15.76	Basalt
3-1, 42-44	471.4		5.75	21.8	3.76			2.86	1	4	16.45	Basalt
4-1, 118-120	481.2	5.69		23.0	4.12	2.77		2.81	2	6	15.88	Basalt
4-4, 95-98	485.5	5.58		23.0	4.12	2.77		2.85	2	5	15.68	Basalt
6-3, 115-118	502.2	5.84		21.4	4.26	2.85		2.84	2	6	16.61	Basalt
7-2, 95-98	509.5	5.77		21.5	3.99	2.88		2.85	2	6	16.53	Basalt
8-3, 139-142	520.4	5.29		22.0	3.99			2.78	4	10	14.71	Altered basalt
9-3, 8-21	528.1	5.52	5.53	22.0	4.12	2.83		2.88	2	6	15.77	Basalt
10-1, 5-17	534.1	4.97		22.0	3.87	2.71		2.64	5	14	13.29	Basalt breccia
11-1, 40-50	543.5	4.16	4.11	22.5		2.48					10.32	Basalt breccia
12-1,121-124	553.2	4.76		22.5	4.12	2.67					12.66	Basalt breccia
13-1, 39-44	561.4			22.0			2.48					Very altered breccia
13-1, 62-65	561.6							2.53	5	12		Serpentinized gabbro
13-1, 65-70	561.7		4.91	22.0	7.10		2.87				14.09	Serpentinized gabbro
14-1, 37-43	565.9		3.99	22.0	6.39		2.56	2.53	4	11	10.15	Serpentinized gabbro
15-1, 74-83	575.3	6.32		22.0	5.55	2.90					18.33	Gabbro
15-3, 120-132	578.2		6.34	22.0			2.99				18.96	Fresh gabbro
16-1, 110-120	584.6		5.88	22.0								Gabbro with calcite veins
18-1, 16-24	601.7		6.06	23.0			2.89	2.85	2	5	17.51	Gabbro
19-1, 119-133	611.7		3.60	23.0				2.59	7	17		Altered gabbro with calcite veins
20-1, 138-139	620.9							2.86	3	9		Gabbro
21-2, 63-65	630.1							2.55	4	11		Gabbro

Note: All values measured at laboratory temperature and pressure. For details of methods, see Explanatory Notes chapter, this volume. V. = vertical; H. = horizontal; T = temperature; water content is corrected.

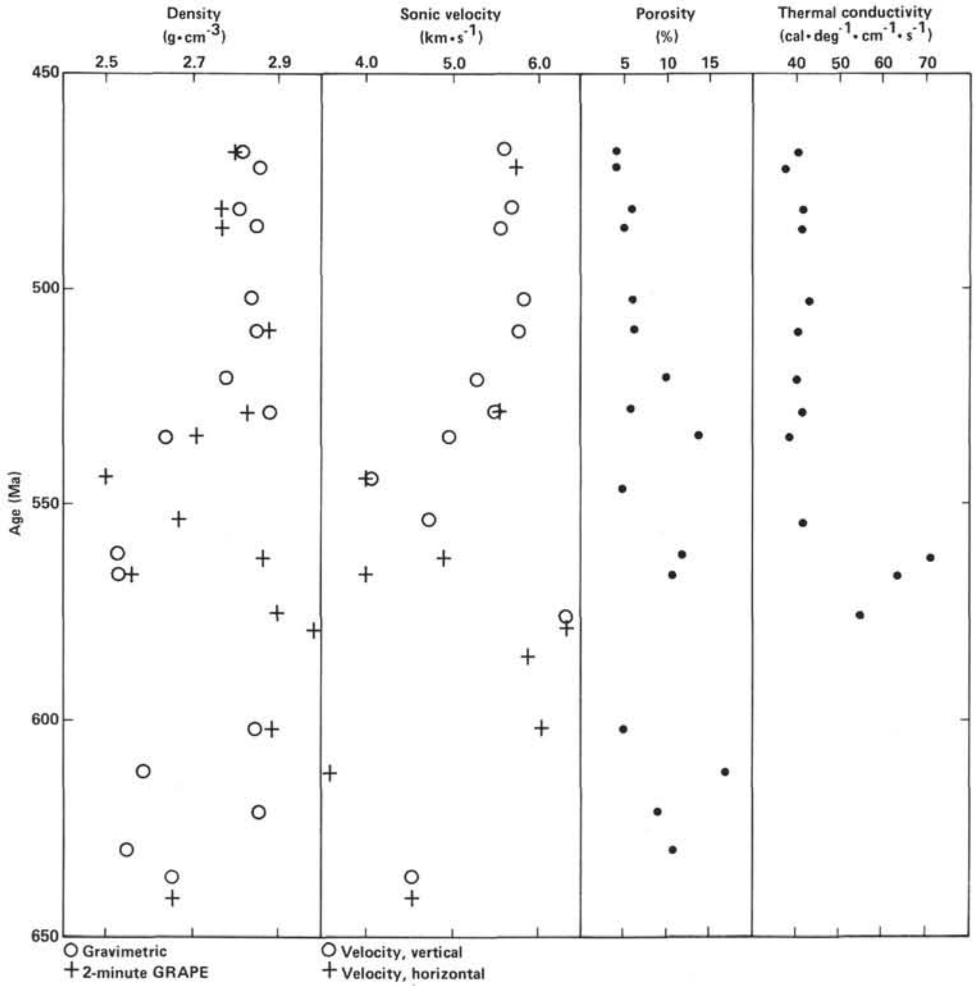

Figure 15. Downhole variation in laboratory measured physical properties, Hole 556.

trend, perhaps showing an effect of secular bottom-water temperature variation and/or a possibility of a higher thermal conductivity in the uppermost sediments.

After continuous coring at Site 558 (MAR-4), thermal conductivity measurements were made on the sedimentary sequence that was similar in age and lithology to that of Site 556. The data show a rise in thermal conductivity as a function of depth and compaction, displaying a similar trend to that determined by Hyndman and others (1977), but with slightly higher values. A mean conductivity for the depth range over which the thermal gradient was determined can thus be estimated as 2.85 (Hyndman) or 3.10 (this study) $\mathrm{mcal \cdot cm^{-1}\, sec^{-1}\, {}^{\circ}C^{-1}}$.

Using a value of 3.0, which is within the error limits of both data sets, and the thermal gradient of $36^{\circ}\mathrm{C\ km^{-1}}$, the heat flow is calculated as $1.08\ \mu\mathrm{cal\ cm^{-2}\ sec^{-1}}$. This is below average for 33-Ma-old crust, but within the range of variation commonly found.

Logging

Operations

After completion of the hole, we decided to run a complete suite of logs, because the basement penetration exceeded 150 m and the lithologies encountered were unusual and complex. The bit was dropped and drill pipe withdrawn until the end of the drill string was 113 m below the mudline. Four logging runs were made using various combinations of tools as given in Table 10.

Within the sediments the caliper logs show that the hole was washed out to more than 16-in. diameter, whereas the diameter in basement was generally of bit size, approximately 10 in. There was a washout within the basement between 561 and 578 m sub-bottom to a diameter of approximately 12 in. Two constrictions were found, one just above basement between 453 and 456 m sub-bottom and the second 40 m below the sediment/basement interface (503–508 m sub-bottom).

There were no serious technical problems with the logging equipment, and complete logs were obtained for all tools. The large-hole diameter in the sediments was greater than the excentralizer extension of the density log (FDC) and the neutron porosity log (CNL), hence these logs were not in continuous contact with the sidewall and resulting data are of doubtful value. Noise on the sonic log is caused by the tool contacting constrictions in the hole and results in localized noisy sections. "Spikes" on the caliper log attached to the sonic tool result from modifications made to allow it to pass down the drill string, but these are easily removed by eye. All

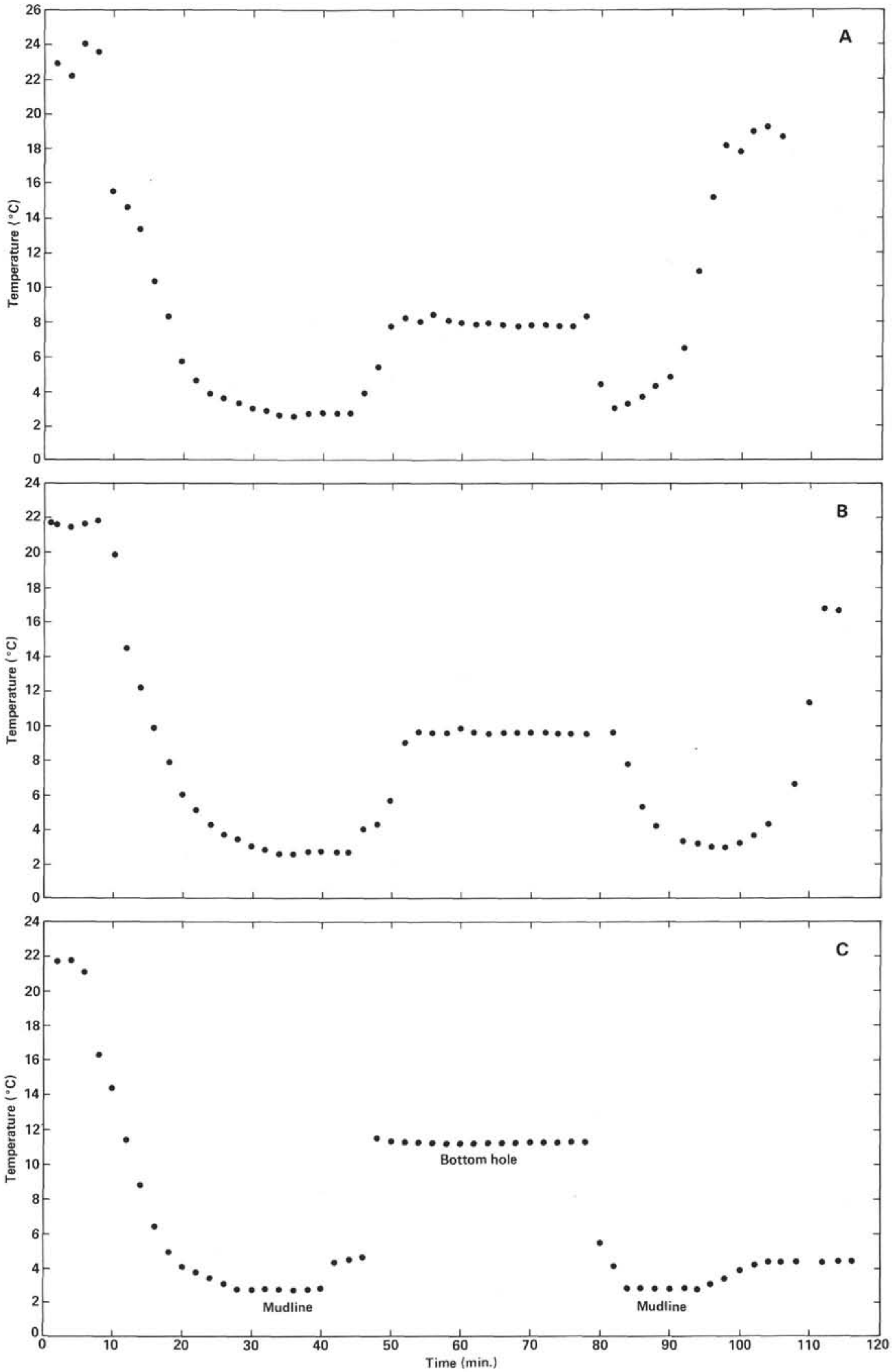

Figure 16. Heat probe measurements in Hole 556. Sub-bottom depths are: A, 97.5 m; B, 145.0 m; C, 192.5 m.

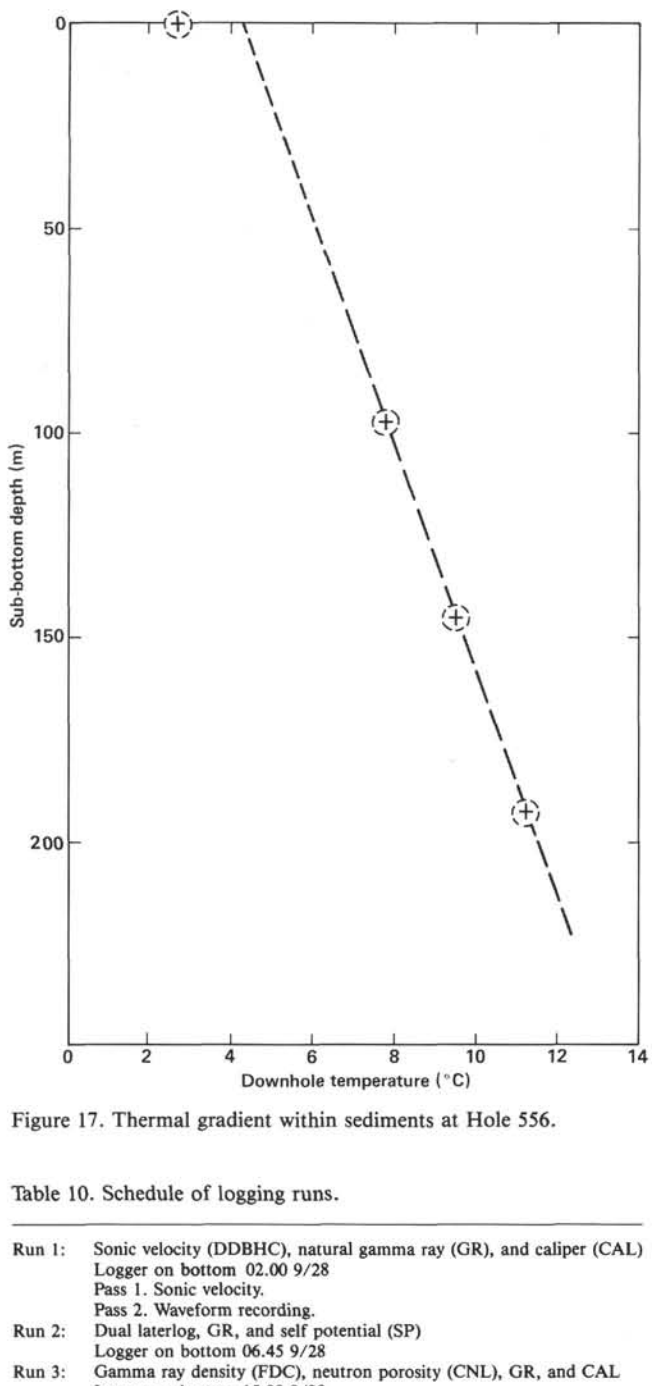

Figure 17. Thermal gradient within sediments at Hole 556.

Table 10. Schedule of logging runs.

Run 1:	Sonic velocity (DDBHC), natural gamma ray (GR), and caliper (CAL) Logger on bottom 02.00 9/28 Pass 1. Sonic velocity. Pass 2. Waveform recording.
Run 2:	Dual laterlog, GR, and self potential (SP) Logger on bottom 06.45 9/28
Run 3:	Gamma ray density (FDC), neutron porosity (CNL), GR, and CAL Logger on bottom 15.00 9/28
Run 4:	High resolution temperature (HRT) Logger on bottom 21.30 9/28 Tool pumped to bottom of drill pipe

three physical property logging runs were started within 20 m of the bottom of the hole.

Sedimentary and Basement Sections

The hole is divided into seven geophysical (log) units (Fig. 18 and Table 11), based on characteristic combinations of physical properties. The boundaries of the units correspond to abrupt simultaneous changes in at least two log curves and generally in three or more. Several excursions (i.e., brief simultaneous changes in several logs that occur within the previously defined units) are noted in Figure 18 (as shown by dashed horizontal lines). Comparison of the boundaries of the geophysical units to the lithologic record from the cores reveals the expected close correlation.

The sedimentary section, Unit 1, is very uniform and both sonic and resistivity logs show gradual changes caused by compaction (Fig. 19). There is a sharp rise in sonic velocity at about 330 m sub-bottom, which may reflect a change in sediment lithology or diagenesis. The curves contain some short-wavelength variations that are difficult to interpret. The density curve is drawn dashed because the curve has many noise spikes and has been filtered by eye. Within the basement, the highest sonic velocities, resistivities, and densities and the lowest porosities correspond to the pillows, massive basalts, and gabbro units. Changes from these values reflect alteration, fracturing and brecciation. A detailed description of the units is given in Table 11. Physical parameter values derived from the logs correlate very well with laboratory sample measurements (see Physical Properties section).

Only one gamma-ray anomaly was noted, at 529 m sub-bottom, corresponding to a low-velocity, low-density, and high-porosity excursion. This may be caused by a localized zone of high clay mineral content within the upper part of the lower basaltic breccia.

Because there is such a close correlation between the log records and lithologic units derived from core description, it is deduced that units are homogeneous and that cored material is probably quite representative of the entire cored section. Where both the lithology and the logs change rapidly within a single core, the logs provide the means of precisely locating the position of the lithology changes.

Downhole Temperatures

The temperature log (high resolution temperature or HRT) was the last log run, giving the hole a period of 24.5 hours to equilibrate. Unfortunately, the hole had closed within the basement section, and the tool could not be lowered more than 20 m below the basement interface; however, the temperature profile above this level is interesting. From the mudline to just above the basement interface, the temperature was nearly uniform at the bottom-water temperature, whereas within the 20 m of basement section, the temperature rose rapidly by 3°C. The absolute calibration of the thermistor used is uncertain within ±2°C, but this does not affect the conclusion that the hole is at bottom-water temperature down to the level of the basement interface. The preexisting temperature was established during drilling (see Heat Flow Measurements section). The logged temperature profile suggests downward flow of bottom water into porous formations just below the sediment/basement interface.

Seawater Drawdown

The geothermal gradient at Site 556 was determined to be 36°C per km. The thickness of sediment was 461

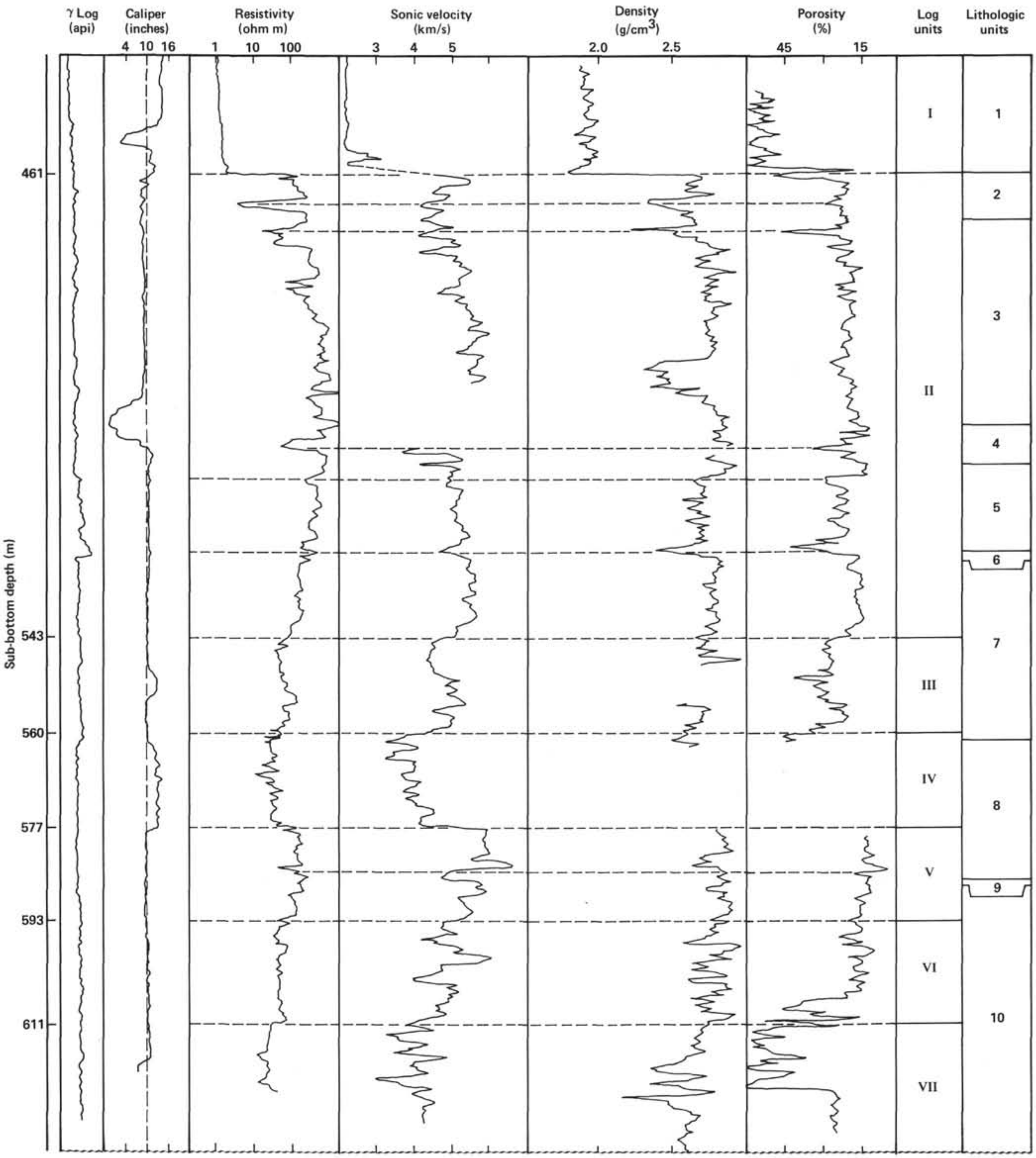

Figure 18. Wireline log curves for the basement section of Hole 556. Curves have been redrawn omitting noise spikes; gaps indicate intervals where noise obscured data.

m, hence a linear gradient would imply a temperature at basement interface of 21°C. If we allow for an increase in conductivity with depth, this value may decrease to about 18°C.

As drilling proceeds, the hole is flushed with seawater pumped from the surface. As it travels down the drill string (about 30 min.), this water cools to equilibrate with ocean water so that it enters the hole at bottom-water temperature. At the cessation of drilling, the hole is uniformly chilled to ocean bottom-water temperature. Because forced-water circulation has now ceased, the hole will tend to return to its equlibrium tempera-

Table 11. Description of geophysical (log) units, Hole 556.

Unit	Sub-bottom depth range (m)	Resistivity (ohm m)	Sonic velocity (km/s)	Density (g/cm^{-3})	Porosity (%)	Lithology	Remarks
I	113–461	1	up to 2.1	up to 1.9	up to 55%	Nannofossil ooze	Only logged from base of drill string.
II	461–543	500	5.4	2.75	20	Basalt breccia, pillow basalts, massive basalts	These values are for the interval 485-500 m.
III	543–560	50	4.6	2.65	27	Lower basalt breccia	
IV	560–577	20	3.8	2.50	50	Serpentinized gabbroic breccia	
V	577–593	100	5.5	2.80	15	Gabbro	Lower sonic velocity occurs in lower half of unit.
VI	593–611	30	4.6	2.70	18	Serpentinized gabbroic breccia	
VII	611–620	15	4.0	2.50	54	Serpentinized gabbroic breccia	

ture at a rate dependent on the duration of chilling (drilling) and the thermal diffusivity of the drilled rock. The return to thermal equilibrium of DSDP holes has been discussed in detail by Hyndman and others (1977). For this study, the simplest treatment has been used, modeling the drilling as a line heat source in an infinite medium. For this model, the temperature disturbance decays approximately as derived by Jaeger (1975):

$$\frac{T}{T_o} = \frac{\ln\left(1 + \frac{t_o}{t}\right)}{\ln\,(4kt_o/a^2 - 0.577)},$$

where T/T_o is the ratio of temperature at time t to equilibrium value T_o; t_o is duration of disturbance (drilling) (122.5 hr.); t is time since the disturbance ceased (25 hr.); k is the diffusivity of the medium (0.003 cm^2/hr.); a is the radius of the hole (12.5 cm).

This equation has been applied to the sedimentary section of Hole 556 where the predrilling temperature was measured by Uyeda heat probe, and the postdrilling temperature was determined by Schlumberger HRT log. The solution predicts a T/T_o value of 0.5 (i.e., temperatures should have returned to half their equilibrium value by the time of the Schlumberger logging). Because the HRT log showed constant bottom-water temperature throughout the sediment section, continuing cooling of the hole by natural drawdown must be assumed.

If we assume that the drill hole acts as a cooling line element within the sedimentary section, we can calculate approximately the quantity of heat that must be removed to prevent reequilibration. For a rise in water temperature of less than 1°C this requires a water flow rate of about 70 m per hour down the hole. This volume of water must flow away from the hole through fractures and joints in the basement.

SUMMARY AND CONCLUSIONS

The principal objective of Leg 82 is to study the evidence for mantle heterogeneity in the vicinity of the Azores Triple Junction. From data collected along the axis of the Mid-Atlantic Ridge (zero age), it appears that the Azores Triple Junction corresponds to the center of a major mantle anomaly in respect to the well-known "depleted" character in the magmaphile elements of typical mid-oceanic crust and mantle. This anomaly is also documented by Sr, Pb, and Nd isotopic ratios. The location of the proposed drill sites forms a grid that makes it possible to sample the oceanic crust between the latitudes of 40 and 32° over a broad span of time.

Site 556 is located on a flow line passing through the Azores Triple Junction, where it is thought that the geochemical anomaly is the highest and should have persisted for the longest period of time. The first site on this flow line was chosen to be on Anomaly 13, which was thought to be a good compromise between the distance from the axis of the ridge, the thickness of sediments, and the location of other proposed sites in the grid. To summarize, the principal objective of drilling at Site 556 was to answer the question: "Was the Azores Mantle Plume producing abnormal (enriched in magmaphile elements) crust at the axis of the ridge 35 Ma?"

The exact position of Site MAR-2 had not been surveyed ahead of time. Although we had intended to drill on Anomaly 13 because of its prominence, a suitable locality could not be found on our approach to the site, because of the rough nature of the basement and the extreme sediment thicknesses. Because smoother basement had been observed in the area of Anomaly 12 and because the sediment thickness there was less than 500 m, the site was moved to Anomaly 12. More precisely, Site 556 is located close to the transition between the positive Anomaly 12 and the negative anomaly between 12 and 13 (about 34 Ma old). The water depth is 3680 m.

The sediments were washed down until basement was felt at a level of 461 m sub-bottom. The last sediment was recovered several meters below in a basaltic breccia. Nannofossils identified within the sediment matrix of the basaltic breccia give an age of 30 to 34 Ma, in agreement with the age of Magnetic Anomaly 12.

Drilling within basement penetrated 177 m before bit destruction. Basalt breccias, pillows, and massive basalts

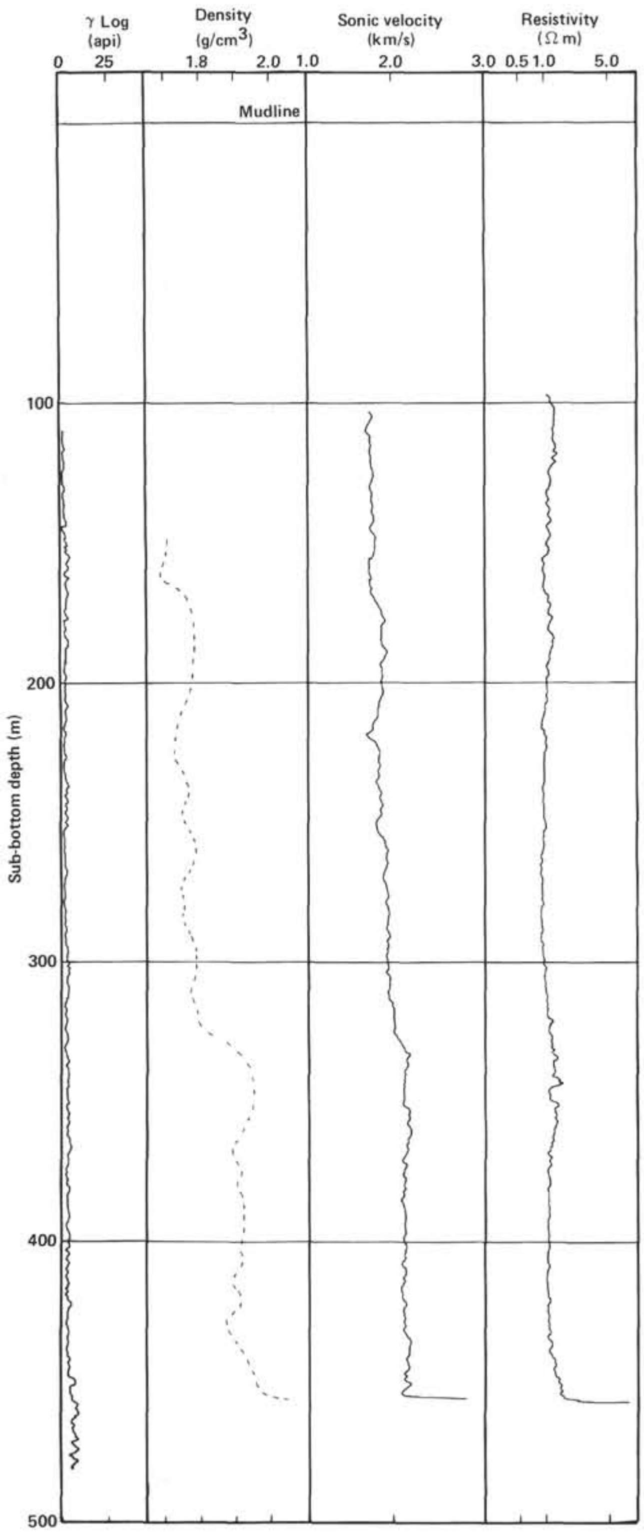

Figure 19. Wireline log curves for the sedimentary section of Hole 556. Density curve is dashed to indicate the low quality of the data. Numbers on the horizontal lines are sub-bottom depth (in m).

were recovered in the upper 99 m of basement, and gabbros and highly altered gabbroic breccias were encountered in the lower part of the basement. The average recovery in the upper basaltic layer was about 64%, whereas recovery in the lower gabbroic unit was only about 20%. Nine lithologic units have been identified within the basement. The macro and micro descriptions of the samples together with the shipboard geochemical analyses make it possible to define five petrographic groups (four basaltic groups and one gabbroic group) within the different lithologic units.

The shipboard geochemical analyses were focused on determining the concentrations of certain key magmaphile trace elements that are critical in determining the depleted or enriched geochemical character of the basalt: Nb, Zr, Ti, Y, and V. Figure 12 shows the concentrations of the elements normalized to chondrites.

The results obtained at Hole 556 show that the geochemical character of the oceanic crust produced at this latitude on the Mid-Atlantic Ridge 34 Ma is typical of normal depleted mid-oceanic basalts. The results demonstrate that the Azores Triple Junction has not been continuously associated with a mantle plume insofar as there is a correlation between mantle plumes and enriched oceanic basalts.

The remanent magnetization inclinations found in the pillow and massive basalt units are negative and consistent with the location of the site near the transition zone between positive and negative anomalies. A narrow range of core average values are found in the upper units (−30 to −35°), and more widely scattered values are found in the lower basaltic units (−21 to −47°).

A complete set of logs were conducted following completion of the hole. Variations in the sonic velocity, resistivity, density, and porosity logs closely follow changes in the lithology within the basement. The temperature profile recorded by the high resolution thermometer showed a nearly uniform bottom-water temperature (about 2°C) all the way down to the sediment/basement interface. This observation contrasts with the thermal gradient of 36°C per km measured at three levels within the sediment when washing down to the basement. This result suggests that a downward flow of deep water was initiated by drilling the basement.

REFERENCES

Aumento, F., Melson, W. G., et al., 1977. *Init. Repts. DSDP*, 37: Washington (U.S. Govt. Printing Office).

Berggren, W. A., and Amdurer, M., 1973. Late Paleogene (Oligocene) and Neogene planktonic foraminiferal biostratigraphy of the Atlantic Ocean (Lat. 30°N to Lat. 30°S). *Rev. Ital. Paleontol. Strati.*, 79:337-391.

Blow, W. H., 1969. Late middle Eocene to Recent planktonic foraminiferal biostratigraphy. *In* Brönnimann, P., and Renz, H. H. (Eds.), *Proc. First Planktonic Conf.*: Leiden (E. J. Brill), pp. 199-422.

Gartner, S., 1977. Calcareous nannofossil biostratigraphy and revised zonation of the Pleistocene. *Mar. Micropaleontol.*, 2:1-25.

Hyndman, R., Von Herzen, R. P., Erickson, A. J., and Jolivet, J., 1977. Heat flow measurements DSDP Leg 37. *In* Aumento, F., Melson, W. G., et al., *Init. Repts. DSDP*, 37: Washington (U.S. Govt. Printing Office), 347-362.

Luyendyk, B. P., Cann, J. R., et al., 1979. *Init. Repts. DSDP*, 49: Washington (U.S. Govt. Printing Office).

Melson, W. G., Rabinowitz, P. D., et al., 1979. *Init. Repts. DSDP*, 45: Washington (U.S. Govt. Printing Office).

Okada, H., and Bukry, D., 1980. Supplementary modification and introduction of code numbers to the low-latitude coccolith biostigraphy zonation (Bukry, 1973:1975). *Mar. Micropaleontol.*, 5: 321–325.

Varet, J., and Demange, J., 1979. Autoclastic submarine breccias in Hole 410, Leg 49, and other DSDP sites. *In* Luyendyk, B. P., Cann, J. R., et al., *Init. Repts. DSDP*, 49: Washington (U.S. Govt. Printing Office), 749–760.

SITE 556 HOLE CORE 1 CORED INTERVAL 0.0–6.5 m

TIME – ROCK UNIT | BIOSTRATIGRAPHIC ZONE | FOSSIL CHARACTER: FORAMINIFERS, NANNOFOSSILS, RADIOLARIANS, DIATOMS | SECTION | METERS | GRAPHIC LITHOLOGY | DRILLING DISTURBANCE | SEDIMENTARY STRUCTURES | SAMPLES | LITHOLOGIC DESCRIPTION

Pleistocene

NN19 N22 early Pleistocene

N22

NN14 CN13

early Pleistocene NN19 (CN13a)

NN19 (CN13a)

Sections: 1, 2, 3, 4, CC

Meters: 0.5, 1.0

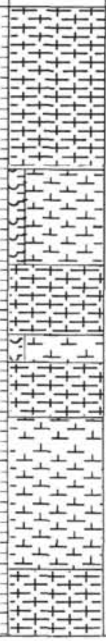

2.5YR N7

5GY 6/1

5Y 7/1

5GY 6/1

2.5YR N7

5GY 6/1

2.5Y N7

5Y 7/1

10YR 6/4

DOMINANT LITHOLOGIES:

(1) NANNOFOSSIL OOZE TO FORAM NANNOFOSSIL OOZE

Light gray (2.5YR N7) with rare black streaks (pyrite?)
Massive bedding slightly mottled

(2) FORAM NANNOFOSSIL OOZE TO NANNOFOSSIL OOZE, in sharp contact with dominant lithology (1)

Light yellowish brown (10YR 6/4)
Massive bedding

Minor lithology:
Siliceous nannofossil ooze, interbedded with dominant lithology (1), possibly gradational

Greenish gray (5GY 6/1) with rare black streaks

SMEAR SLIDE SUMMARY (%):

	1, 88	2, 6	2, 70	3, 94	4, 99	4, 124	CC
	D	D	D	D	D	D	D
Composition:							
Feldspar	Tr	Tr	–	–	–	–	–
Clay	–	–	–	–	–	Tr	2
Volcanic glass	–	Tr	–	Tr	–	–	–
Palagonite	Tr	–	Tr	Tr	Tr	Tr	Tr
Pyrite	–	Tr	Tr	–	–	–	–
Carbonte unspec.	–	–	–	–	–	–	3
Foraminifers	10	5	3	14	5	15	5
Calc. nannofossils	82	80	80	85	93	85	90
Diatoms	3	10	10	Tr	2	–	–
Radiolarians	5	3	5	Tr	Tr	–	–
Sponge spicules	Tr	2	2	Tr	Tr	–	–
Silicoflagellates	Tr	–	Tr	Tr	Tr	–	–

SITE 556 HOLE CORE H1 CORED INTERVAL 6.5–97.5 m

TIME – ROCK UNIT | BIOSTRATIGRAPHIC ZONE | FOSSIL CHARACTER: FORAMINIFERS, NANNOFOSSILS, RADIOLARIANS, DIATOMS | SECTION | METERS | GRAPHIC LITHOLOGY | DRILLING DISTURBANCE | SEDIMENTARY STRUCTURES | SAMPLES | LITHOLOGIC DESCRIPTION

Pliocene

late Pliocene (NN18)

late Pliocene NN18 (CN12d)

late early Pliocene (N9, NN15)

N19 – late early Pliocene

NN15 (CN11b)

Sections: 1, 2, 3, 4, 5, 6, CC

Meters: 0.5, 1.0

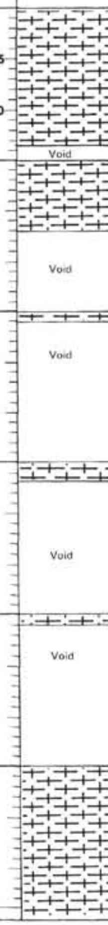

2.5Y N7

DOMINANT LITHOLOGY FORAM NANNOFOSSIL OOZE

Light gray (2.5Y N7) with green streak (Section 1) possibly altered ash

Massive bedding

Warning! – wash core, stratigraphic position is questionable

SMEAR SLIDE SUMMARY (%):

	CC
	D
Composition:	
Feldspar	Tr
Palagonite	Tr
Foraminifers	15
Calc. nannofossils	80
Discoasters	5

SITE 556 HOLE CORE H2 CORED INTERVAL 97.5–145.0 m

TIME – ROCK UNIT	BIOSTRATIGRAPHIC ZONE	FORAMINIFERS	NANNOFOSSILS	SECTION	METERS
upper Miocene	late Miocene (NN10–11)	Miocene (not determined/reworking/contamination)	NN10–11 (CN8–9d)	1, 2, 3, CC	0.5, 1.0

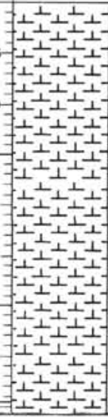

2.5Y N7

2.5Y N7

LITHOLOGIC DESCRIPTION

DOMINANT LITHOLOGY NANNOFOSSIL OOZE

Light gray (2.5Y N7) to white

Massive bedding

Warning! – wash core, stratigraphic position questionable

SMEAR SLIDE SUMMARY (%):

	1, 120	2, 50
	D	D
Composition:		
Heavy minerals	Tr	–
Clay	5	–
Palagonite	–	Tr
Pyrite	–	Tr
Foraminifers	5	9
Calc. nannofossils	85	76
Discoasters	5	15

SITE 556 HOLE CORE H3 CORED INTERVAL 145.0–192.5 m

TIME – ROCK UNIT	BIOSTRATIGRAPHIC ZONE	FORAMINIFERS	NANNOFOSSILS	SECTION	METERS
upper Miocene	earliest late Miocene (N14, NN9) *Globorotalia nepenthes/G. menardii*	N14	NN9 (CN7)	1, 2, 3, CC	0.5, 1.0

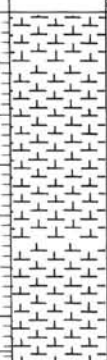

2.5Y N7

2.5Y N7

LITHOLOGIC DESCRIPTION

DOMINANT LITHOLOGY NANNOFOSSIL OOZE

Light gray (2.5Y N7)

Massive bedding

Warning! – wash core, stratigraphic position questionable

SMEAR SLIDE SUMMARY (%):

	1, 70
	D
Texture:	
Silt	2
Clay	98
Composition:	
Palagonite	Tr
Foraminifers	2
Calc. nannofossils	88
Fish remains	Tr?
Discoasters	10

SITE 556 HOLE CORE H4 CORED INTERVAL 192.5–461.5 m

TIME – ROCK UNIT	BIOSTRATIGRAPHIC ZONE	FORAMINIFERS	NANNOFOSSILS	SECTION	METERS
middle Miocene	middle Miocene (NN6–7)		CN4 (NN5) CN5 (NN6–7)	1, 2	0.5, 1.0
upper Oligocene	late Oligocene (P21/22, NP23–24)	P21/P22 (upper part P21/P22)	NP23–24 (CP18–19)		

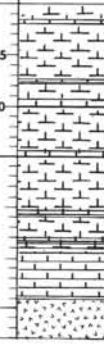

2.5Y N8 to 5Y 8/1

5Y 7/1

2.5Y N8

5Y 8/1

5YR 8/2

LITHOLOGIC DESCRIPTION

DOMINANT LITHOLOGIES:

(1) NANNOFOSSIL OOZE WITH MINOR CHALK, Section 1–Section 2, 90 cm

White (2.5Y N8–5Y 8/1

Rare faint blackish streaks

Massive bedding, except near contact with dominant lithology (2) where irregular bedding is distinguished by faint color changes

(2) NANNOFOSSIL CHALK, Section 2, 90–143 cm

Pinkish white

Massive bedding, but fractured by drilling

(3) LIMESTONE BASALT BRECCIA, Section 2, 143 cm and Core Catcher.

See Core 2 for description

Warning! – wash core, stratigraphic position questionable, except for recovered basalt.

SMEAR SLIDE SUMMARY (%):

	1, 76	2, 108	CC
	D	D	D
Composition:			
Quartz	–	1	–
Feldspar	–	–	1
Heavy minerals	–	Tr	–
Volcanic glass	–	1	–
Palagonite	–	–	Tr
Carbonate unspec.	5	2	3
Foraminifers	–	1	3
Calc. nannofossils	95	95	93
Sponge spicules	–	Tr	–

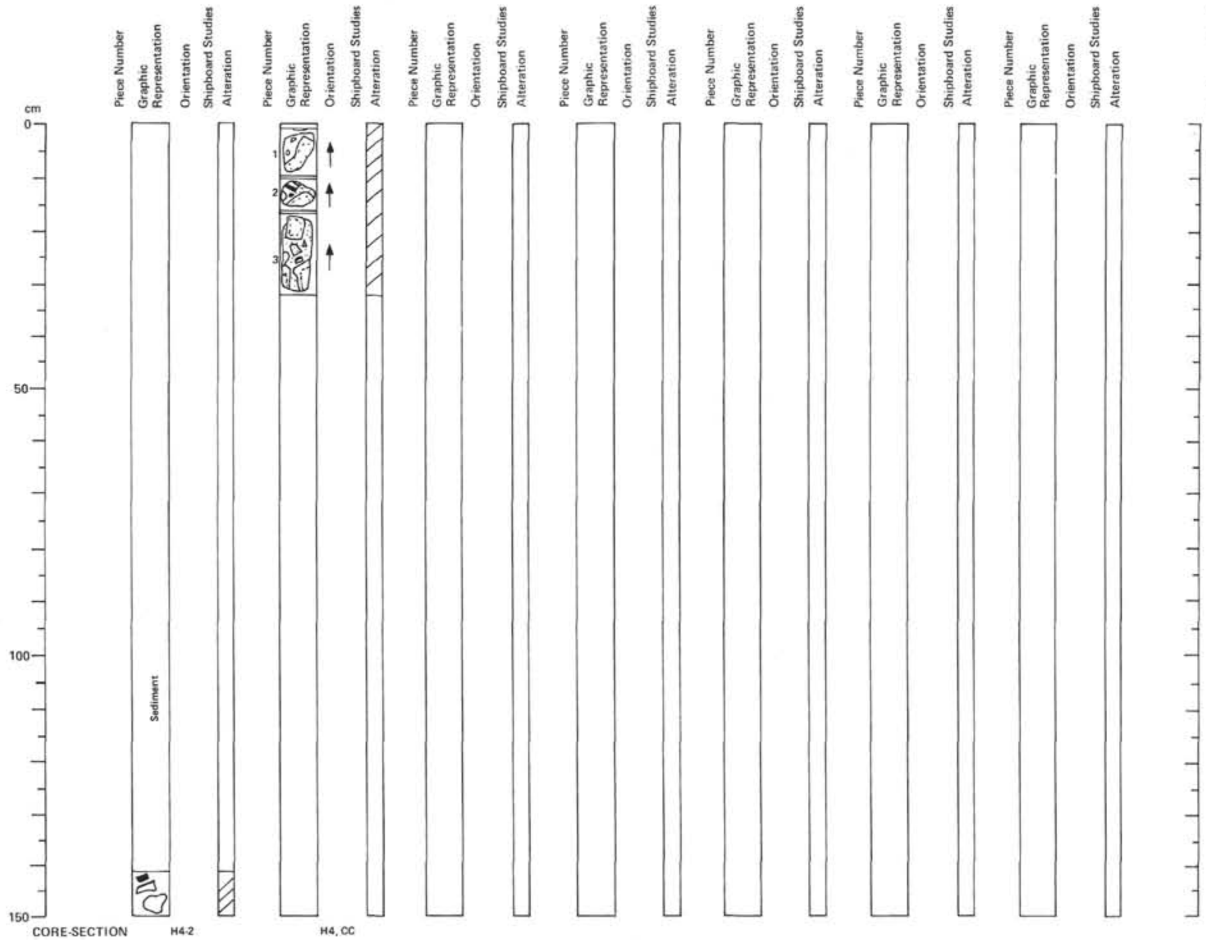

SITE 556, CORE H4

Depth 192.5–461.5 m

SECTION 2

Chalk – a clear calcite cemented breccia: 2 clasts moderately altered, fine grained aphyric basalt. Glass fragment weathered to dark brown palagonite. Minor fresh glass at center.

SECTION CC

Basalt breccia. Basalt is medium gray–gray (7.5YR N5), moderately altered and aphyric. Fine grained plagioclase and olivine (plagioclase ~0.5 mm, olivine up to 2 mm). Olivine is completely replaced by smectite. Vesicles are very rare and not filled.

Some of the basalt pieces show a vitric rim, which is mostly altered (in Piece 2 it looks like fresh glass).

The breccia is indurated by a calcite cement.

The cement, which fills up nearly all space between the basalt pieces, sometimes shows drusy cavities.

SITE 556 HOLE CORE 2 CORED INTERVAL 461.5–471.0 m

TIME – ROCK UNIT	BIOSTRATIGRAPHIC ZONE	FOSSIL CHARACTER: FORAMINIFERS	NANNOFOSSILS	RADIOLARIANS	DIATOMS	SECTION	METERS	GRAPHIC LITHOLOGY	DRILLING DISTURBANCE	SEDIMENTARY STRUCTURES	SAMPLES	LITHOLOGIC DESCRIPTION
a) from Core 3, Section 1, 0–5 cm; lower Oligocene	latest early Oligocene NP23 (CP17)		Bottom of NP23 (CP17)			1, 2, 3, 4, 5, 6	0.5, 1.0	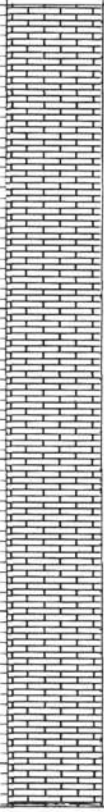				vug; vug; vug

DOMINANT LITHOLOGY LIMESTONE BASALT BRECCIA

Poorly sorted, with clast size ranging from boulders to coarse sand. Boulder size clasts are prominent at three intervals in the core (Section 6, base of Section 4, and base of Section 2).

Volcaniclasts are dominated by fresh, gray (7.5YR N5) to weathered, pinkish gray (7.5YR 6/2) basalt (moderately plagioclase-phyric) along with both fresh and altered, grayish green (5G 4/2) to dark brown (7.5YR 3/2) volcanic glass.

Biogenic limestone (nannofossil limestone and chalk) pinkish white (5YR 8/2) to light gray (10YR 7/1) not only makes up the matrix of the breccia but also provides subrounded intraclasts, and fracture filling in the basalt clasts. Both limestone clasts and matrix are recrystallized discontinuously, as veins, to sparite and in places the entire limestone matrix and clasts have been recrystallized to sparite with solution vugs. Also, basalt clasts are rimmed by very fine microcrystalline calcite.

Please note that the original recovered interval has been expanded by spacers separating broken sections of core.

[a] Note: base of this lithology is nanno chalk in Core 3, Section 1, 0–5 cm in contact with basalt flow.

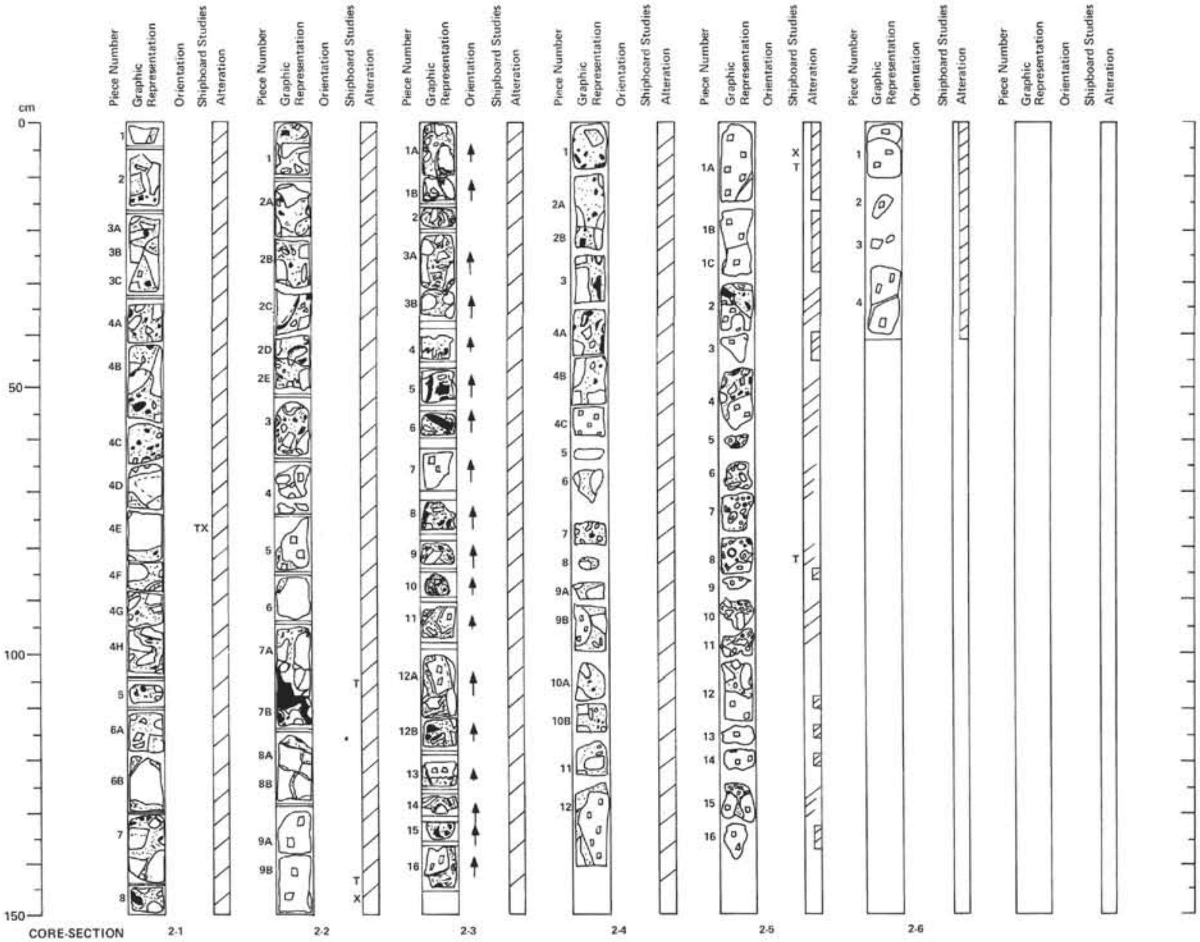

SITE 556, CORE 2 Depth 461.5–471.0 m

SECTION 1

Basalt breccia – indurated calcareous chalk matrix with ~5% drusy clear calcite.

Clasts:

1 – Fine grained, medium gray (7.5YR N5) aphyric to sparsely phyric basalt. Dark brown (7.5YR 4/4) altered olivine? (to 1 mm) varying 0–2% rarely to ~ 5%. Light brown–pinkish gray (7.5YR 6/2) weathered margins to 1 cm thick on some clasts.

2 – Dark brown altered glass fragments and occasional glass rims. Some unaltered glass in centers of larger pieces.

Thin Section: Intergranular aphyric basalt; round vesicles (0.5–1%) filled with calcite.

SECTION 2

Basalt breccia as in Section 1.

Clasts as in Section 1 with addition of: sparsely plagioclase phyric basalts at 65–70, 75–85, and 130–150 cm. Equant plagioclase phenocrytts to 5 mm ingreasing downhole to ~3%.

95–115 cm: Strong development of dark green–grayish green (5G 4/2) pumpellyite(?) in glass fragments and glass rim. Chalk matrix stained pink.

110 cm: Fresh glass fragment.

Thin Section: Intersertal, sparsely plagioclase-phyric (<2%) basalt. Olivine in groundmass (~5%) is altered to clay. Other groundmass minerals: plag (30%), cpx (40%), magnetite (3%); mesostasis (15%).

SECTION 3

0–5 cm: Drusy calcite vein.

Basalt breccia as in Sections 1 and 2.

Clasts: Basalt and glass as in Sections 1 and 2 becoming moderately plagioclase phyric downhole.

55–57 cm: Fresh glass fragment.

SECTION 4

Basalt breccia – matrix as in Sections 1–3.

Clasts:

1 – Few reworked chalk fragments.

2 – Sparsely to moderately plagioclase phyric basalt as in Sections 2–3.

3 – Altered glass as in Sections 1–3 becoming larger with larger fresh centers.

45 cm: Fresh glass.

130 cm: Drusy calcite vein.

SECTION 5

0–70 cm: Basalt breccia – chalk matrix. Large clasts all fresh to moderately weathered, moderately plagioclase phyric basalt as in Sections 2–4. Smaller angular fragments of weathered glass with fresh cores as in Sections 1–4.

32 cm: Fresh glass.

70–130 cm: Calcite cemented polymict breccia. Basalt clasts as above, however generally weathered light brown–pinkish gray (7.5YR 6/2) and more rounded. Few well rounded weathered glass fragments. Tabular to well rounded reworked chalk clasts abundant in parts. Cement is white, finely crystalline calcite with numerous drusy vug linings. Solution channel(?) – above basement.

130 cm: Probable start of basalt pillows.

Thin Section: Intergranular, moderately plagioclase-phyric (2–3%) basalt. Glomerophyric clusters of plagioclase, which often have many liquid inclusions. Groundmass: ol (20%), pl (30%), cpx (40%); vesicles are rare and filled with clay.

SECTION 6

Moderately plagioclase phyric basalt as in Sections 2–5. No matrix present – probably first flow material.

35 cm: 2 mm clear drusy calcite vein.

SITE 556 HOLE CORE 3 CORED INTERVAL 471.0–480.0 m

TIME – ROCK UNIT	BIOSTRATIGRAPHIC ZONE	FOSSIL CHARACTER: FORAMINIFERS	NANNOFOSSILS	RADIOLARIANS	DIATOMS	SECTION	METERS	GRAPHIC LITHOLOGY	DRILLING DISTURBANCE	SEDIMENTARY STRUCTURES	SAMPLES	LITHOLOGIC DESCRIPTION
						1	0.5 1.0	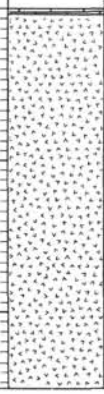				BASALT LIMESTONE BRECCIA AND PLAGIOCLASE PHYRIC BASALT Section 1, 0–5 cm: Basalt limestone breccia, See Core 2 for description. The remaining core is described in the Visual Core Descriptions for Igneous Rocks.
						2						
						3						

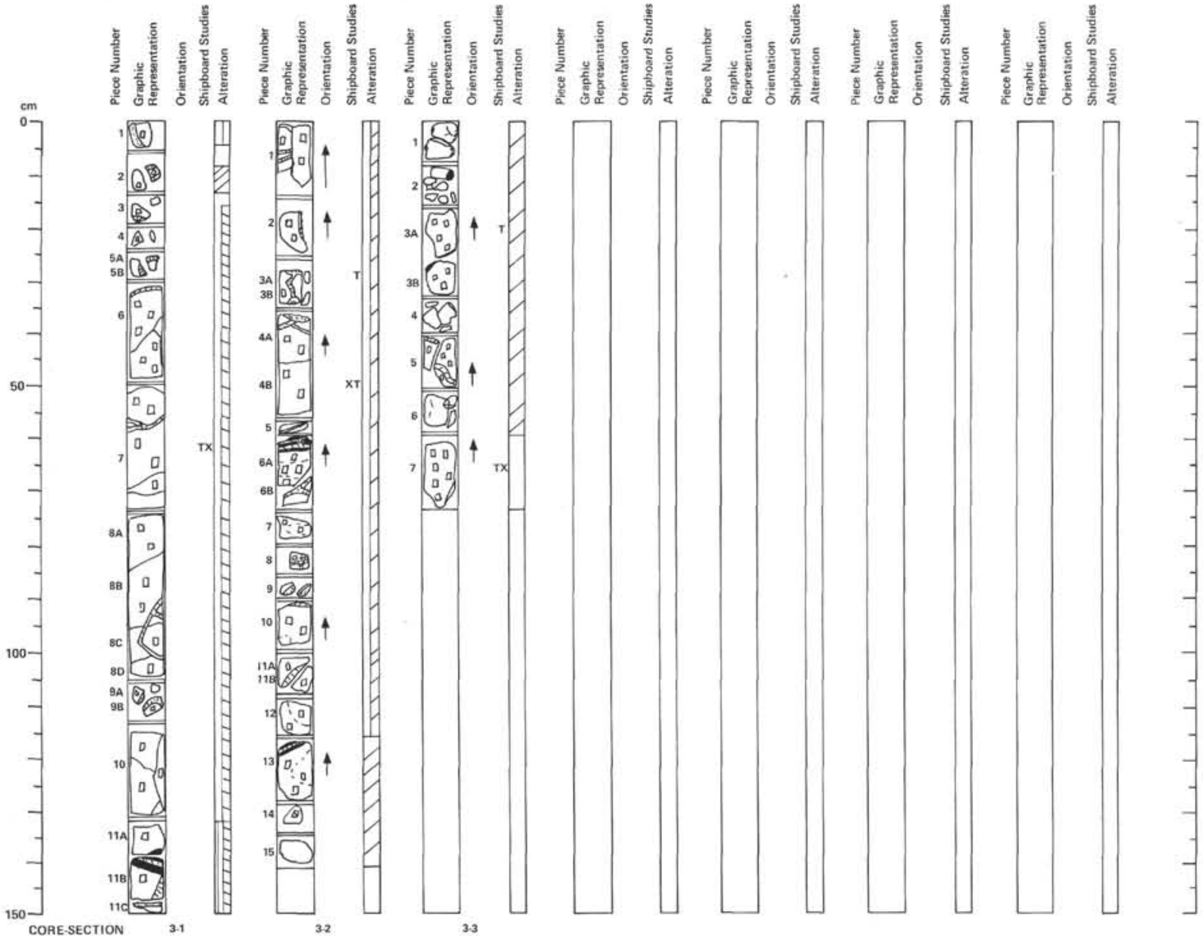

SITE 556, CORE 3 Depth 471.0–480.0 m

SECTION 1

LIMESTONE BASALT BRECCIA AND PLAGIOCLASE PHYRIC BASALT

0–5 cm: Limestone basalt breccia, see description of Core 2.

5–150 cm: Fine grained, moderately phyric basalt, dark gray (2.5YR N4). Equant plagioclase phenocrysts (~5 mm) up to 5%. Minor olivine (~1 mm) that is weathered dark grayish brown (2.5Y 4/2). Minor calcite veins are present.

138 cm: ~1 cm, thick glass band (wedge shaped) about 50% weathered to dark brown (7.5YR 3/2).

Thin Section at 63–65 cm: Moderately plagioclase phyric (5–7%), hyalophitic basalt; traces of olivine phenocrysts (mostly altered). Mesostasis (20–23%) devitrified and partially altered (1–3%) to clay; groundmass: ol (5%), plag (35%), cpx (35%). Vesicles (~1%) are filled with clay.

SECTION 2

PLAGIOCLASE PHYRIC BASALT

Same as in Section 1 although slightly more weathered with ~1% round amygdules (1 mm) filled with dark clay minerals. Calcite veins (1–2 mm wide) are common.

61 and 115 cm: Intervals of fresh glass, heavily veined by carbonate.

Thin Section at 30–33 cm: Sparsely plagioclase-phyric (~2%), hyalophitic basalt; groundmass: ol (3%), plag (30%), cpx (30%); mesostasis (~23%) is devitrified glass, partly altered to clay (chlorite?). Rare vesicles (<1%) filled with clay; fractures and veins filled with calcite.

SECTION 3

PLAGIOCLASE PHYRIC BASALT

Similar to Sections 1 and 2, medium gray (2.5Y N5) with prismatic plagioclase phenocrysts (up to 7 mm), 2%. Calcite veins are common.

Thin Section at 65–67 cm: Plagioclase-phyric (~5%) hyalopilitic basalt; olivine phenos also present (~2%); groundmass: pl (30%), cpx (<10%), ol (<1%), opaques (<1%); mesostasis (~50%) devitrified glass.

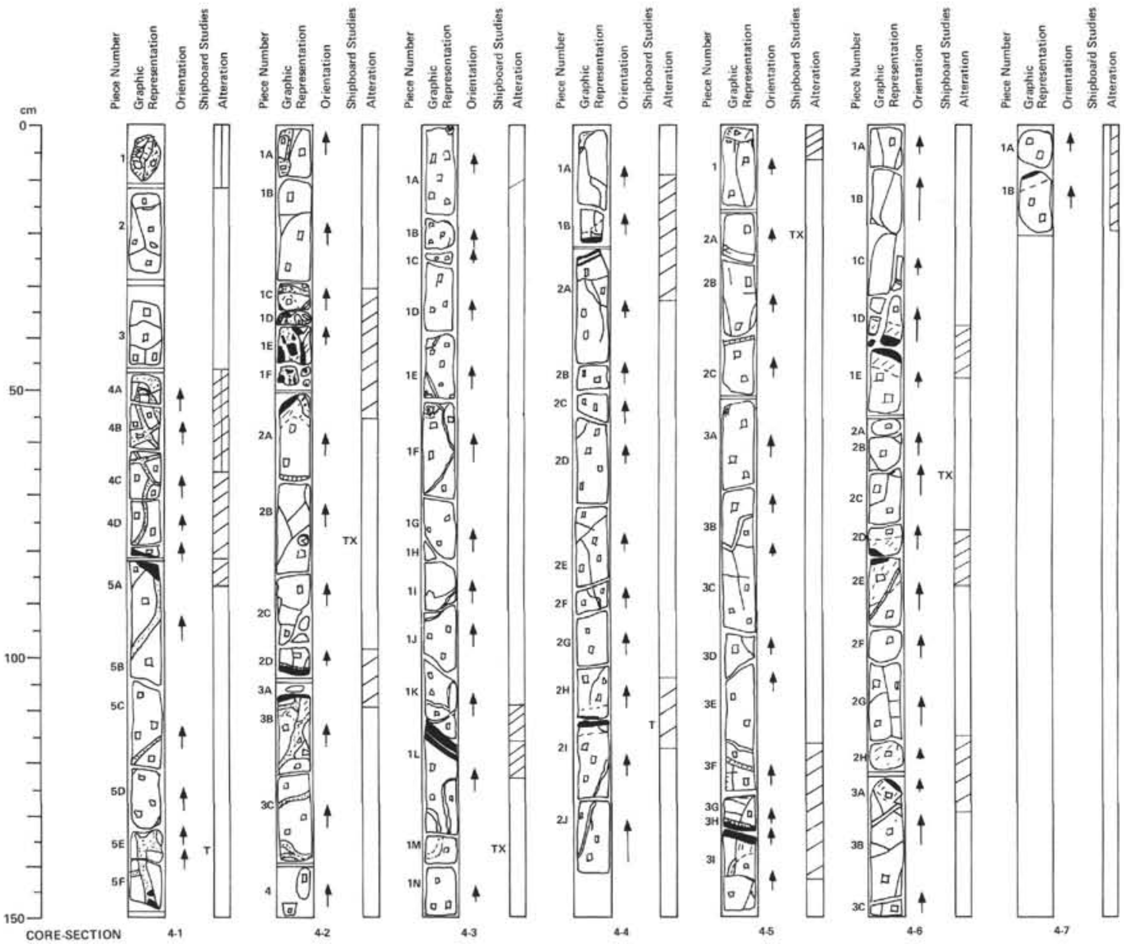

SITE 556, CORE 4

Depth 480.0–489.0 m

SECTION 1

PLAGIOCLASE PHYRIC BASALT (BRECCIA)

0–10 cm: Fine grained, phyric basalt breccia, grayish brown (2.5Y 5/2) with plagioclase phenocrysts (4 mm). Finer matrix cemented by calcite.

10–150 cm: Fine grained, phyric basalt, dark gray (7.5YR N4). Plagioclase phenocrysts are common (5–10% and often partially reabsorbed, size is <10 mm. Olivine (1%) is mostly altered to smectite.

79–84 cm: Vitric rims separating two pillows?

Infilling the fractures is pale yellow (5Y 7/3) nannofossil chalk. Geopetal structures are common, showing that the sediment has filtered into the basalt after its emplacement. In some places this sediment has been completely recrystallized to calcite.

Thin Section at 45–47 cm: Volcanic intralclastic chalk is composed of the following: volcaniclastics (< 2 mm) 10%, foraminifers 5%, intraclasts (micrite) 30% and with a micrite matrix 55%. Clasts are poorly sorted, angular to subrounded; but do show stratification (geopetal).

SECTION 2

PLAGIOCLASE PHYRIC BASALT

Plagioclase phenocrysts (<10 mm to 15 mm) and fine- to medium-grained, dark gray (7.5YR N4/0) phyric basalt make up 5–10%. Fresh olivine (~2–3 mm in diameter) is rare. Olivine is usually altered to smectite. Vesicles are either filled with smectite or with calcite.

33–54 and 101–108 cm: Vitric rims occurring between different pillows. Close to the glass the basalt is moderately altered. Fractures that occur in fresh regions are filled with pale yellow (5Y 7/3) nannofossil chalk.

Thin Section at 80–88 cm: Plagioclase-phyric (~ 10%), vitrophyric basalt; olivine-phenocrysts up to 1%; groundmass: plag (40%), ol (2%); devitrified glass (45%); segregation vesicles are rare and filled with smectite(?).

SECTION 3

PLAGIOCLASE PHYRIC BASALT

0–110 cm: Same unit as Section 2.

51–56 cm: Sediment-dendritic pattern, penetrating the basalt from a fracture.

110–150 cm: Fine grained gray (2.5Y N5) plagioclase phyric (<5%) basalt. Plagioclase phenocrysts are rounded (partial resorbed), upper portion has glass rim.

120–134 cm: has 'chlorite?' filled amygules (2–4%) and fewer phenocrysts.

128–137 cm: Alteration zone.

SECTION 4

APHYRIC AND PLAGIOCLASE PHYRIC BASALT

0–22 cm: Fine to medium grained aphyric basalt. Color medium gray (2.5YR N5/0). Fractures filled with carbonate. Vitric rim at the bottom.

22–140 cm: Medium grained phyric basalt. Color dark gray (2.5YR N4/0). Vitric rims at top and bottom with moderately altered zones beside them. Fractures filled with carbonate. Plagioclase phenocrysts (< 10 mm). Percentage of phenocrysts increases from top to bottom (5–15%).

112 cm: Vitric rim with fractures filled by smectite and carbonate.

Thin Section at 110–113 cm: Plagioclase-glomerophyric (3–5%), vitrophyric to tachylitic basalt; groundmass: plag (35%), cpx (~ 2%); glass of groundmass is mostly devitrified (55%) and shows dots of ore minerals (magnetite?).

SECTION 5

PLAGIOCLASE PHYRIC BASALT

Medium grained phyric basalt. Color dark gray (2.5YR N4/0). Plagioclase phenocrysts (< 15 mm) 5–10%. Vesicles partly round and partly irregular shaped. Fractures partly filled with carbonate.

130–135 cm: Vitric bottom of upper and vitric top of lower unit.

Thin Section at 32–34 cm: Plagioclase-glomerophyric (3–5%), vitrophyric to tachylitic basalt; groundmass: plag (35%), cpx (2%); glass is devitrified (~55%) and shows dots of ore; vesicles (<1%) are filled with clay.

SECTION 6

PLAGIOCLASE-PHYRIC BASALT

0–42 cm: Same as bottom of Section 5. Vitric rim at bottom.

42–150 cm: Fine grained gray (2.5Y N5/0) basalt with vitric rim at top and bottom. Plagioclase-phyric (~5–10%, <14 mm). Fractures are filled with carbonate.

82–122 cm: Vitric rims.

SECTION 7

PLAGIOCLASE-PHYRIC BASALT

Moderately plagioclase-phyric basalt as in Section 6.

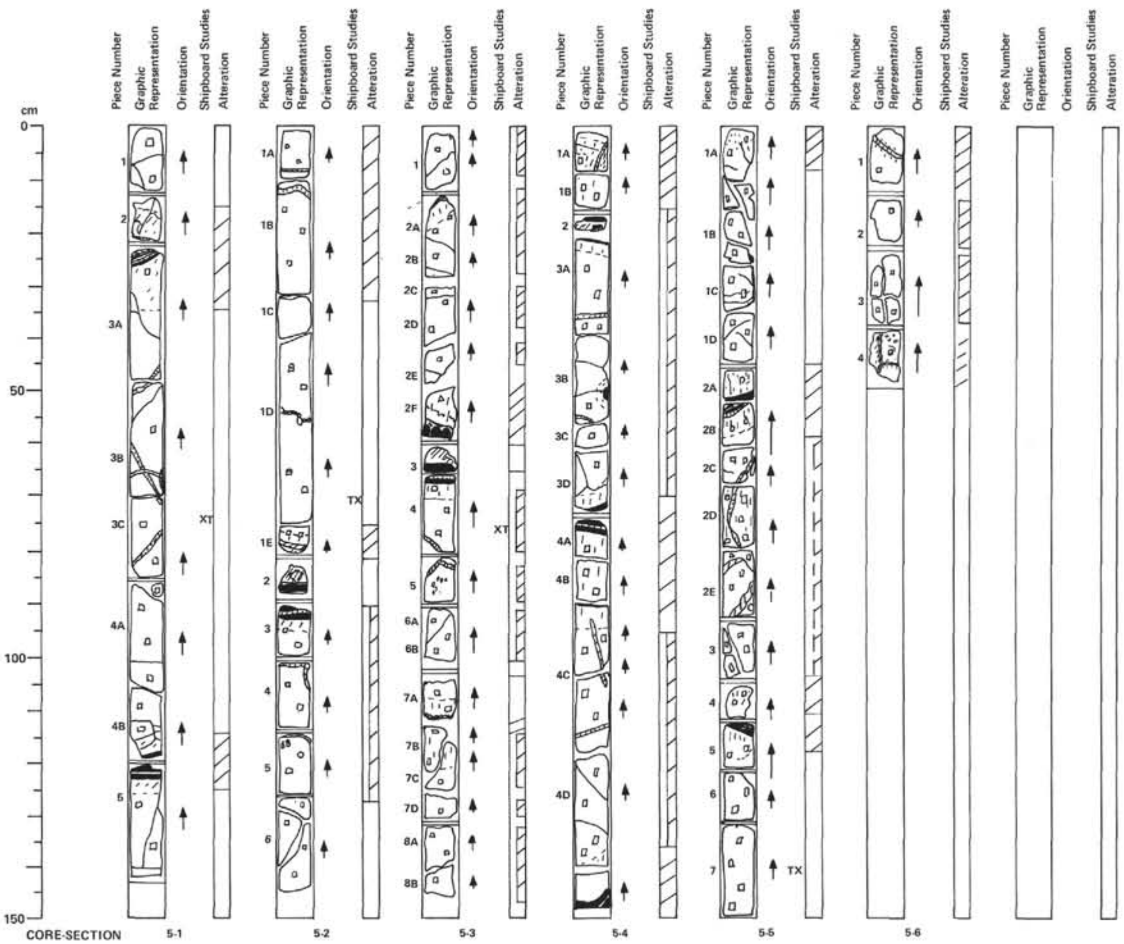

SITE 556, CORE 5 Depth 489.0–498.0 m

SECTION 1

PLAGIOCLASE PHYRIC BASALT

Medium grained, plagioclase-phyric basalt. Color medium gray (7.5YR N5/0). Plagioclase about 5 mm to 8 mm (~5%) and mostly anhedral (resorbed). Round amygdules filled with smectite. At 55 cm patchy vesicles filled with (smectite?) clay minerals occur. At the top of Pieces 3 and 5 there are multiple vitric cooling rims. Calcitic and clayey fracture fillings are common.

0–23 cm: Lower part of pillow.

23–118 cm: Separate pillow.

118–143 cm: Upper part of pillow.

Thin Section at 75–78 cm: Intersertal to intergranular plagioclase-phyric basalt; plagioclase occurs in glomerophyric clusters and is often resorbed; groundmass: plag (50%), cpx (40%); mesostasis (10%) looks like devitrified glass.

SECTION 2

PLAGIOCLASE PHYRIC BASALT

Moderately plagioclase phyric basalt throughout as in Section 1 and above. Minor carbonate veins (shown with hatched [=] pattern). Color gray (7.5YR N5).

1–32 cm: Vesicular < 5% rounded vesicles filled with moderate green (5G 5/6) clays(?) and/or white calcite.

Thin Section at 70–73 cm: Hyalophitic, plagioclase-phyric (~5%) basalt; olivine phenocrysts are present (~1%) but altered or corroded (skeletons). Groundmass: plag (35%), cpx (4%), ol (1%); glass (devitrified) (55%) with opaques; like the olivine, cpx is often replaced by clay minerals.

83–87 cm: Fresh glass and carbonate.

SECTION 3

PLAGIOCLASE PHYRIC BASALT

Moderately plagioclase phyric basalt throughout the core section as in Sections 1 and 2. Minor carbonate veins (shown by hatched [=] pattern). (Gradational alteration indicated by [··], as per legend.) Color gray (7.5YR N5)

82–90 cm: Note the calcite veins within the top of the sample. Irregular vesicles (denoted by) filled with dark greenish clays.

SECTION 4

PLAGIOCLASE PHYRIC BASALT

Sparsely to moderately plagioclase phyric basalt as in Sections 1–3. Phenocryst abundance gradually decreasing downhole.

SECTION 5

PLAGIOCLASE PHYRIC BASALT

0–5 cm: < 5% small vesicles mostly empty, some with calcite. Sparsely to moderately plagioclase phyric basalts as in Sections 1–4, dark gray (7.5YR N4).

50 cm: Fresh to moderately altered glass with calcite vein (bottom of upper pillow).

54 cm: Fresh to moderately altered glass (top of pillow).

65–70 cm: Moderate sized calcite vein.

85–90 cm: Pinkish gray (7.5YR 7/2) vein of carbonate cement with small pieces of basalt and altered glass.

100 cm: Larger (12 mm) equant plagioclase phenocryst.

113–115 cm: Glass with calcite vein containing angular pieces of fresh glass with altered rims; top of pillow.

Thin Section at 140–143 cm: Moderately plagioclase-phyric (~3%), intergranular to intersertal basalt; plagioclase phenocrysts often show liquid inclusions. Groundmass: plag (50%), cpx (30%), ol (~1%); mesostasis (15%) is devitrified glass, containing opaques (magnetite?).

SECTION 6

PLAGIOCLASE PHYRIC BASALT

Slightly to moderately plagioclase phyric basalts, as in Sections 1–5.

38–46 cm: Irregular vesicles filled with calcite.

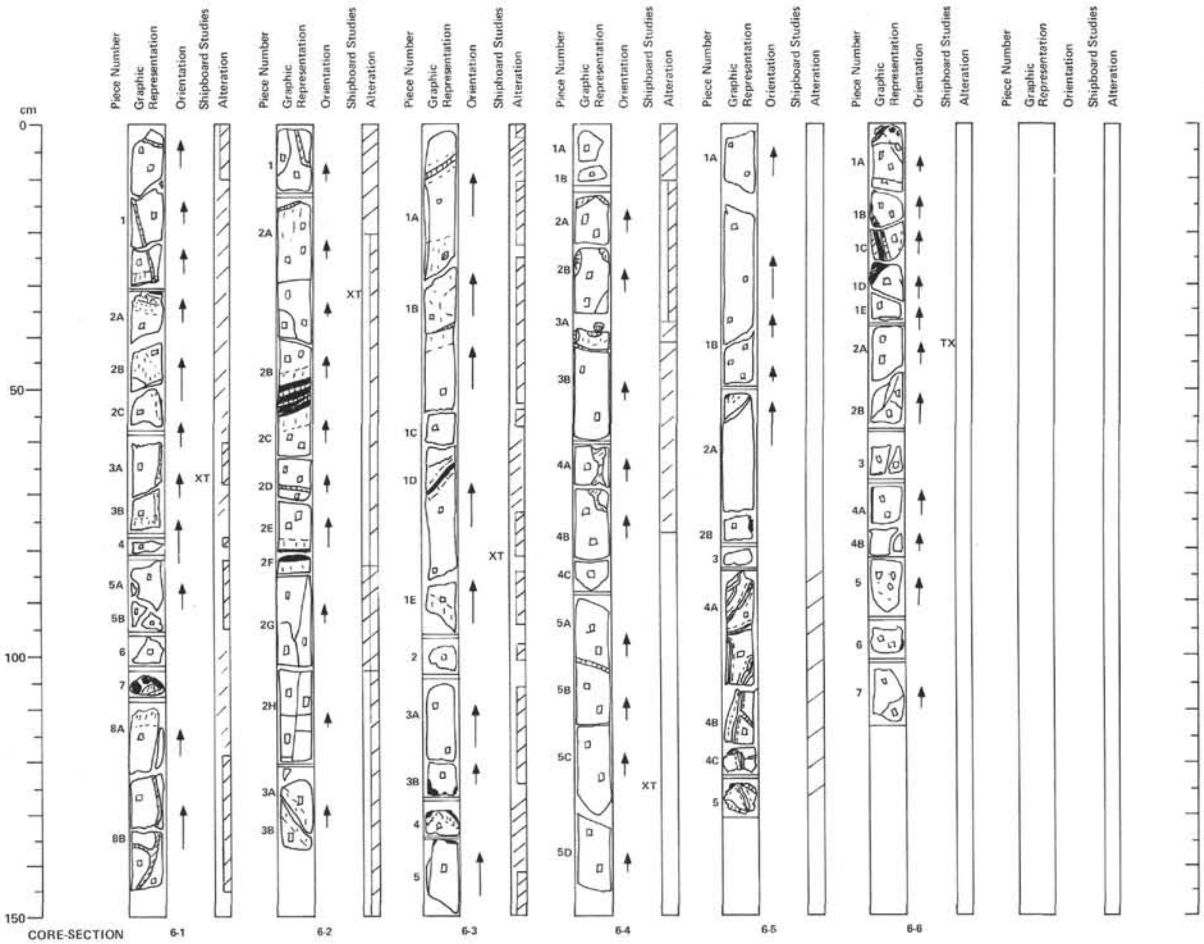

SITE 556, CORE 6 — Depth 498.0–507.0 m

SECTION 1

PLAGIOCLASE PHYRIC BASALT

Slightly to moderately plagioclase phyric basalt decreasing in frequency and becoming more rounded down the core. Irregular vesicles found throughout, often with greenish clay or calcite included. Color 7.5YR N6/0.

33–40 cm, Piece 2A: Altered multiple glass rinds separated by calcite veins. Small unaltered pieces of glass remain. Irregular vesicles throughout entire unit 2.

101–107 cm, Piece 7: Altered glass and calcite, dark brown to black glass, white calcite, ruddy orange zone between the two (color 5YR N6/6).

Thin Section at 65–68 cm: Sparsely plagioclase-phyric (~2%) intergranular basalt; groundmass: cpx (45%), plag (30%), ol (20%), magnetite (5%); olivine is mostly altered to clay minerals.

SECTION 2

PLAGIOCLASE PHYRIC BASALT

Sparsely plagioclase phyric basalt as in Section 1. Phenocrysts (~3%) prismatic to rounded, up to ~4 mm maximum dimension. Minor calcite veins to ~1 mm. Light brown weathering along many cracks.
many cracks.

Thin Section at 32–35 cm: Moderately plagioclase-phyric (~5%) basalt, minor ol-phenocrysts are present (<1%); groundmass: plag (45%), cpx (45%), ol (5%), magnetite (5%); vesicles occur up to 1% and are filled with clay; olivine and partly cpx are replaced by clay minerals.

SECTION 3

PLAGIOCLASE PHYRIC BASALT

Sparsely plagioclase phyric basalt as in Sections 1 and 2.

0–60 cm: 2–3% vesicles to 1 mm. Most filled with dark green (5G 5/2) clay(?) or chlorite.

0–45 and 90–95 cm: Weathered zones greenish brown (2.5Y 5/4) in color in contrast to normal light brown (7.5YR 6/4).

Thin Section at 80–83 cm: Moderately plagioclase-phyric (~3%) intergranular to intersertal basalt containing traces of olivine phenocrysts; the normally zoned plagioclase-phenocrysts show liquid inclusions; groundmass: cpx (45%), plag (35%), ol (0.5%), magnetite (5%); mesostasis (~5%) is altered to clay, olivine is replaced by clay minerals, too

SECTION 4

PLAGIOCLASE PHYRIC BASALT

Sparsely plagioclase phyric basalt as in Sections 1–3. Calcite veins open in several places to drusy cavities.

25 cm: Dark green chlorite(?) in cavity in calcite vein (XRD – chlorite and montmorillonite [dioctahedral]).

SECTION 5

PLAGIOCLASE PHYRIC BASALT

Moderately plagioclase phyric basalts to sparsely plagioclase phyric down core. Color dark gray (7.5YR N4).

80 cm: Major(?) break – increase in occurrence and complexity of calcite vein pattern. Noticeable small (<0.1 mm) orange brown patches in irregular vesicles, iddingsite? (probably clay alteration product). Alteration along calcite veins. (Steroscopic examination further suggests highly weathered olivines–iddingsite?.) Gradient in color most noticeable from 80 cm down, gray (7.5YR N6). Less crystalline, more massive character.

SECTION 6

PLAGIOCLASE PHYRIC TO APHYRIC BASALT

Fine grained, sparsely plagioclase phyric to aphyric basalt with small plagioclase laths and 1–2% equant plagioclase phenocrysts (similar to 85–130 cm in Section 5).

Color medium gray (7.5YR N6); red brown altered olivines.

17–30 cm: Large calcite vein to fresh altered glass

Thin Section at 44–47 cm: Aphyric, intergranular basalt; microphenocrysts: plag (2–3%); groundmass: cpx (50%), plag (25%), ol (10%), clay minerals (5–10%).

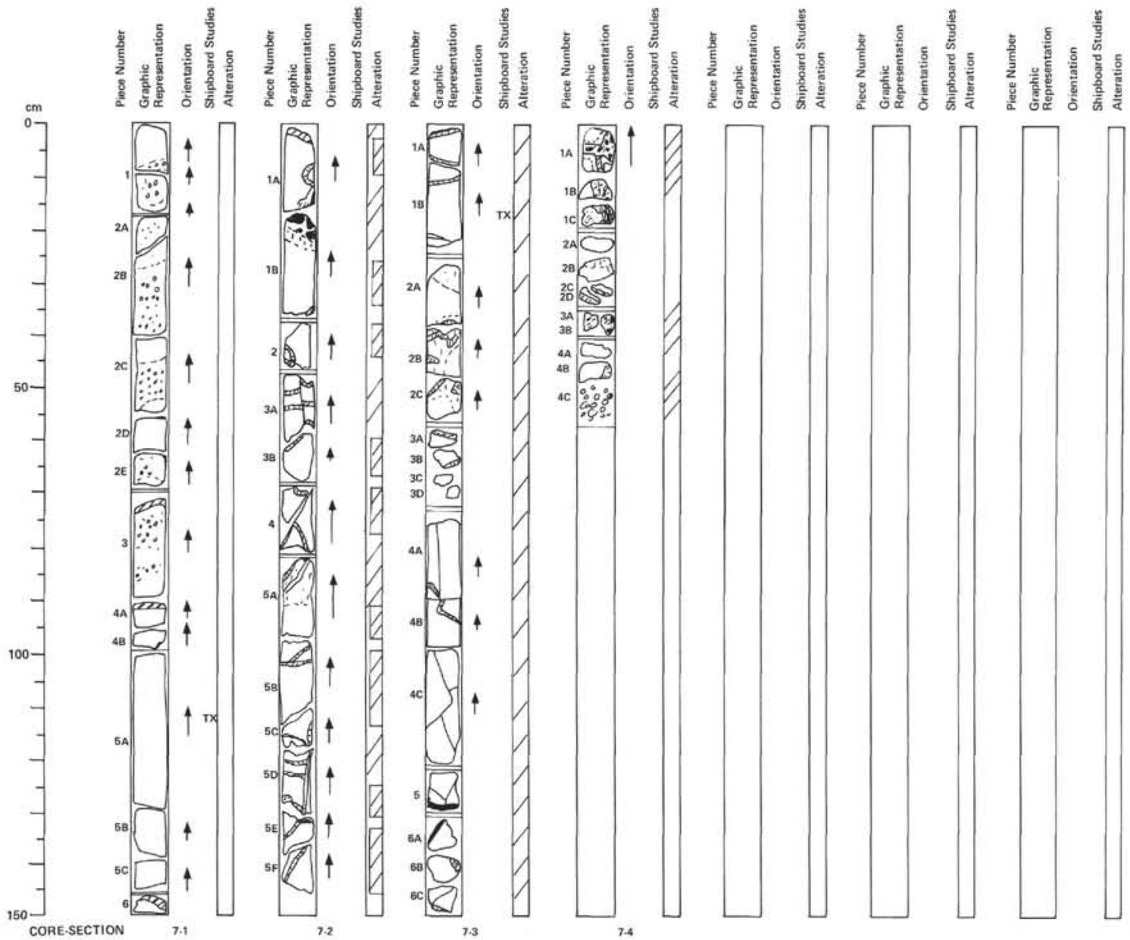

SITE 556, CORE 7 — Depth 507.0–516.0 m

SECTION 1

APHYRIC BASALT

Fine grained, light gray (7.5YR N6) aphyric basalt to sparse equant plagioclase phenocrysts up to 3 mm. Varying amounts (up to 3–4%) of vesicles (≤3%) up to 1 mm, most are empty, but some are filled with calcite. Sparse altered red-brown (7.5YR 6/8) olivine(?) phenocrysts up to 1 mm.

Thin Section at 113–115 cm: Intergranular to subophitic sparsely plagioclase phyric (1–3%) basalt. Plagioclase phenocrysts show liquid inclusions, their approximate composition is An_{88}. Groundmass: plag (40%), cpx (35%), ol (10%), magnetite (5%). Olivine and mesostasis are partly replaced by clay.

SECTION 2

APHYRIC BASALT

Aphyric, fine grained basalt with patches of slightly plagioclase phyric basalt mainly in the top 35 cm. Color light gray (7.5YR N6).

13–20 cm: Glass fragments imbedded in and reacted with calcite.

Irregular vesicles throughout, extensive about the calcite veins. Vesicles empty, or containing green clay or calcite. Altered olivine crystals (<1.5 mm) to iddingsite product.

SECTION 3

APHYRIC BASALT

Aphyric fine grained basalt with scattered equant plagioclase phenocrysts as in Section 2. Vesicles scarce.

Thin Section at 17–19 cm: Aphyric to sparsely plagioclase-phyric (< 1%) intergranular to intersertal basalt; plagioclase laths are resorbed. Groundmass: plag (35%), cpx (35%), ol (10%), magnetite (5%). Round vesicles (<1%) are filled with clay. Parts of olivine and mesostasis are replaced by clay.

SECTION 4

APHYRIC BASALT

Vesicular aphyric basalt, light gray (7.5YR N6). High degree of calcite vein intrusion, causing distinct alteration about veins, light brown (10YR N6/2) in color. Glass fragments in Pieces 1A and C.

35–38 cm, Pieces 3A and B: Calcareous sediment(?) positive acid test.

48–57 cm, Piece 4C: Gravel, mixture of small aphyric basalt and calcite chips.

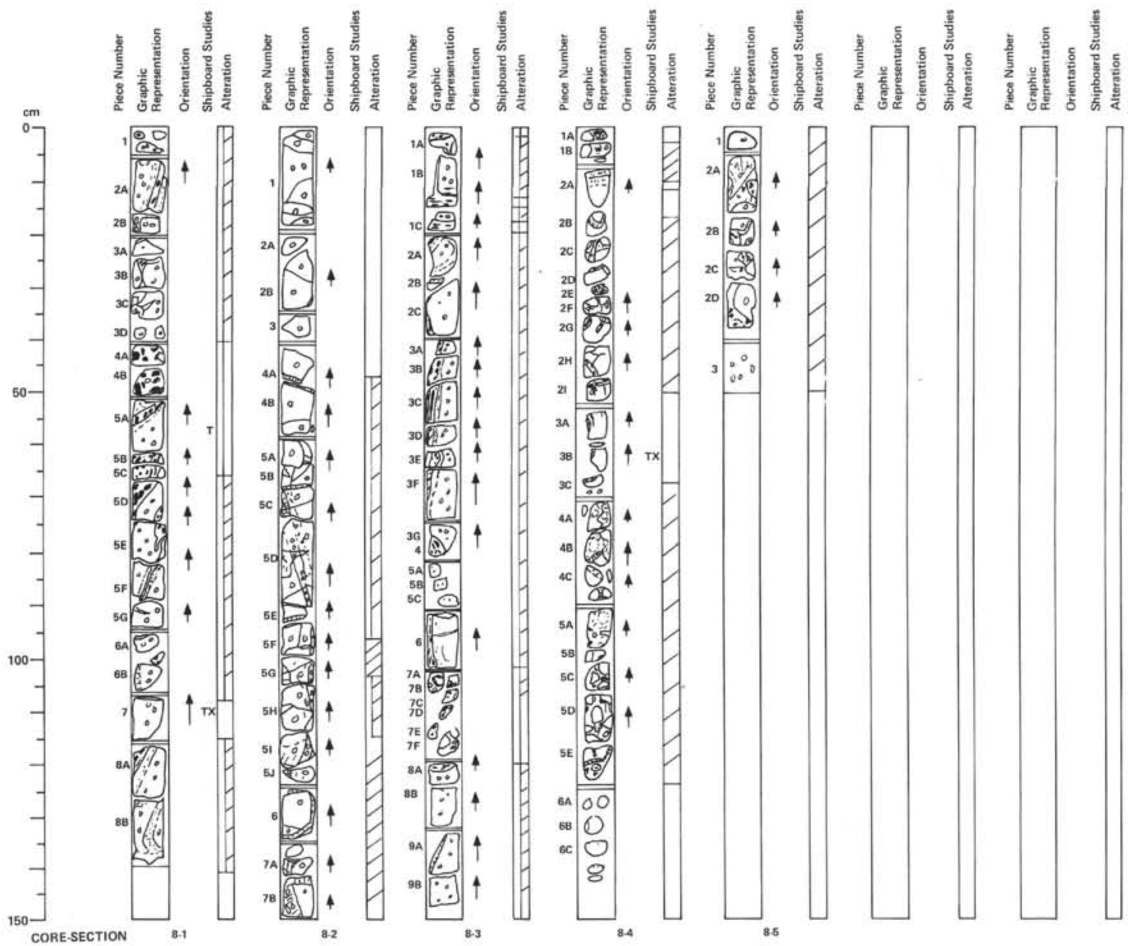

SITE 556, CORE 8 Depth 516.0–525.0 m

SECTION 1

OLIVINE MICRO-PHYRIC BASALT

0–5 cm: Moderately plagioclase and olivine micro-phyric basalt, plagioclase ~ 5% anhedral and partially resorbed, olivine 5–7% altered.

5–140 cm: New unit – moderately olivine micro-phyric basalt, color gray (7.5YR N6/0), fine grained. Olivines are altered, 5% rounded vesicles.

40–50 and 60–68 cm: Broken pieces of glass and/or basalt which have altered to palagonite. Some pieces of palagonite have basalt cores. All pieces are cemented with micrite and then spary calcite cement.

Thin Section taken to compare altered and fresh basalt, and cemented palagonite pieces.

Thin Section at 110–113 cm: Sparsely phyric to aphyric intersertal to intergranular basalt. Microphenos: ol (3%), plag (1%), cpx (1%); groundmass: cpx (45%), plag (30–35%), magnetite (3%); segregation vesicles (1%) filled with devitrified glass and carbonate; olivine is completely altered to clay.

SECTION 2

OLIVINE MICRO-PHYRIC BASALT

Moderately olivine micro-phyric, gray (7.5YR N6/0) basalt. Olivine is mostly altered into smectite. Olivine: ~5–7%; size ≧1 mm. There are some large equant (some >5 mm), light-colored phenocrysts in the upper 35 cm of this section (plagioclase?). Vesicles are common and empty. The whole section is highly fractured. Some fractures are filled with sparry calcite cement (see Pieces 4, 6, and 7). From 68 to 120 cm a fracture occurs which is filled with highly palagonitized basalt breccia. The same occurs in Piece 7. These brecciated fractures have palagonite edges.

Piece 5C, 68–74 cm:

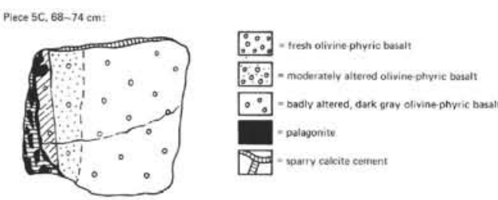

SECTION 3

OLIVINE MICRO-PHYRIC BASALT

See Section 2 description for details of this moderately olivine micro-phyric basalt (≈10% olivine).

Rare (2 mm) partially resorbed plagioclase phenocrysts are found in Pieces 1B, 8–10 cm; 1C, 23–24 cm; and 3E, 62 cm.

SECTION 4

OLIVINE MICRO-PHYRIC BASALT

Moderately olivine micro-phyric basalt; color light brownish gray to gray (2.5Y 6/2–2.5Y 6/0). Olivine (up to 10%), mostly altered (diameter = 0.8–1 mm). Almost whole section is brecciated and shows palagonitization and calcite cementation in and close to the fractures and veins.

Thin Section at 63–66 cm: Hyalophitic basalt; groundmass: cpx (40%), plag (25–30%), ol (<5%), magnetite (3%); rest: devitrified glass (25–30%); vesicles (3%) are round and filled with calcite, some of them show segregation. Olivine is replaced by clay.

SECTION 5

OLIVINE MICRO-PHYRIC BASALT (BRECCIA)

Larger basalt pieces: light brownish gray (2.5Y 6/2) olivine micro-phyric basalt, moderately altered; with mostly empty round vesicles. Pieces are fairly rounded. Smaller pieces: basalt as above and palagonite pieces. The breccia is cemented by calcite.

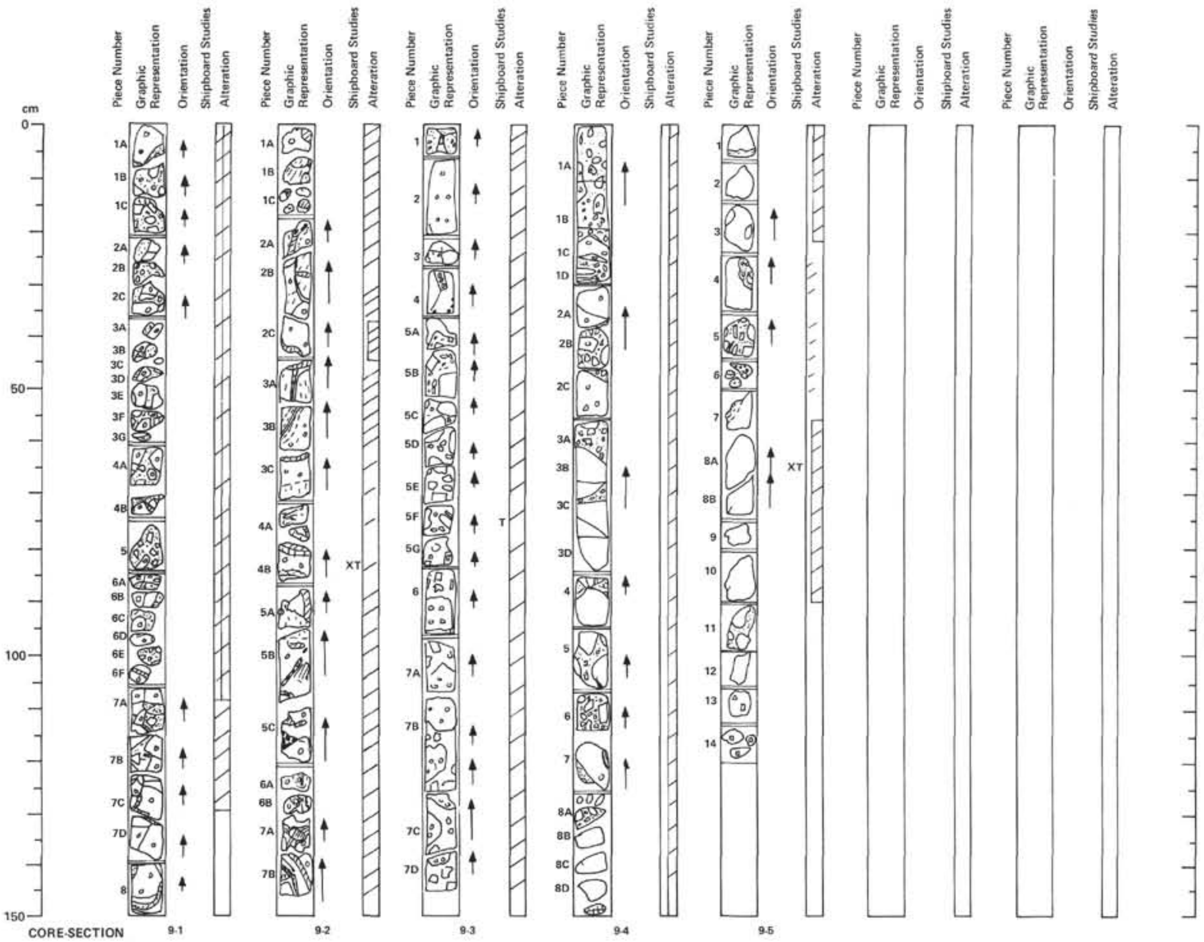

SITE 556, CORE 9 Depth 525.0–534.0 m

SECTION 1

OLIVINE MICRO-PHYRIC BASALT

0–105 cm: Moderately to badly altered, vesicular, olivine micro-phyric, medium-grained basalt breccia. Olivine (5–10%) diameter >1 mm and altered to smectite.

From 0–~50 cm: "Matrix" consists of angular – rounded palagonite pieces.

From 50– ~110 cm: Calcite cementation increases.

From ~ 110 cm–bottom of section: The basalt is fairly fresh. Here the narrow fractures are filled by carbonate cement. Color gray (2.5Y N5/0). Most of the vesicles in the basalt throughout the whole section are not filled.

SECTION 2

OLIVINE MICRO-PHYRIC BASALT

Olivine microphenocrystic basalt light gray (7.5YR N/6) in color. Calcite veins infiltrate the basalt, pattern quite complex and frequent down core. Alteration of basalt about calcite veins yield clay/basalt mixture, light brown *(10YR N6/2) in color. General alteration to brown throughout, very noticeable in Pieces 3A, B, and C and 5A, B,* and C. Interpreted as brecciated basalt transition zone; just fractured, slightly moved to stationary.

Irregular vesicles throughout, size ranging up to 1 mm in diameter. Often empty, some filled with calcite or clay alteration product.

107–118 cm, Piece 5C: Glass altered to palagonite surrounded by calcite alteration rim. Subsequent product is ruddy orange (7.5YR N7/6) in color.

120–145 cm: Calcite rim with palagonatized glass.

SECTION 3

OLIVINE MICRO-PHYRIC BASALT AND BASALT BRECCIA

0–30 cm: Moderately olivine (5–7%) micro-phyric gray (7.5YR N5) fine-grained basalt. Olivines are altered to smectite (~0.5 mm) 5% round vesicles.

27–143 cm: Breccia – made up of angular and subrounded pieces of moderately olivine microphyric gray fine grained basalt. These pieces range in sizes from 10 cm to a few mm. The degree of alterations is not a function of size (i. e. smaller pieces are fresher then larger pieces). The matrix contains carbonate.

Thin Section, 72–75 cm: Basalt breccia matrix, basalt lithic and glass fragments, subangular to subrounded, no sorting or stratification noticed, size range coarse sand to clay-size. XRD shows no clay minerals. Micritic calcite is common.

SECTION 4

BASALT BRECCIA (OLIVINE MICRO-PHYRIC)

Fresh to moderately altered basalt breccia. Upper half is olivine micro-phyric (<5%, <1 mm). From ~55 cm to the bottom basalt is aphyric. Vesicles occur anywhere, partly empty, partly filled with smectite. Color of basalt is gray to light brownish gray *(2.5Y N6–2.5Y 6/2). Color of "matrix" is light yellowish gray (2.5Y 7/2).*

SECTION 5

BASALT BRECCIA (APHYRIC)

Aphyric basalt, exceptions as noted. Color 10YR N6/1. Hints of central phases of brecciated basalt zone.

35–42 cm: Brecciated basalt, carbonate cement.

44–50 cm: Brecciated basalt pieces, carbonate cement.

91–92 cm, Piece 11: Hazy brecciated basalt transition zone. Calcite cement light brown gray (10YR 6/2).

106–110 cm, Piece 13: Plagioclase phyric basalt, clasts up to 3.5 mm in diameter.

111–116 cm: Pieces of slightly plagiophyric basalt.

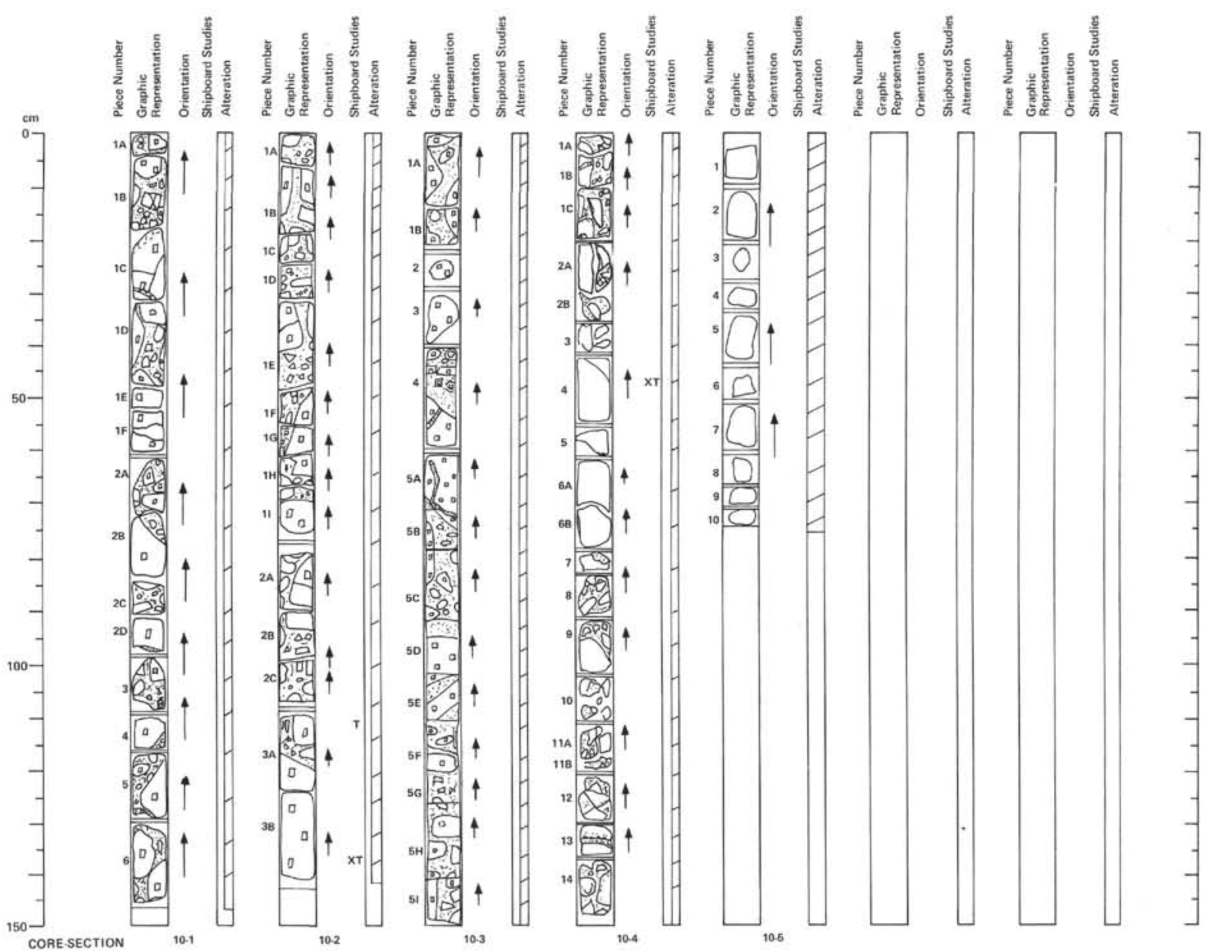

SITE 556, CORE 10 Depth 534.0–543.0 m

SECTION 1

BASALT BRECCIA (PLAGIOCLASE PHYRIC)

Basalt: Moderately plagioclase-phyric, gray (2.5Y N5/0). Vesicles are common and mostly filled with smectite.

At 30 cm: Narrow calcitic vein.

"Matrix": Olive (5Y 5/3) with many angular pieces of basalt.

115–128 cm: Partly calcite-cemented with some open cavities.

SECTION 2

BASALT BRECCIA (PLAGIOCLASE PHYRIC)

Basalt breccia.

Angular clasts of moderately plagioclase phyric light gray (2.5Y N5/0) basalt.

~ 5% equant plagioclase phenocrysts to about 2 mm.

Matrix: Indurated light gray-green (5Y 5/3) calcareous(?) ooze.

Thin Section, 36–39 cm: Moderately plagioclase-phyric (5%) intersertal basalt; plagioclase-phenocryst composition An_{80}; groundmass: cpx (40%), plag (30%), ol (5–10%), magnetite (3–5%); mesostasis (15–20%) is altered; olivine is replaced by clay.

SECTION 3

BASALT BRECCIA (PLAGIOCLASE PHYRIC)

Becoming less plagioclase phyric dwnwards, but otherwise exactly as Section 2.

SECTION 4

BASALT BRECCIA (like Sections 2 and 3).

Clasts: Angular, fine grained, medium gray (5Y 5/1) aphyric to very sparse small olivine and plagioclase phenocrysts.

Matrix: Indurated light gray green (5Y 5/3) calcareous(?) ooze.

SECTION 5

BASALT BRECCIA (APHYRIC TO PLAGIOCLASE PHYRIC)

Medium gray aphyric fine grained basalt with occasional plagioclase phenocrysts to 2 mm.

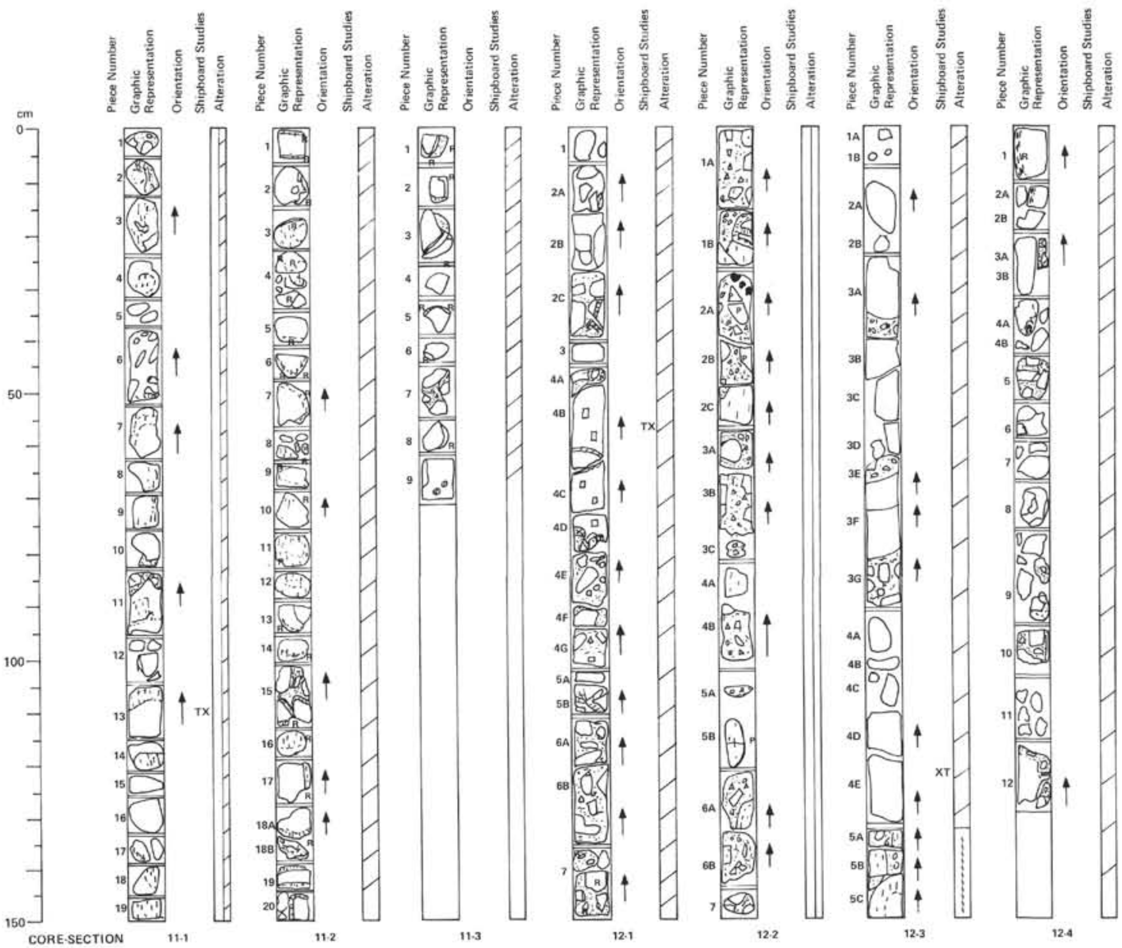

SITE 556, CORE 11 — Depth 543.0–552.0 m

SECTION 1

BASALT BRECCIA (APHYRIC)

Clasts: Angular, fine grained, medium gray (2.5Y N6) aphyric with very sparse plagioclase phenocrysts and *altered olivine. Sparse vesicles throughout (up to 1 mm), some empty, some filled with calcite and/or green clays.* Slight to moderate weathering (~~).

17 cm: Larger (1 cm) cavity filled with calcite and dark green clays(?).

Matrix: Indurated, dark olive gray (5Y 4/3).

Thin Section at 110–112 cm: Aphyric to sparsely plagioclase-phyric (1–2%) intersertal to subophitic basalt. Groundmass: plag (40%), cpx (30%), magnetite (5%); mesostasis (20–25%) partly altered to clay; segregation vesicles (1%) filled with carbonate; olivine is also altered to clay.

140–150 cm: Medium red (5YR 5/3) alteration (oxidation?) and dark red (5YR 3/3) alteration.

SECTION 2

BASALT BRECCIA (APHYRIC)

Mostly single pieces of basalt, but at 25–35 cm; 103–113 cm and 130–135 cm there are angular to subrounded basalt clasts in dark gray green (5GY 3/2) chlorite(?) carbonate matrix.

Basalt itself is fine grained, aphyric medium gray (2.5Y N5).

Extensive red (5R 4/6) alteration in bands or on surface (indicated by R).

SECTION 3

BASALT BRECCIA (APHYRIC)

Light gray (2.5Y N5) aphyric basalt subrounded clasts in dark green (5GY 3/2) chlorite(?) matrix.

Red (5R 4/6) alteration bands in many pieces (indicated by R).

44–52 cm: Chlorite(?) – carbonate matrix.

52–70 cm: No matrix present.

SITE 556, CORE 12 — Depth 552.0–561.0 m

SECTION 1

BASALT BRECCIA (APHYRIC TO PLAGIOCLASE PHYRIC)

0–133 cm: Basalt breccia.

Clasts: Medium to fine grained, medium gray (5Y 4/1) aphyric to sparsely plagioclase phyric basalt.

Matrix: greenish gray (5Y 5/3) silt, fine sand size sedimentary matrix (non-carbonate) with ~5% fine carbonate veins.

Thin Section at 55–57 cm: Identical to Core 10, Section 2, Piece 3B.

135–137 cm: See Core 12, Section 2.

SECTION 2

BASALT BRECCIA (APHYRIC)

Section 1, 137–150 cm and Section 2, 0–150 cm: Altered basalt breccia (hyaloclastic).

Clasts:

1 – Angular fine grained aphyric basalt clasts to ~ 8 cm maximum dimension. Almost entirely altered light brownish gray (10YR 6/1) to red (2.5YR 4/4).

2 – Black devitrified pillow fragments (marked P) grading to light brown (10YR 6/1) interiors.

3 – Rounded to angular glass fragments. Some fresh, most altered rusty brown or green (10GY 3/2).

Matrix: White to light green (10Y 4/2).

SECTION 3

BASALT BRECCIA (APHYRIC)

0–130 cm: Basalt breccia as in Section 2.

130–150 cm: Altered basalt breccia. Aphyric basalt clasts with red (2.5YR 4/4) altered rims in reddish matrix of comminuted basalt fragments. Chlorite along fracture surfaces in matrix.

SECTION 4

CHALK BASALT BRECCIA (APHYRIC)

More basalt breccias as in Section 3.

More red (5R 5/4) alteration rims.

33–40 cm and 52–57 cm: Reddish (5R 5/4) micritic chalk.

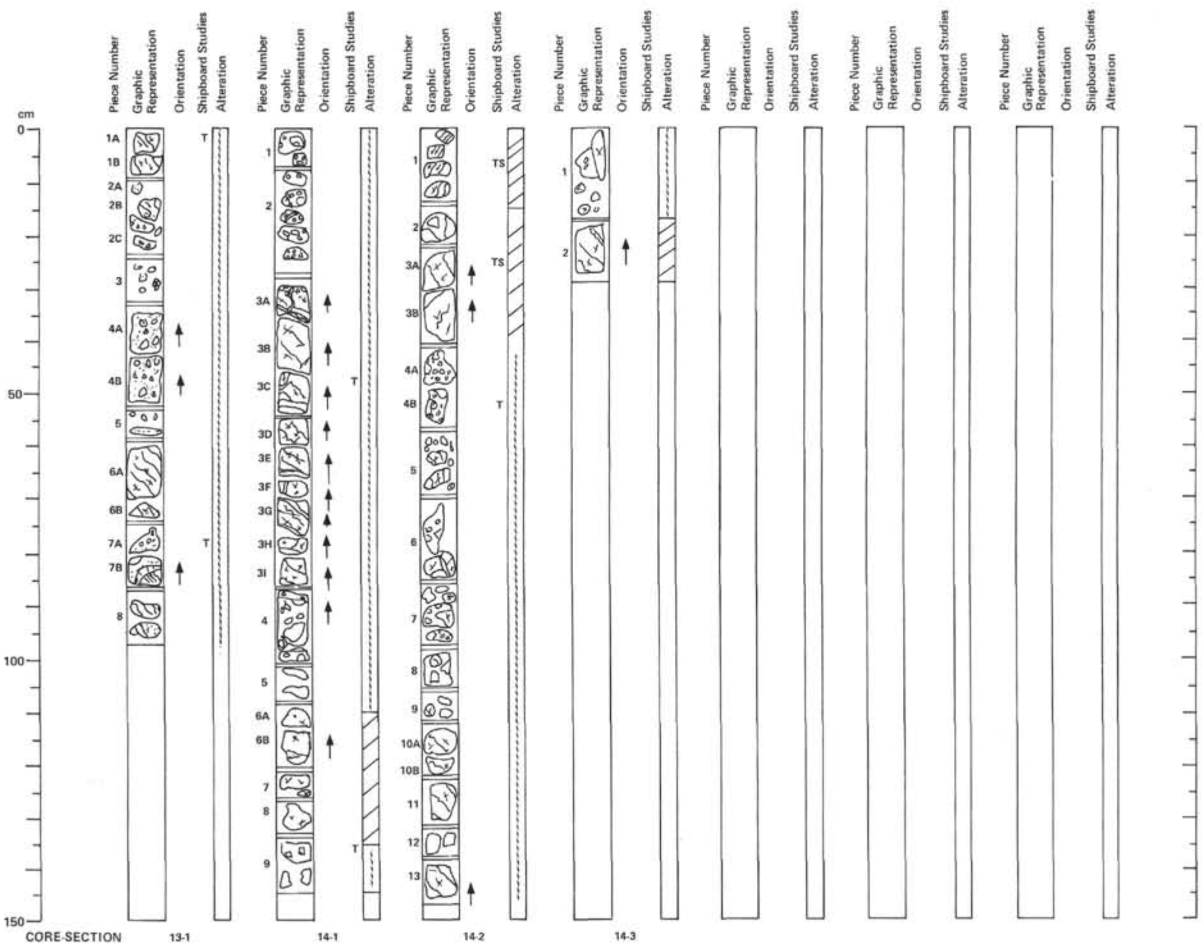

SITE 556, CORE 13 Depth 561.0–570.0 m

SECTION 1

SERPENTINIZED GABBRO BRECCIA

Clasts:

1 – Serpentinized gabbro greenish black (5Y 2/2) weathering greenish brown (5Y 5/3). Weakly foliated 10–15% altered pyroxene (opx?), brown (10YR 6/4 to 10YR 5/4) in color.

Minor angular clasts of:

Black clinopyroxene
White plagioclase
Gabbro

Matrix: Nondescript brownish green (2.5Y 5/4) fine grained mterial.

Thin Section at 6–9 cm: Serpentinite (serpentinized noritic?), holocrystalline; phenocrysts; opx (10%), plag (~1%), groundmass: serpentine (80%), magnetite (5%), hematite (3%) – probably after magnetite.

SITE 556, CORE 14 Depth 565.5–574.5 m

SECTION 1

SERPENTINIZED GABBRO BRECCIA

0–30 cm: Clasts – large plagioclase crystal (3 cm) black clinopyroxene. See Core 13, Section 1 description.
30–86 cm: Serpentinized gabbro with calcite veins.
86–107 cm: Polymict breccia with carbonate cement.
107–134 cm: Moderately altered gabbro with ≈10% pyroxene.
134–144 cm: Polymict breccia with plagioclase clasts.

SECTION 2

SERPENTINIZED GABBRO BRECCIA

0–15 cm: Moderately altered serpentinized gabbro. Pyroxene is brown (altered).
15–23 cm: Polymict breccia with clasts of gabbro.
23–40 cm: Serpentinized gabbro with ≥15% opx.
40–56 cm: Polymict breccia with gabbro clasts 3 cm–3 mm in size.
56–70 cm: Serpentinized gabbro.
70–111 cm: Polymict breccia.
111–145 cm: Serpentinized gabbro.

Thin Section at 8–11 cm: Clast of holocrystalline (granitic) gabbro, bearing plag (60%), cpx (40%) and traces of magnetite. Plagioclase has approximate composition of An_{60}. Adjacent to cpx occurs light brown amphibole (~10% of cpx) and chlorite (5% of cpx). White prehnite occurs in scattered patches (~15%), serpentine and carbonate are found in small veinlets.

SECTION 3

SERPENTINIZED GABBRO BRECCIA

0–17 cm: Polymict breccia – matrix is not carbonate. The rock is so friable that the clasts of serpentinized gabbro and matrix are disassociating.
17–29 cm: Moderately altered gabbro.

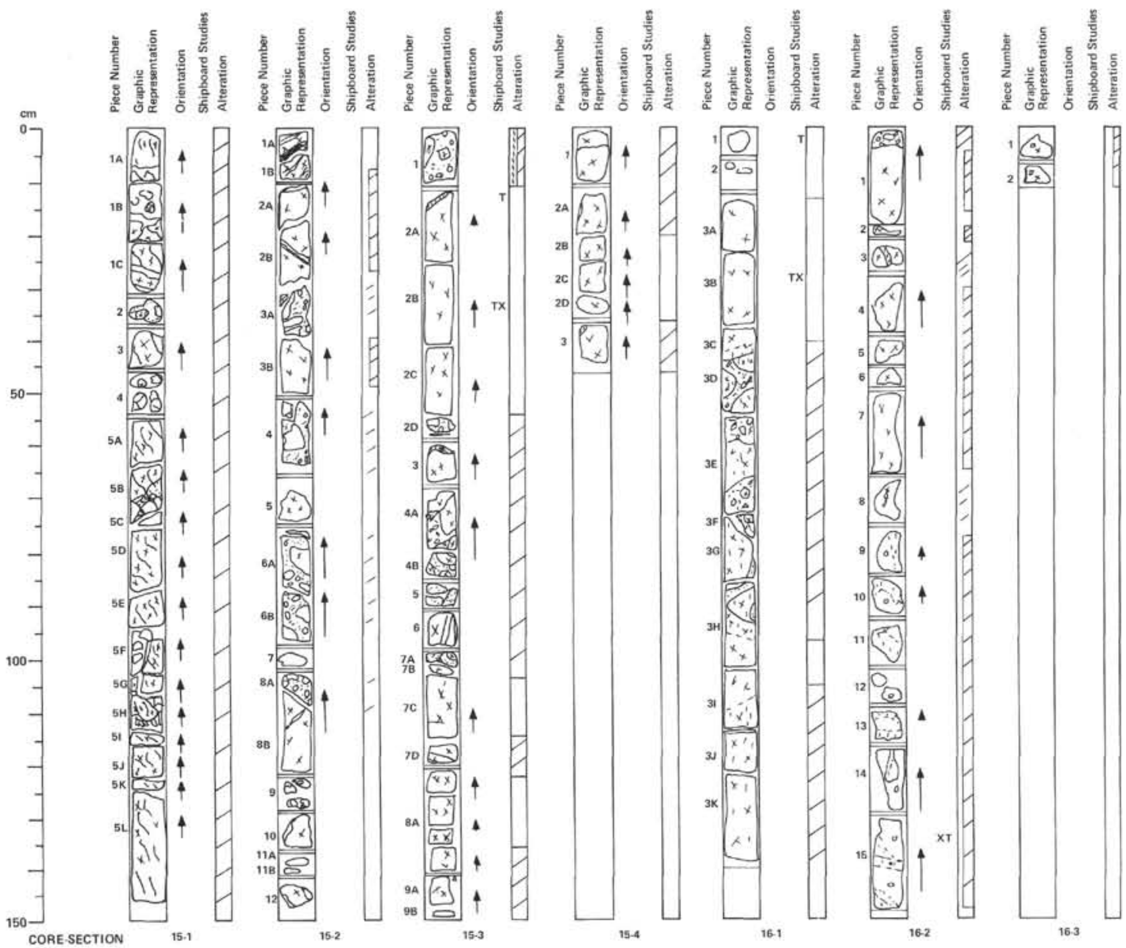

SITE 556, CORE 15 Depth 574,5–583.5 m

SECTION 1

SERPENTINIZED GABBRO BRECCIA

Similar to Core 14, Sections 2 and 3 with clasts of gabbro.

Medium brown (4.5YR 5/6) pyroxene (10%); size 1–5 mm and plagioclase plus <1% dark green cpx(?).

0–15 cm: Polymict breccia.

15–30 cm: Moderately altered gabbro.

30–53 cm: Polymict breccia.

53–90 cm: Moderately altered gabbro with some breccia.

90–140 cm: Moderately altered gabbro.

SECTION 2

SERPENTINIZED GABBRO BRECCIA

Slightly serpentinized gabbro with altered brown pyroxenes infiltrated by calcite veins.

30–38 cm, Piece 3A: Polymict breccia of clasts of gabbro *(serpentinized)* containing altered brown pyroxene.

53–64 cm, Piece 4: Polymict breccia with clasts of gabbro slightly serpentinized with brown pyroxenes.

67–74 cm, Piece 5: Gabbro of brown slightly altered pyroxenes.

76–107 cm, Pieces 6A–8A: Polymict breccia with clasts of serpentinized gabbros (serpentine obvious) with brown pyroxenes.

104–119 cm, Piece 8B: Same as for 0–30 cm, except amount of serpentine is increasing.

120–124 cm, Piece 9: Polymict breccia with clasts (small) of serpentinized gabbro.

126–133 cm, Piece 10: Same as for 0–30 cm, except highly serpentinized rim.

134–139 cm, Piece 11: Polymict breccia with clast of gabbro.

141–145 cm, Piece 12: Same as for 0–30 cm.

SECTION 3

SERPENTINIZED GABBRO BRECCIA

Piece 1: Polymict gabbro breccia, gray gabbro clasts contain large pyroxene which is partly altered. Some clasts are serpentinized (dark green color). Matrix of breccia is serpentine, too.

Piece 2: Gabbro as above, but very fresh and masive.

60–103 cm: Polymict gabbro breccia as in Piece 1, but all are altered and brown colored.

103–150 cm: Gabbro, mostly fresh. Pyroxene is altered in some pieces (7A, 7B, top of 7C, 7D, top and bottom of 8A, and 9A, and B).

Thin Section at 15–17 cm: Holocrystalline (granitic) gabbro with plag (45%), cpx (35%), opx (5%), magnetite (3%), amphibole (5%). Carbonate, hematite and rutile (1–2%) probably pseudomorphs after olivine.

Thin Section at 34–37 cm: Holocrystalline (granitic) gabbro with plag (60%), opx (20%), cpx (15%), amph (~1%); 10% of pyroxene replaced by green brown amph.

SECTION 4

SERPENTINIZED GABBRO BRECCIA

Fresh to moderately altered dark gray gabbro containing large opx (<1 cm). At upper edge of Piece 3A occurs yellow greenish brecciated gabbro with serpentine matrix.

SITE 556, CORE 16 Depth 583.5–592.5 m

SECTION 1

SERPENTINIZED GABBRO BRECCIA

0–10 cm: Anorthosite(?) vein. Coarse white plagioclase with minor opx(?).

15–40 cm: Fresh gabbro becoming altered (opx turns brown) at lower end.

40–95 cm: Gabbro breccia: Angular gabbro and minor gabbro (~1 cm) clasts in nondescript greenish brown (5Y 6/3) matrix.

Thin Section, Piece 1: Holocrystalline (granitic), partly altered anorthosite; contains plag (80%), cpx (20%). Amphibole (2%) and chlorite (5–10%) are replacing cpx (around cpx), prehnite occurs up to 20% in veinlets and patches replacing plagioclase.

92–136 cm: Moderately altered gabbro.

Thin Section at 3–6 cm: Holocrystalline (granitic) gabbro with plag (60%), opx (20%), cpx (20%) and traces of magnetite. Plagioclase approximately An_{60}. Pyroxene (10%) is replaced by amphibole.

SECTION 2

SERPENTINIZED GABBRO BRECCIA WITH APHYRIC BASALT (CLAST?)

0–3 cm: Polymite breccia, clasts are altered gabbro (serpentinized) with brown pyroxenes.

30–75 cm: Moderately altered gabbro with large phenocrysts of brown (altered?) pyroxene diameter ≈4.0 mm. Dark red clay alteration product.

68–75 cm, Piece 8: Highly(?) altered gabbro with altered brown pyroxene, surface is impregnated with dark red with altered brown clay alteration product.

75 cm: Major unit break.

75–145 cm: Slightly olivine micro-phyric basalt, somewhat altered in places and light gray (10YR N6/2) in color. Alteration light gray brown (10YRN 6/4) in color. Transition is rather sharp and sudden, occurring immediately after Piece 8. Alteration shown to light brown gray by

Thin Section at 138–141 cm: Aphyric intergranular to intersertal basalt; groundmass: plag (50%), cpx (20%), magnetite (5%); mesostasis (20%) is devitrified glass. Vesicles are filled with clay.

SECTION 3

APHYRIC BASALT (CLAST?)

Slightly olivine micro-phyric basalt, olivines altered and discolored. Smaller phenocrysts of plagioclase are also present. Diameter <1 mm. Color basalt 10YR N6/2.

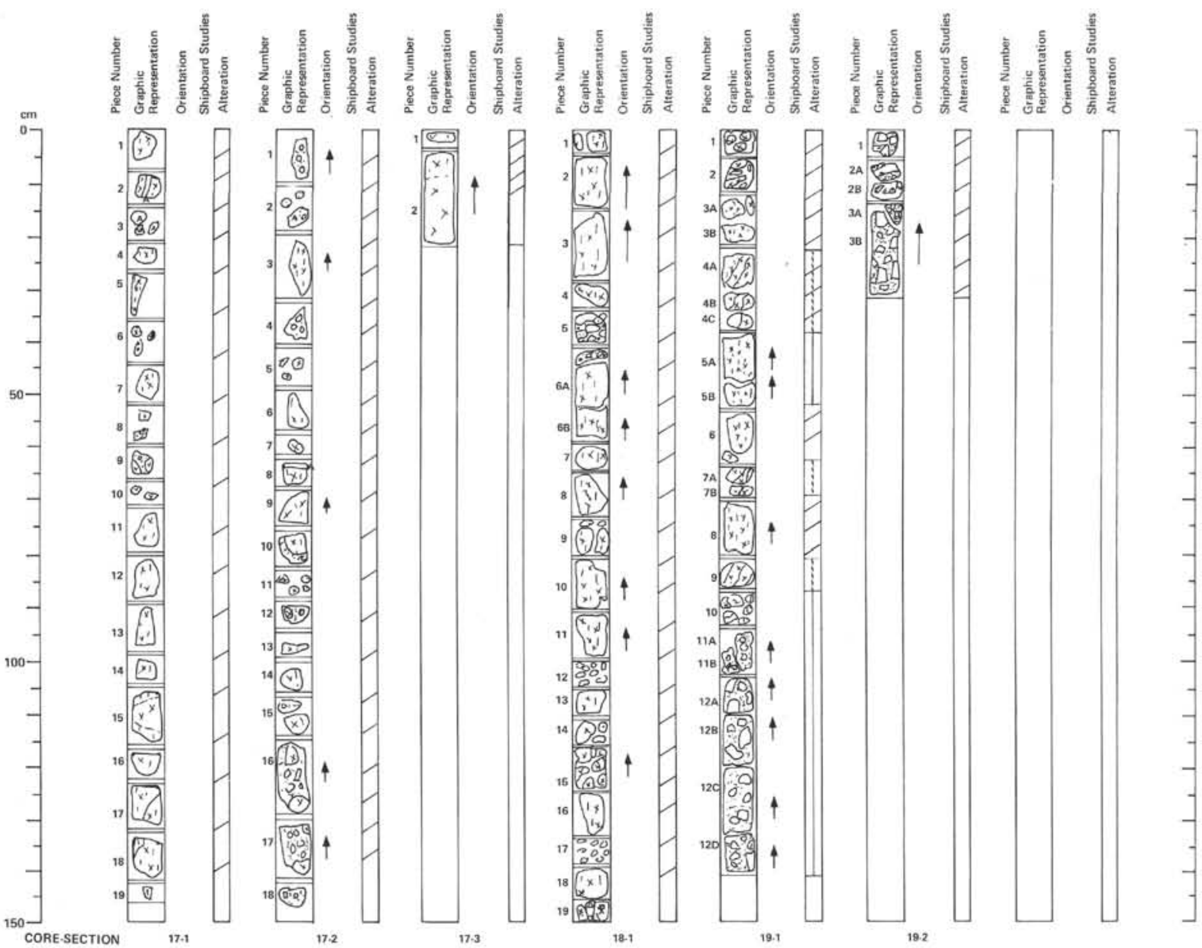

SITE 556, CORE 17 Depth 592.5–601.5 m

SECTION 1

TALC-SERPENTINE GABBRO BRECCIA

Moderately altered gabbro as in Core 16. Anorthosite veins (A) at 10–20 cm. Breccia matrix in Pieces 6, 8, and 9 – same as Core 16.

SECTION 2

TALC-SERPENTINE GABBRO BRECCIA

Gabbro breccia as in Section 1.

SECTION 3

TALC-SERPENTINE GABBRO BRECCIA

Gabbro (clast) as in Section 1

SITE 556, CORE 18 Depth 601.5–610.5 m

SECTION 1

TALC-SERPENTINE GABBRO BRECCIA

Gabbro breccia as in Sections 1–3.
36–40 cm: Chlorite (talc) rich matrix.
100–105 cm: Rubble.
118–125 cm: Matrix.
134–139 cm: Rubble.

SITE 556, CORE 19 Depth 610.5–619.5 m

SECTION 1

TALC-SERPENTINE GABBRO BRECCIA

0–15 cm: Breccia with gabbro clasts.
15–23 cm: Serpentinized gabbro (breccia).
23–38 cm: Serpentinized gabbro.
38–53 cm: Breccia in gabbro clasts.
53–62 cm: Serpentinized gabbro breccia.
62–69 cm: Serpentinized gabbro.
69–79 cm: Moderately altered gabbro.
79–86 cm: Serpentinized gabbro.
86–93 cm: Highly altered (dark red brown – 10R 3/4) gabbro and breccia rubble.
93–138 cm: Breccia to predominantely anorthorite clasts and dark green (5G 3/2) chlorite(?) rich matrix with dark red brown (10R 3/4) alteration.

SECTION 2

TALC-SERPENTINE GABBRO BRECCIA

As in Section 1, 93–138 cm.

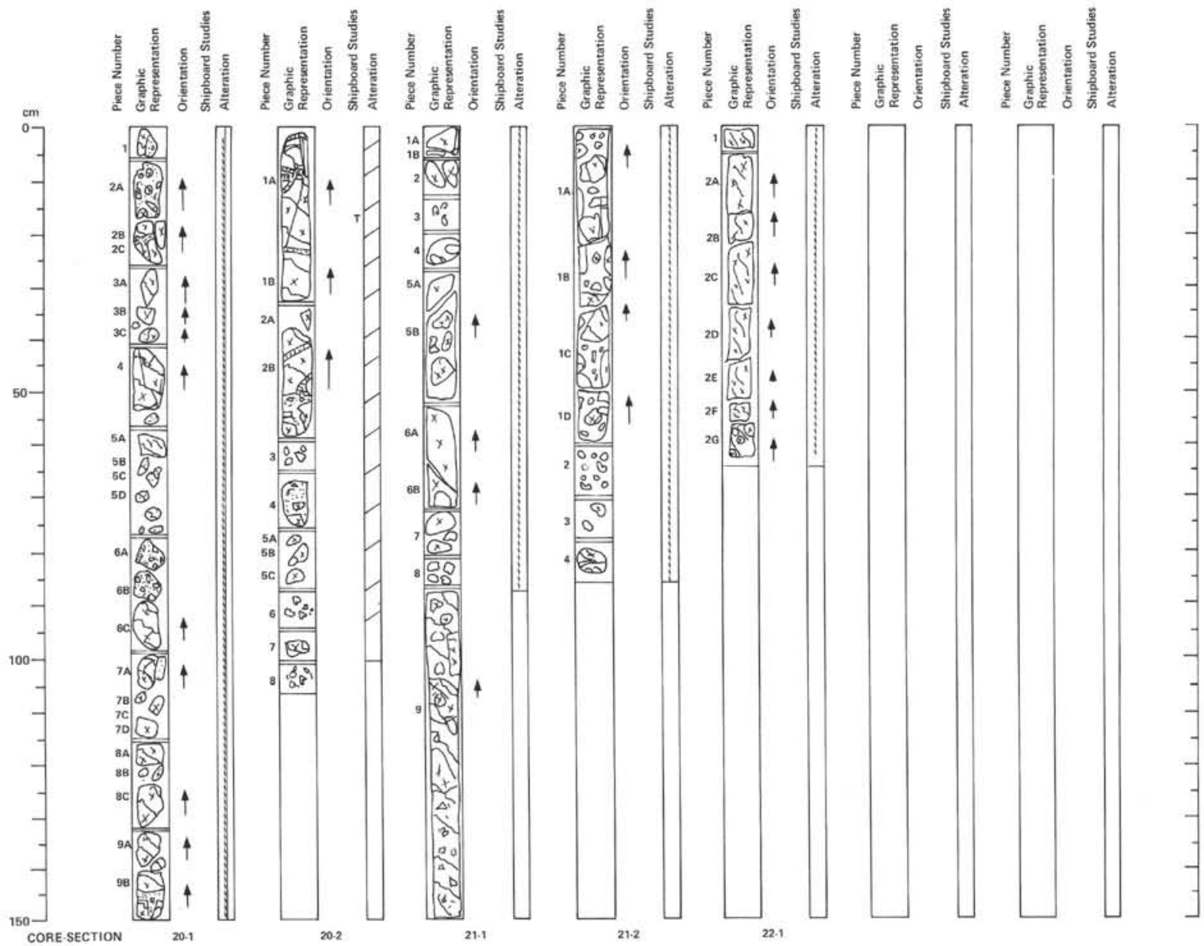

SITE 556, CORE 20 — Depth 619.5–628.5 m

SECTION 1

TALC-SERPENTINE GABBRO BRECCIA

Highly altered predominately serpentinized gabbro breccia. A high amount of the "matrix" is green talc. Orthopyroxene is very common (~15–20%). In Piece 9 the talc is dark green and predominant.

SECTION 2

TALC-SERPENTINE GABBRO BRECCIA

0–56 cm: Massive dark gray greenish serpentinized gabbro with large opx (size up to 13 mm). Upper and lower parts are highly fractured; veins filled with calcite. At the bottom between 50 and 56 cm brecciation occurs.

56–105 cm: Continuation of brecciation. Breccia is cemented by calcite.

CC = Calcite cement.

SITE 556, CORE 21 — Depth 628.5–637.5 m

SECTION 1

TALC-SERPENTINE GABBRO BRECCIA

0–20 cm: Serpentinized gabbro.

20–87 cm: Breccia. Serpentinized gabbro, gabbro and anorthosite (talc rims) clasts in talc-rich matrix.

87–150 cm: Foliated, serpentinized breccia. Clasts of dark green black serpentinized (5Y 2.5/2) gabbro in serpentinized matrix of small angular gabbro fragments and nondescript light gray green (5G 5/2) material.

SECTION 2

TALC-SERPENTINE GABBRO BRECCIA

Serpentinized breccia with clasts of gabbro. Veins of calcite run between the clasts. Serpentinization appears to have taken place before formation of the breccia, since the clasts fabric is different.

Gabbro contains orthopyroxene and plagioclase.

70–80 cm: Talc present.

SITE 556, CORE 22 — Depth 637.5–639.0 m

SECTION 1

TALC-SERPENTINE GABBRO BRECCIA

Foliated serpentinized gabbro, partly brecciated (similar to Core 21, Section 1, 87–150 cm).

Piece 2G: Clasts of dark green black (5G 2/1). Serpentinized gabbro in serpentinized matrix of small angular clasts of gabbro and nondescript light gray green (5G 6/1) material.


0 cm
25
50
75
100
125
150
1-1
1-2
1-3
1-4
1,CC
H1-1
H1-2
H1-3
H1-4
H1-5
H1-6
H2-1

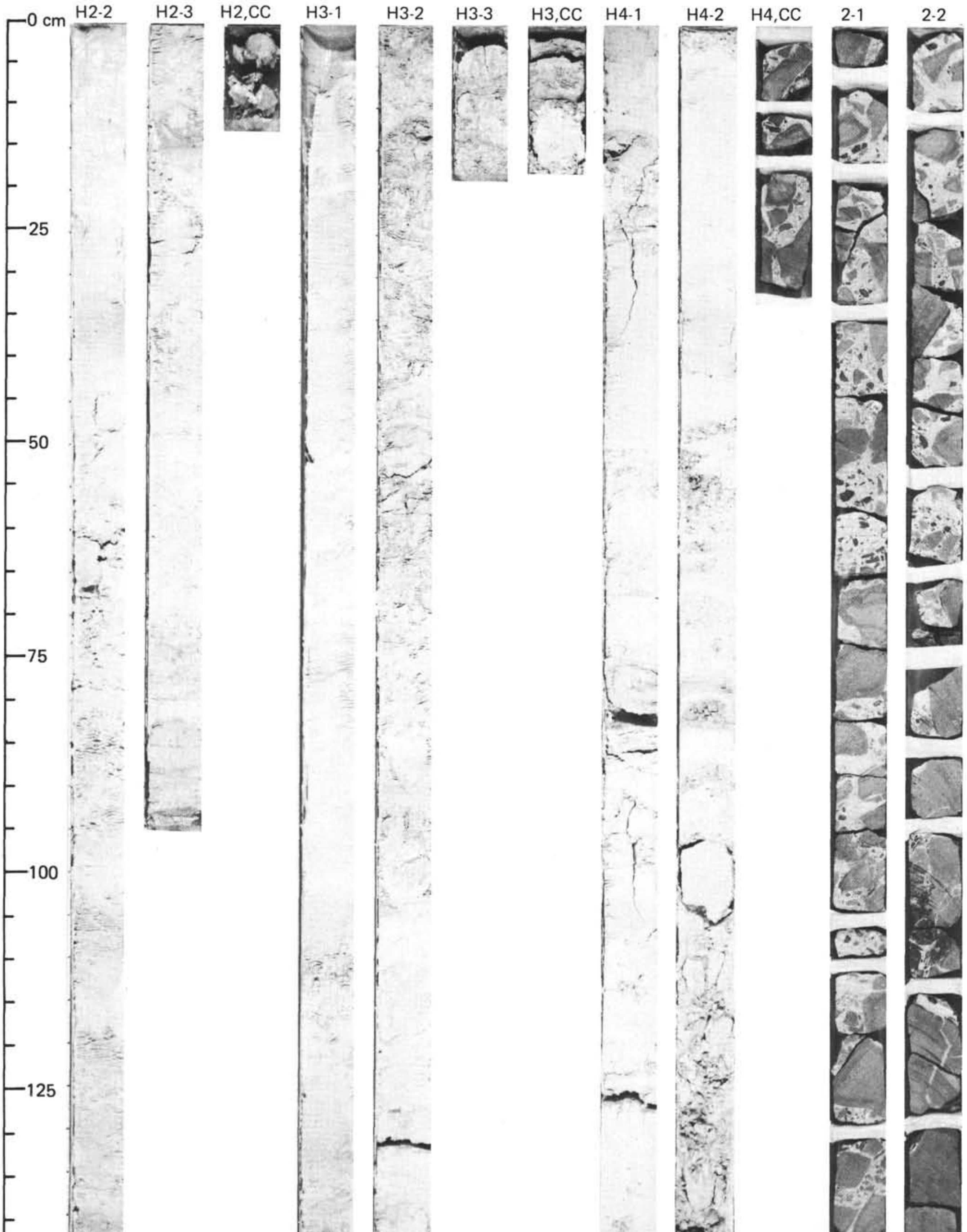
0 cm
25
50
75
100
125
150
H2-2
H2-3
H2,CC
H3-1
H3-2
H3-3
H3,CC
H4-1
H4-2
H4,CC
2-1
2-2


2-3
2-4
2-5
2-6
3-1
3-2
3-3
4-1
4-2
4-3
4-4
4-5
0 cm
25
50
75
100
125
150

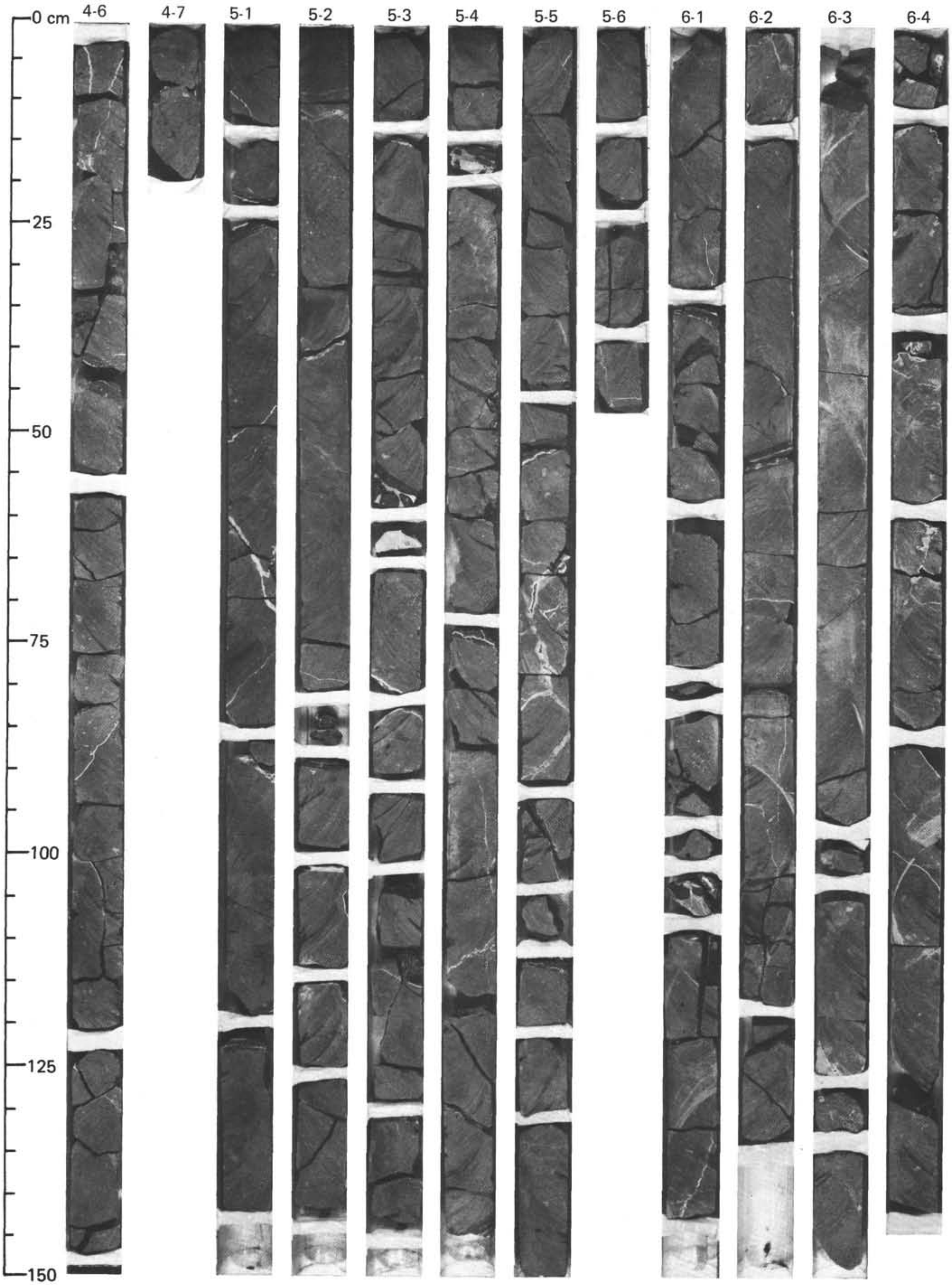
0 cm
25
50
75
100
125
150
4-6
4-7
5-1
5-2
5-3
5-4
5-5
5-6
6-1
6-2
6-3
6-4

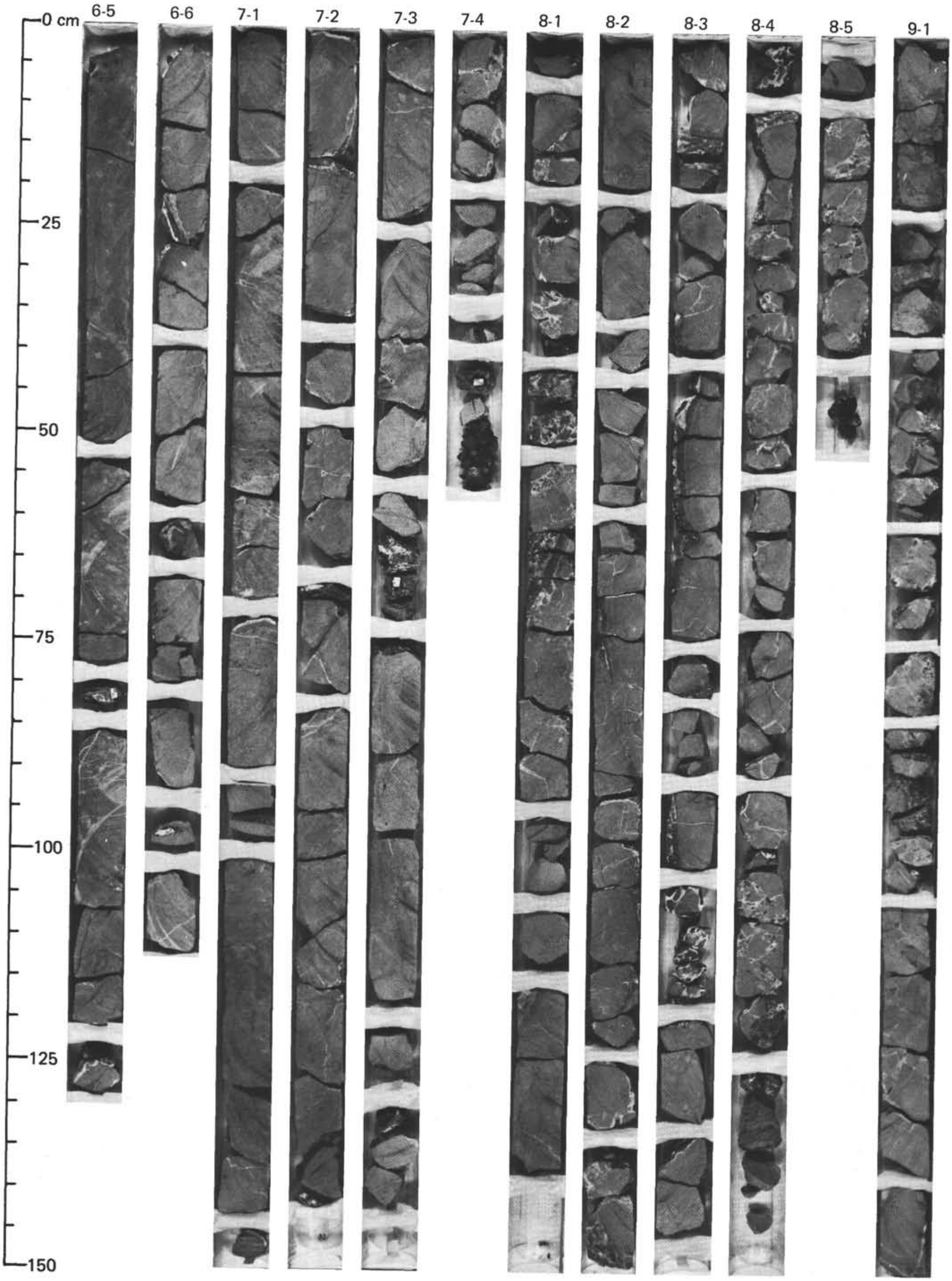
0 cm
25
50
75
100
125
150
6-5
6-6
7-1
7-2
7-3
7-4
8-1
8-2
8-3
8-4
8-5
9-1

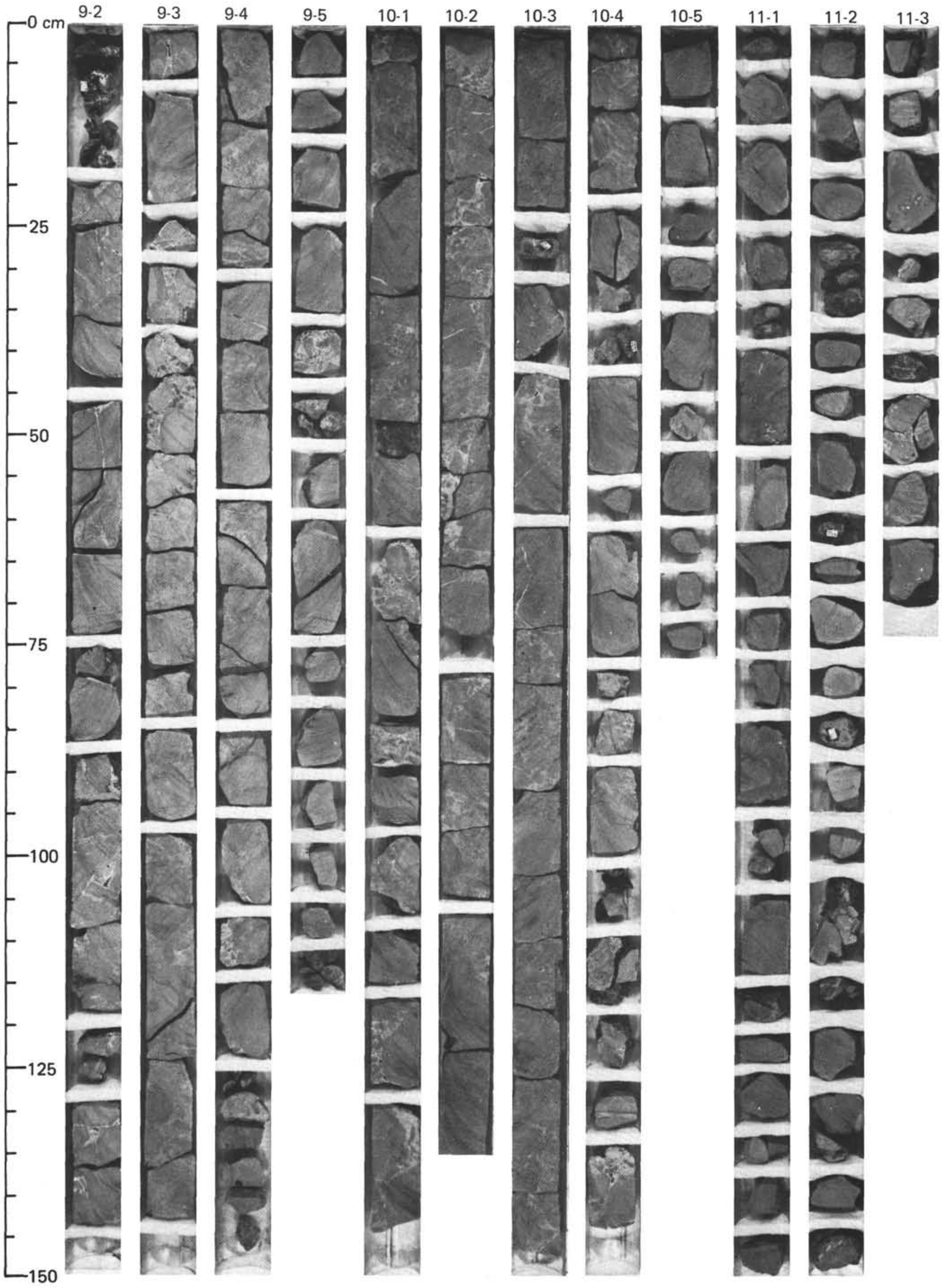
0 cm
25
50
75
100
125
150
9-2
9-3
9-4
9-5
10-1
10-2
10-3
10-4
10-5
11-1
11-2
11-3

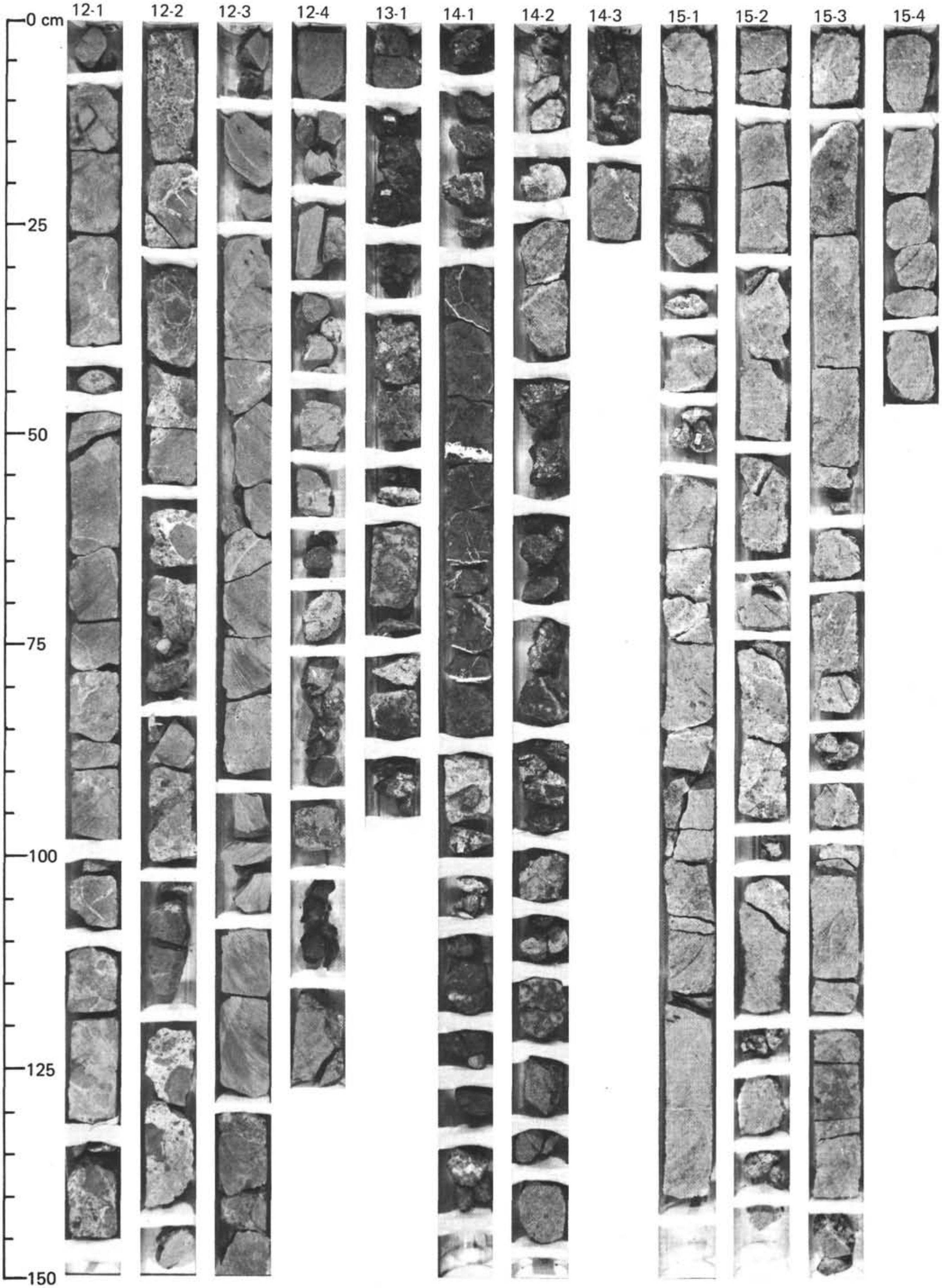
0 cm
25
50
75
100
125
150
12-1
12-2
12-3
12-4
13-1
14-1
14-2
14-3
15-1
15-2
15-3
15-4

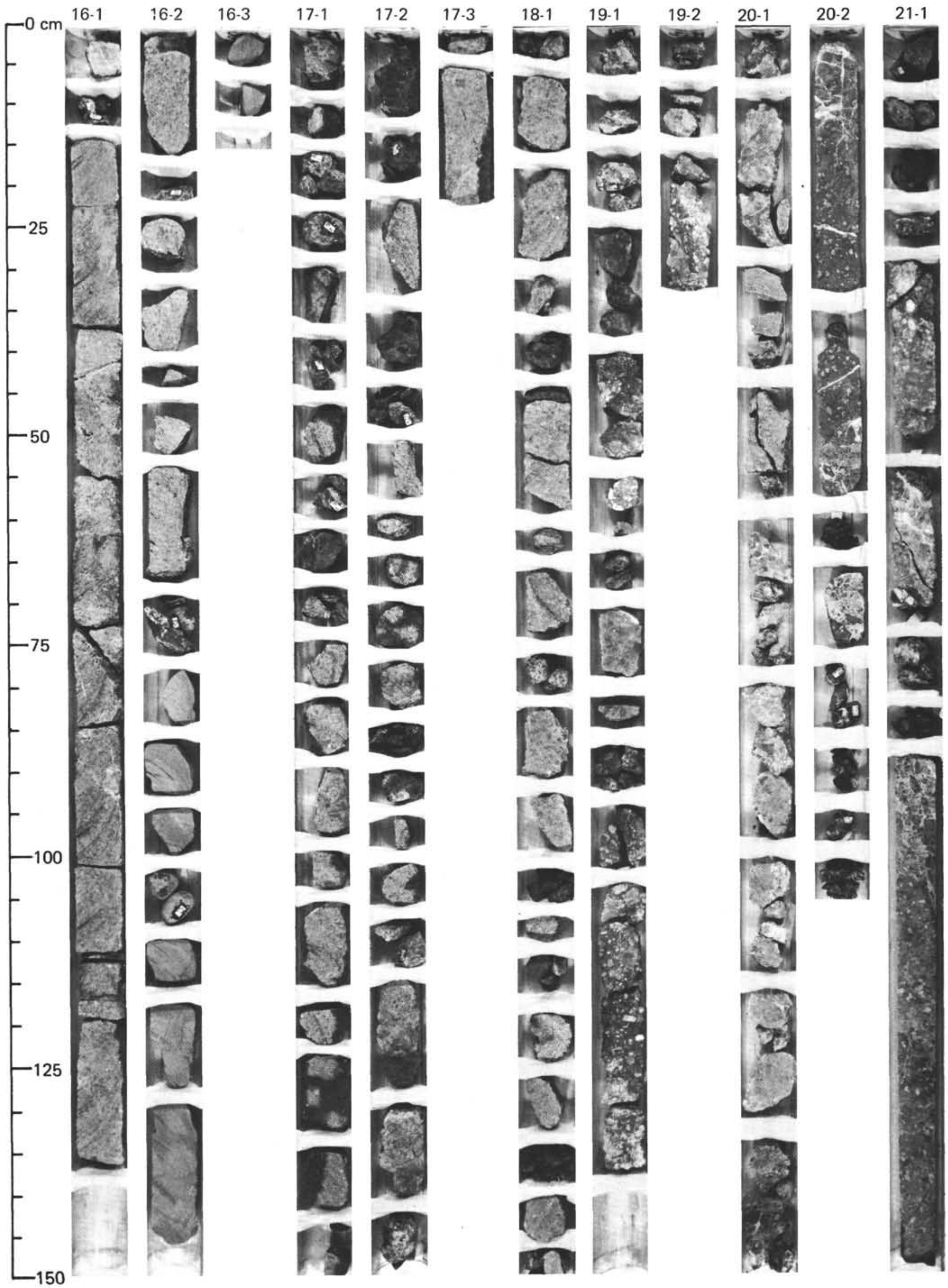
0 cm
25
50
75
100
125
150
16-1
16-2
16-3
17-1
17-2
17-3
18-1
19-1
19-2
20-1
20-2
21-1

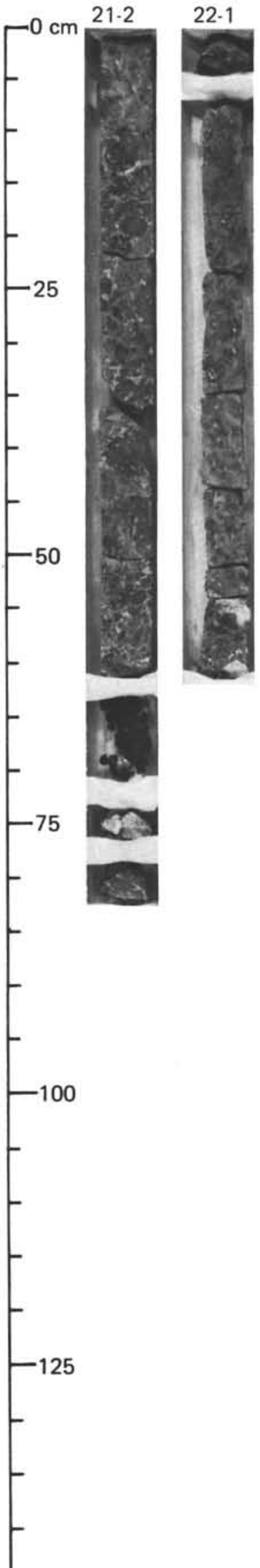
0 cm
25
50
75
100
125
150
21-2
22-1